DOCTORAL THESIS

Precise Beam Control System for Solar Power Satellite

Author:
Raza Mudassir

Supervisor:
Associate Professor
Koji Tanaka

A thesis submitted in fulfillment of the requirements
for the degree of Doctor of Philosophy

in the

The Graduate University for Advanced Studies, SOKENDAI
Department of Space and Astronautical Science, School of Physical Sciences

Abstract

The Graduate University for Advanced Studies, SOKENDAI
Department of Space and Astronautical Science, School of Physical Sciences

Doctor of Philosophy

Precise Beam Control System for Solar Power Satellite

by Raza Mudassir

Solar Power Satellite (SPS) has been proposed to provide continuous renewable energy from solar power. SPS will receive power from sun and transmit to rectenna on ground in form of microwaves. Challenges for SPS are efficient microwave power transmission, construction and control of large structure in space, large scale power generation, space transportation, etc. My study is focused to solve issues regarding efficient microwave power transmission. Many designs of SPS have been studied, and one of them is Tethered SPS. Its size is 2.375 km x 2.5 km, and rectenna of 3.5 km diameter will provide 1 GW power. Tethered SPS will use power generation and transmission modules with size of 0.5 m x 0.5 m, and 23,750,000 modules will be required. SPS will be installed in geostationary equatorial orbit (GEO) to transmit power continuously. For Tethered SPS, required accuracy of beam forming is .0005°. Flexible structures will be used for large array antenna system and space environment conditions will deform the antenna system. It is required to compensate effect of deformation for achieving the required accuracy.

Hardware retrodirective method and software retrodirective method have been studied previously to fulfill the requirements of power transmission, but both have some limitations. Hardware retrodirective method uses phase conjugate signals generated by a hardware microwave circuit, so it is not flexible regarding frequency. Refinements for amplitude tapering are difficult to apply, and filtering of unwanted signals is also not possible. Software retrodirective method consists of a direction finding system and a beam forming system. It needs high uplink power of pilot signal for direction finding in order to achieve required high beam control accuracy. The software retrodirective system also requires phase synchronization among huge number of power emitting devices installed on 23,750,000 modules. REV method that can correct phase error caused by an antenna deformation or temperature changes takes long processing time. Objectives of my study are improvement of software retrodirective method regarding direction finding and proposal of digital retrodirective method.

To solve issue of high uplink power for software retrodirective method, i proposed to increase SNR of pilot signal with high gain pilot signal receiving antennas and to use long baseline. Dipole array antennas were used to receive pilot signal and they were installed on power transmitting antennas. Phase comparison monopulse method was used to measure phase difference for 2x2 and 4x4 dipole array antennas. Error of angle of arrival was determined by using the measured values of phase difference. 1m, 2.5m and 5m baselines were used to compare effect of different baselines on the accuracy of direction finding. Results indicated that for 60 dB SNR with

using 4x4 array and 5m baseline, required accuracy of .0005° was achieved. Estimation was performed to determine uplink power for SPS and It was resulted that 6 kW uplink power is required with 54.4 dB gain of pilot signal transmitting parabolic antenna. Number of pilot signal receiving antennas was also decreased with using long baseline.

However, with larger receiving antenna by using an antenna array and with the longer baseline, deformation of the antenna is more susceptible. I evaluated effect of antenna deformation experimentally. Antenna deformation experiments were performed with dipole array antennas to estimate effect of antenna deformation on direction finding. Cases of partial antenna array deformation and whole antenna array deformation were considered. Phase error was minimum for one element deformation and was maximum for whole array deformation.

I proposed digital retrodirective method that generates phase conjugate signals by the software methods, as alternative to hardware and software retrodirective methods. Digital signal processing was used to detect phase of pilot signal and to generate conjugate phase for power signal by a new algorithm. Each set of pilot signal and power signal antenna worked independently to perform precise beam forming. A reference signal was used to provide standard frequency, phase and timing among retrodirective array antennas. For antenna deformation compensation, change of pilot signal phase was determined and power signal was generated accordingly.

Experimental evaluation for the digital retrodirective system and the algorithm was performed with using one dimensional retrodirective array. Patch subarray was used as power signal transmitting antenna and dipole antenna was used as pilot signal receiving antenna. Frequencies of power signal and pilot signal were 5.8 GHz and 2.45 GHz respectively. No deformation, forward deformation and backward deformation cases were considered for the evaluation. Results showed that digital retrodirective method performed well for all the cases. Regarding compensation for deformation cases, beam pointing error was .21° rms. Comparison was carried out between REV method and digital retrodirective method for compensation of antenna deformation. Antenna Radiation patterns for both methods were in good agreement, but long processing time was required for REV method.

Regarding application for SPS, estimation was performed for digital retrodirective method with two dimensional retrodirective array. 8x8 subarray was used and appropriate results for beam forming were obtained. Configuration to provide reference signal for large scale antenna system of SPS was also presented. GPS antennas were used to supply reference signal for a group of retrodirective array antennas and synchronization was not required among the groups of antennas.

Hence, the digital retrodirective method used digital processing circuit, which solved issues of hardware retrodirective method as flexibility regarding frequency, amplitude tapering modifications, etc. Issues of synchronization among antenna modules and processing time of antenna deformation compensation for software retrodirective method were also solved by digital retrodirective method. Number of pilot signal receiving antennas is increased with digital retrodirective method and it can increase cost. So, there is a trade-off between efficiency of beam forming and cost.

Conclusively, studies were performed to resolve issues of previously studied methods to do efficient microwave power transmission for SPS. Direction finding experiments were performed with high gain antennas and long baseline to decrease uplink power of pilot signal. Required uplink power for SPS was decreased with using the proposed methodology. Evaluation was also done for effect of antenna deformation on direction finding. Digital retrodirective method was proposed as alternative to the conventional methods and experiments were conducted to verify the algorithm. Results indicated that proposed method was able to solve issues of conventional methods to do precise beam forming for SPS.

Acknowledgements

Firstly, I would like say thanks to my advisor, Assoc. Prof. Koji Tanaka for providing me opportunity to work in Tanaka lab. I am also grateful for his support and guidance in research work.

Secondly, I am thankful to Japanese Ministry of education, Culture, Sports, Science, and Technology (MEXT) for granting me a scholarship to do graduate studies in Japan.

Finally, I will appreciate SOKENDAI for providing well facilitates for graduate studies and also supporting for attending conferences and experiments.

Contents

Abstract iii

Acknowledgements vii

1 Introduction 1
- 1.1 Tethered SPS . . . 1
- 1.2 Hardware Retrodirective Method . . . 2
- 1.3 Direction Finding and Beam Forming Method . . . 3
- 1.4 Research Problem . . . 3
- 1.5 Research Objective . . . 4
- 1.6 Thesis Outline . . . 5

2 Literature Review 7
- 2.1 Solar Power Satellite . . . 7
  - 2.1.1 SPS in Japan . . . 9
- 2.2 Wireless Power Transmission towards SPS . . . 11
  - 2.2.1 19th Century . . . 11
  - 2.2.2 20th Century . . . 12
  - 2.2.3 21th Century . . . 16
- 2.3 Hardware Retrodirective System . . . 18
- 2.4 Direction Finding and Beam Forming Method . . . 19

3 Precise Direction Finding 21
- 3.1 Introduction . . . 21
- 3.2 Phase comparison monopulse . . . 21
- 3.3 USRP . . . 23
- 3.4 Antenna . . . 24
  - 3.4.1 Half Wavelength Dipole antenna . . . 24
  - 3.4.2 Microstrip Patch antenna . . . 25
  - 3.4.3 Array antenna . . . 26
  - 3.4.4 Phased Array . . . 27
  - 3.4.5 Planar Array . . . 28
- 3.5 DF with Array Antenna . . . 29
  - 3.5.1 Simulation Setup of Antennas . . . 30
  - 3.5.2 Experimental setup for DF . . . 32
  - 3.5.3 Results and Discussion . . . 34
    - Radiation Pattern of Antenna . . . 34
    - Analysis for Degradation of AOA . . . 36
    - Comparison of Baseline . . . 37
    - Comparison of Array Size . . . 38
    - Analysis for Approximation . . . 41
    - Analysis of Ambiguity . . . 44

3.6 Effect of Deformation on DF . . . 46
3.6.1 Experimental Setup . . . 46
3.6.2 Results and Discussion . . . 51
3.7 Summary . . . 55

4 Digital Retrodirective Method **57**
4.1 Introduction . . . 57
4.2 Concept of Digital Retrodiretive method . . . 58
4.2.1 Algorithm of Digital Retrodiretive method . . . 60
4.3 DSP Circuit . . . 61
4.4 Experimental Setup . . . 62
4.4.1 Experimental Setup for Bistatic Pattern Measurement . . . 62
4.4.2 Detailed Experimental Setup Configuration . . . 63
4.5 Results and Discussion . . . 66
4.5.1 No Deformation Case . . . 66
4.5.2 Deformation case . . . 68
4.6 Summary . . . 74

5 System Study of WPT Technologies for SPS **75**
5.1 Introduction . . . 75
5.2 Estimation of Uplink Power . . . 75
5.3 Array Size Estimation . . . 76
5.4 Configuration of Pilot Signal Receiving Antennas for SPS . . . 77
5.5 Application of Digital Retrodirective Method for SPS . . . 78
5.6 Summary . . . 80

6 Conclusion **81**

List of Figures

1.1 Tethered SPS . . . 2
1.2 Construction Scenario of Tethered SPS . . . 2
1.3 Retrodirective method . . . 3
1.4 Conventional MPT methods . . . 4

2.1 Concept of SPS by Peter Glaser . . . 7
2.2 NASA Reference Model . . . 8
2.3 Sun Tower SPS . . . 9
2.4 SPS 2000 . . . 10
2.5 Different types of SPS Models . . . 11
2.6 Tesla Tower . . . 12
2.7 Goldstone Experiment . . . 13
2.8 ISY-METS . . . 14
2.9 SHARP experiment . . . 15
2.10 MILAX Experiment . . . 16
2.11 BBM Transmitting Antenna . . . 17
2.12 BBM Microwave Module . . . 17
2.13 Hardware Retrodirective Experiment . . . 18
2.14 Phased array model by Kyoto Uni . . . 19
2.15 DOA experiment by JAXA . . . 20

3.1 Software Retrodirective Method . . . 22
3.2 Phase Comparison Monopulse . . . 22
3.3 USRP . . . 24
3.4 Half Wavelength Dipole antenna . . . 25
3.5 Patch Antenna . . . 26
3.6 Array Antenna . . . 27
3.7 Phased Array Antenna . . . 28
3.8 Planar Array Antenna . . . 29
3.9 DF Setup . . . 30
3.10 2x2 dipole Antenna Array . . . 31
3.11 4x4 dipole Antenna Array . . . 31
3.12 Patch Subarray . . . 32
3.13 DF Experiment in Anechoic Chamber . . . 33
3.14 4x4 dipole Array Setup . . . 33
3.15 4x4 dipole Antenna Array on Tx Panel . . . 34
3.16 1 dipole Antenna Pattern . . . 35
3.17 Comparison of radiation pattern of 4x4 dipole Array . . . 35
3.18 Effect of 4x4 dipole Antenna Array on Tx Panel . . . 36
3.19 Checking for Degradation of AOA . . . 37
3.20 Effect of Baseline on error of AOA . . . 38
3.21 Comparison of Theory and Experimental data . . . 41

3.22 Comparison of Experiment and Approximation for Error of AOA . . . 42
3.23 Comparison of Experiment and Approximation for Standard Deviation 43
3.24 Cos Function. 45
3.25 Phase Measurement. 45
3.26 2x2 dipole Antenna Array without Deformation 47
3.27 2x2 dipole Antenna Array with 1 element Deformation 47
3.28 2x2 dipole Antenna Array with 2 element Deformation 48
3.29 2x2 dipole Antenna Array with whole antenna Deformation 49
3.30 Partial Antenna Deformation 50
3.31 Whole Array Deformation 50
3.32 Simulation for 1 element Deformation 51
3.33 Simulation for 2 element Deformation 52
3.34 Phase Change for 1 element Deformation 53
3.35 Phase Change for 2 element Deformation 53
3.36 Phase Change for whole antenna deformation 54
3.37 Error of AOA for Deformation 54

4.1 Digital Retrodirective method concept. 59
4.2 Digital Retrodirective method concept for Deformation. 59
4.3 Digital Retrodirective method algorithm. 60
4.4 Digital Retrodirective algorithm. 62
4.5 Bistatic radiation pattern measurement. 63
4.6 Digital Retrodirective method experimental setup. 64
4.7 Configuration for Refernce signal. 64
4.8 Patch subarrays with dipole antennas. 65
4.9 Forward antenna deformation configuration. 66
4.10 Backward antenna deformation configuration. 66
4.11 No deformation with Digital Retrodirective method for pilot signal from 0°. 67
4.12 No deformation with Digital Retrodirective method for pilot signal from 5°. 68
4.13 Deformation analysis for phase. 69
4.14 Probability density function of phase error. 70
4.15 Forward deformation with digital Retrodirective method. 71
4.16 Comparison of Digital Retrodirective method with REV method. . . . 72
4.17 Backward deformation with Digital Retrodirective method. 73
4.18 Comparison of no deformation and deformation case. 73

5.1 Uplink pilot SIgnal. 76
5.2 Configuration of 4x4 array for SPS. 77
5.3 Configuration of 8x8 subarray. 79
5.4 Simulation for of 8x8 deformed subarray. 79
5.5 Configuration of reference signal for large scale. 80

List of Tables

3.1 Phase Standard Deviation. 39
3.2 Error of AOA for 4x4 array. 39
3.3 Error of AOA for 2x2 array. 40
3.4 Comparison of Theory and Approximation for error of AOA. 40
3.5 Approximation for error of AOA. 42
3.6 Approximation for Phase Standard Deviation. 43
3.7 Phase data for Turntable position. 46

4.1 Root-mean square (RMS) phase error measurement.. 69

5.1 Uplink Power Estimation. 76
5.2 Array Size and Gain. 77
5.3 Uplink power with noise level. 77

List of Abbreviations

DOA	**D**irection of **A**rrival
AOA	**A**ngle of **A**rrival
DF	**D**irection **F**inding
SPS	**S**olar **P**ower **S**atellite
SSPS	**S**pace **S**olar **P**ower **S**ystem
WPT	**W**ireless **P**ower **T**ransfer
MPT	**M**icrowave **P**ower **T**ransfer

Dedicated To My Parents.

Chapter 1

Introduction

Due to issue of CO_2 emission from fossil fuels for power generation, demand for renewable energy sources is increasing and has become international concern. Among the renewable energy sources, solar arrays and wind energy are big sources to provide clean power. But these sources depend on local environment and power supply is unstable and rapidly changes. Solar Power Satellite (SPS) is an option to provide continuous clean power. SPS has been studied since 1960s and it is one of best applications of microwave power transmission (MPT). It will be installed in geostationary orbit (GEO), 36000 Km above earth. It will have 3 parts: solar energy collector, DC power to microwave converter and antenna to transmit power to ground. For solar energy collector, solar cells will be used. To convert DC power to microwave power, microwave tube or semiconductor system will be used. Large antenna array will be used to transmit higher power. SPS system also needs a ground segment to collect transmitted power from SPS. A rectenna will be used to receive microwave power and rectification will be done to convert to DC power. Then, this DC Power will go to existing power network.

Targets of research and development for SPS are as [1]:

- Technology (Transportation of large structure to outer space, construction and control, highly efficient and safe power generation, efficient microwave power transmission, operation and maintenance, etc.).
- safety (Effects on human body, atmosphere, ionized layer, aircrafts, electronic devices, etc).
- Economic Performance (cutting the cost of transportation to space, etc).

1.1 Tethered SPS

Many studies have been conducted for SPS worldwide and different models are suggested. A basic model, suggested by Japan is Tethered SPS, shown in Figure 1.1 and 1.2. Its size is 2.375 km x 2.5 km and size of subpanel is 100 m x 95 m. Area of structural unit panel is 5 m x 0.5 m and power generation and transmission module will have 0.5 m x 0.5 m size. 23.75 million modules are required for the tethered SPS. Rectenna on ground will be size of 3.5 km diameter and output power from rectenna is 1 GW [2].

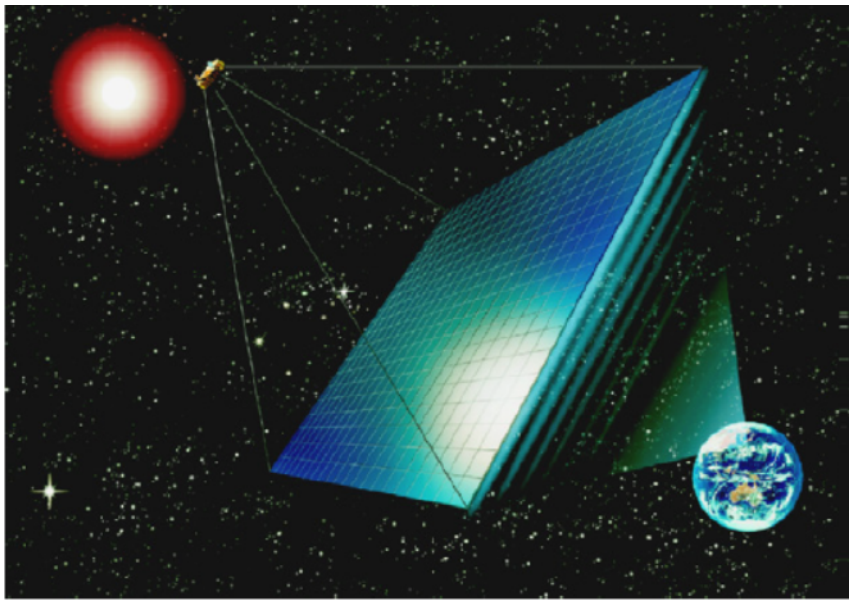

FIGURE 1.1: Tethered SPS.

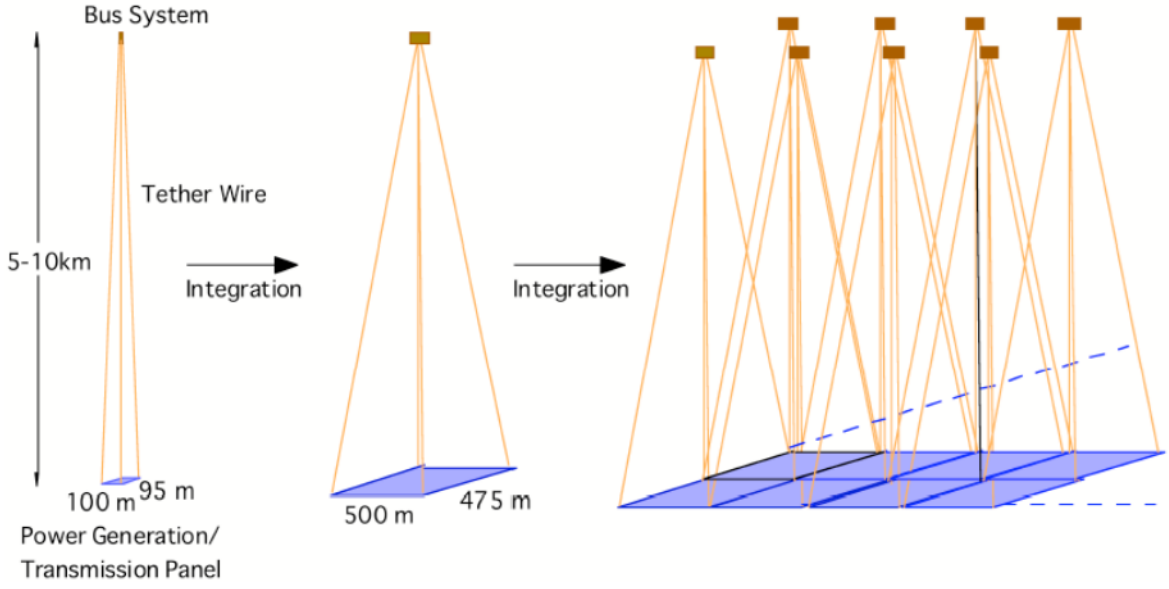

FIGURE 1.2: Construction Scenario of Tethered SPS.

1.2 Hardware Retrodirective Method

For the case of wireless power transmission, experiments have been conducted since the Nikola Tesla's experiment about wireless power transmission [2]. A lot of MPT experiments for case of SPS also have been conducted after idea of SPS was given by peter Glaser in 1960s [3-6]. Different technologies are studied to perform MPT for SPS and one of them is Hardware Retrodirective. It uses analog RF devices with phase conjugation circuit to do beamforming. Pilot signal from receiver is sent to the transmitter and then, power signal is transmitted towards location of receiver.

1.3 Direction Finding and Beam Forming Method

Direction finding and Beam Forming method, also known as software retrodirective method was proposed as alternative to hardware retrodirective method. It uses direction finding (DF) methods to detect angle of pilot signal. Experiments have been conducted with different direction of arrival (DOA) methods to do DF of pilot signal. Phased array antenna system with digital beamforming techniques is used for power transmission. With use of digital beamforming, flexibility is achieved to transmit power beam. Figure 1.3 shows a basic configuration about working of retrodirective beamforming system for SPS. Pilot signal is sent from ground location of rectenna towards SPS and then, microwave power is transmitted towards rectenna from SPS.

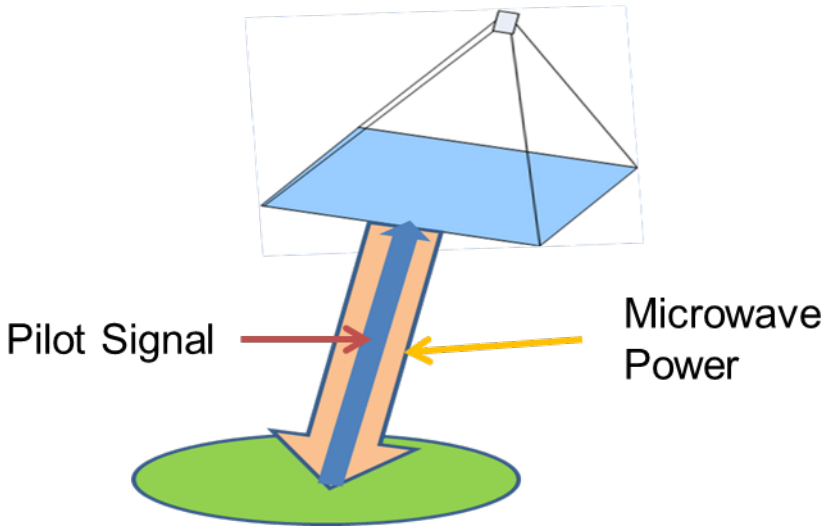

FIGURE 1.3: Retrodirective method.

1.4 Research Problem

For case of tethered SPS, required accuracy of beam forming with 10% of control error is .0005°. Beam forming includes pilot signal DF and power signal transmission, so required accuracy of DF is also .0005°.

Surface of SPS will not be flat in space due to environmental conditions, and deformation of the surface will lead to error in DF and beamforming. So, it is required to explore effect of antenna deformation for efficient power transmission.

Hardware retrodirective and DF & Beam Forming methods have been studied to solve issues of required accuracy of power transmission from SPS and to compensate effect of surface deformation in orbital motion. Figure 1.4 compares hardware retrodirective method and DF & Beam Forming method regarding microwave power transmission. Hardware Retrodirective system has difficulty to implement amplitude tapering refinements, not flexible regarding frequency and not useful for filtering the unwanted signals, etc. For DF & Beam Forming method, synchronization is required among 23.75 million antenna modules. It uses REV method to correct antenna deformation, and REV method needs several hours for processing. Uplink power in megawatts is estimated for achieving the required accuracy of power

transmission. A standard signal as reference is required for phase and frequency by hardware retrodirective method and DF & Beam Forming method.

	Hardware Retrodirective	Direction Finding and Beam forming (Software Retrodirective)
Principle	• Phase conjugation of pilot signal for power transmission	• Direction Finding by Amplitude / Phase Comparison • Beam forming with phase array antenna
Advantages	• No phase shifter for beam forming • Synchronization is not required for beam forming	• Flexible regarding beam forming • Digital beam forming techniques can be used
Issues	1. Amplitude tapering etc. refinements are difficult to use 2. Not flexible regarding frequency 3. Security function can not be used 4. Pilot signal antenna is required for each power transmitting antenna 5. Standard of Phase/frequency is required	1. Synchronization is required among 23.75 million modules 2. Correction of antenna deformation by REV method takes several hours for whole SPS 3. High uplink power of pilot signal to get required accuracy of direction finding 4. Standard of Phase/frequency is required

FIGURE 1.4: Conventional MPT methods.

1.5 Research Objective

My goal is to achieve the .0005° accuracy for power transmission and to compensate effect of antenna deformation effectively. My study objectives to achieve this goal are given below:

- Improvement of System Study of SPS with respect to required accuracy of pilot signal direction finding with less uplink power
- Estimation of antenna deformation effect on direction finding
- Development of Digital Retrodirective method with using digital signal processing (alternative to Hardware retrodirective and Direction Finding and Beam Forming)
- Deformation correction by Digital Retrodirective method

1.6 Thesis Outline

This Thesis is organized as follows: Chapter 2 is about literature review of SPS, wireless power transmission via radio waves, hardware retrodirective method and DF & Beam Forming method. Some history of previous work for models of SPS and microwave power transmission technologies is given.

Chapter 3 describes DF & Beam Forming method. Data is discussed about phase comparison monopulse method, antenna types, equations for finding error of angle of arrival, etc. Setup and results of the experiments with using array antennas and long baseline are reported. Results of experimental data are also discussed for effect of antenna deformation on DF.

Chapter 4 gives data about proposed digital retrodirective method. Algorithm for the method is discussed, and experimental results are given for evaluation of the method. Deformation experiments are performed to find effectiveness of the method.

Chapter 5 is about system study for SPS by using proposed technologies. Estimation of uplink power is done and application of digital retrodirective method for SPS is discussed.

Chapter 6 concludes the thesis by mentioning about study objective and results from the experiments.

Chapter 2

Literature Review

2.1 Solar Power Satellite

Concept of SPS was given by Peter Glaser in 1968, shown in Figure 2.1 [3]. After Glaser's idea, many research projects were conducted about designing of SPS.

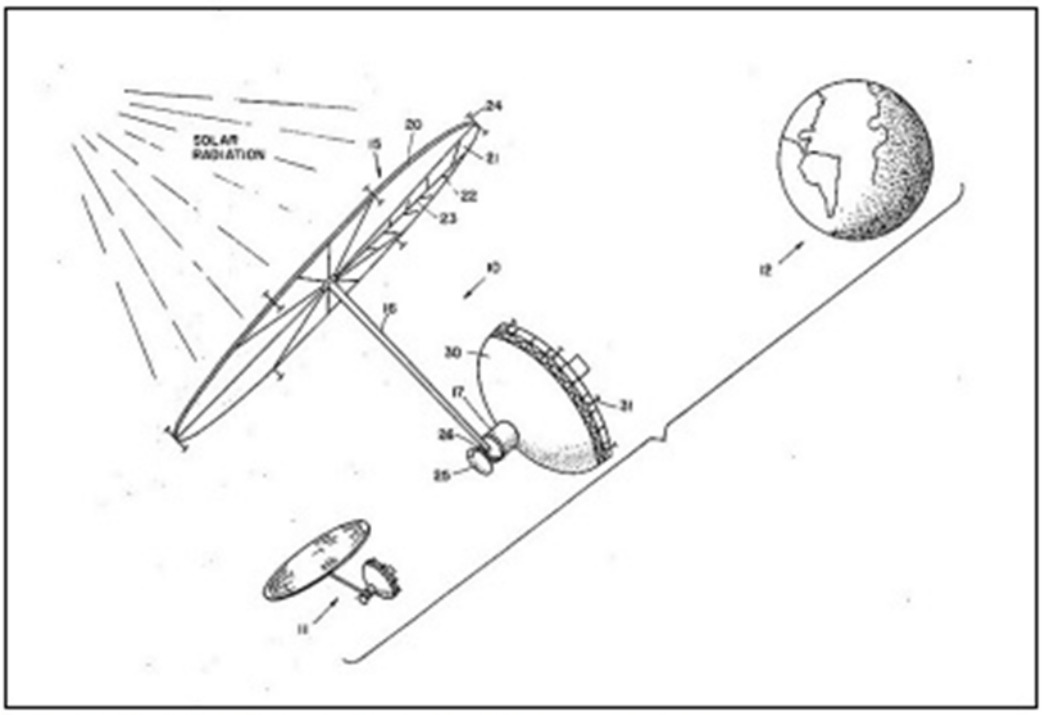

FIGURE 2.1: Concept of SPS by Peter Glaser.

A feasibility study about SPS was done by NASA/DOE in 1978-1980. A reference model was proposed by them in 1979, as shown in Figure 2.2. Transmitting power from the reference model was 6.72 GW at 2.45 GHz. Number of antenna elements in SPS was 100 million with $.75\lambda$ antenna spacing.

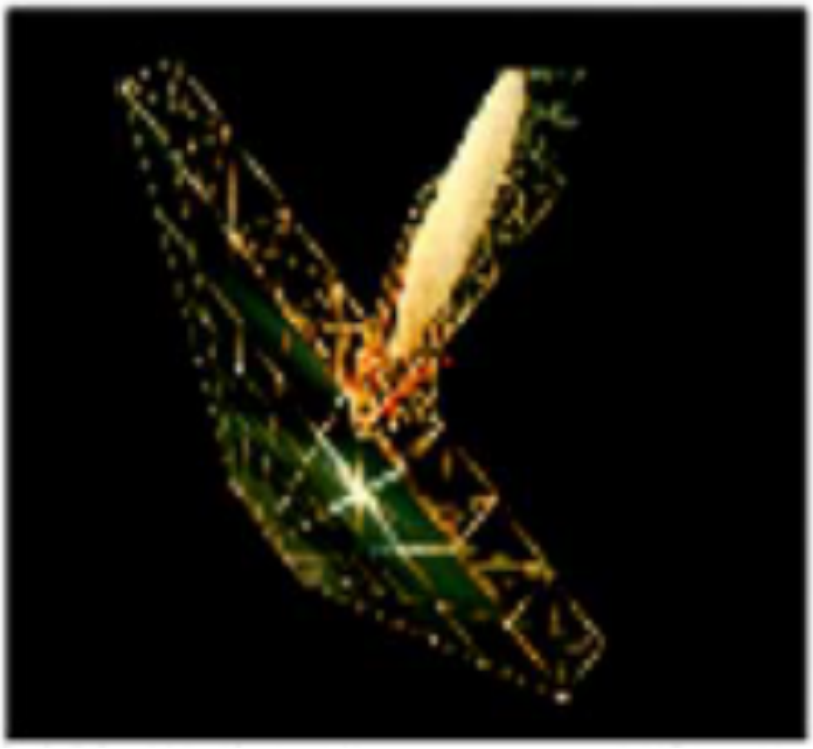

FIGURE 2.2: NASA Reference Model.

Sun Tower concept was given in 1995, shown in Figure 2.3. Power transmission level would be 200 MW with 5.8 GHz frequency. Antenna array for transmission was circular and approximately 260 m diameter [7].

In 2001, another model for SPS was proposed, named as Integrated Symmetrical Concentrator (ISC). It was having capacity of 2.1 GW.

FIGURE 2.3: Sun Tower SPS.

European space agency proposed idea of Sail Tower SPS. Transmitting power was 450 MW with 2.45 GHz. Thin film technology was proposed and new mechanisms were suggested for deployment of solar sails.

In 2011, a study was conducted by International Academy of Astronautics (IAA) and a model for SPS was proposed [7].

2.1.1 SPS in Japan

In 1992, a model of SPS was designed by New energy and Industrial Technology Development Organization (NEDO). Out pout power from SPS was 1 GW with 2.45 GHz.

SPS 2000 model was proposed by group of Institute of Space and Astronautical Sciences (ISAS) in 1993. Its shape was like triangular prism, as in Figure 2.4.

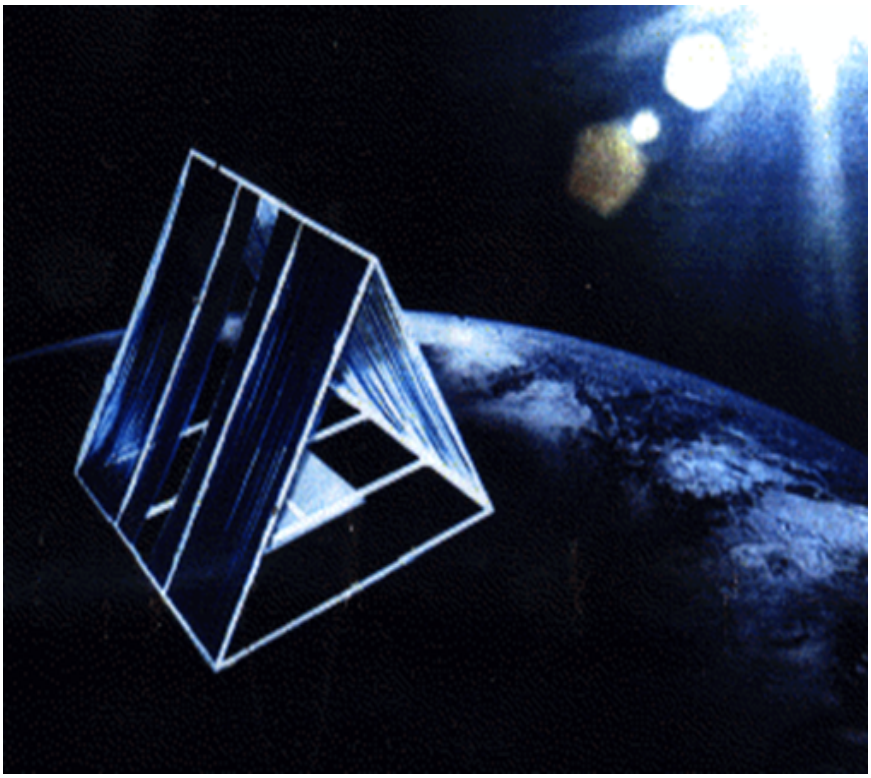

FIGURE 2.4: SPS 2000.

Japan Aerospace Exploration agency (JAXA), formally known as National Space Development Agency (NASDA) gave a model for SPS in 2001. 1 GW was output power from SPS with 5.8 GHz frequency.

Unmanned Space experiment Space Flyer (USEF) gave concept of Tethered – SPS in 2001-2002 study. Power generation/transmission panel was suspended by multi-tether.

Some concepts of SPS, discussed are shown in Figure 2.5. They are categorized by sunlight concentrating mirror and power collection, distribution [12]. For the bus power models, weight of power collection cables is extremely large. To concentrate sunlight using mirror leads to difficulties in attitude control and requires highly challenging technologies. For the Tethered-SPS, attitude control will be by gravity gradient. No mechanism like rotary joint is used to track sun, so simple configuration resolves technical difficulties in past SPS models [9].

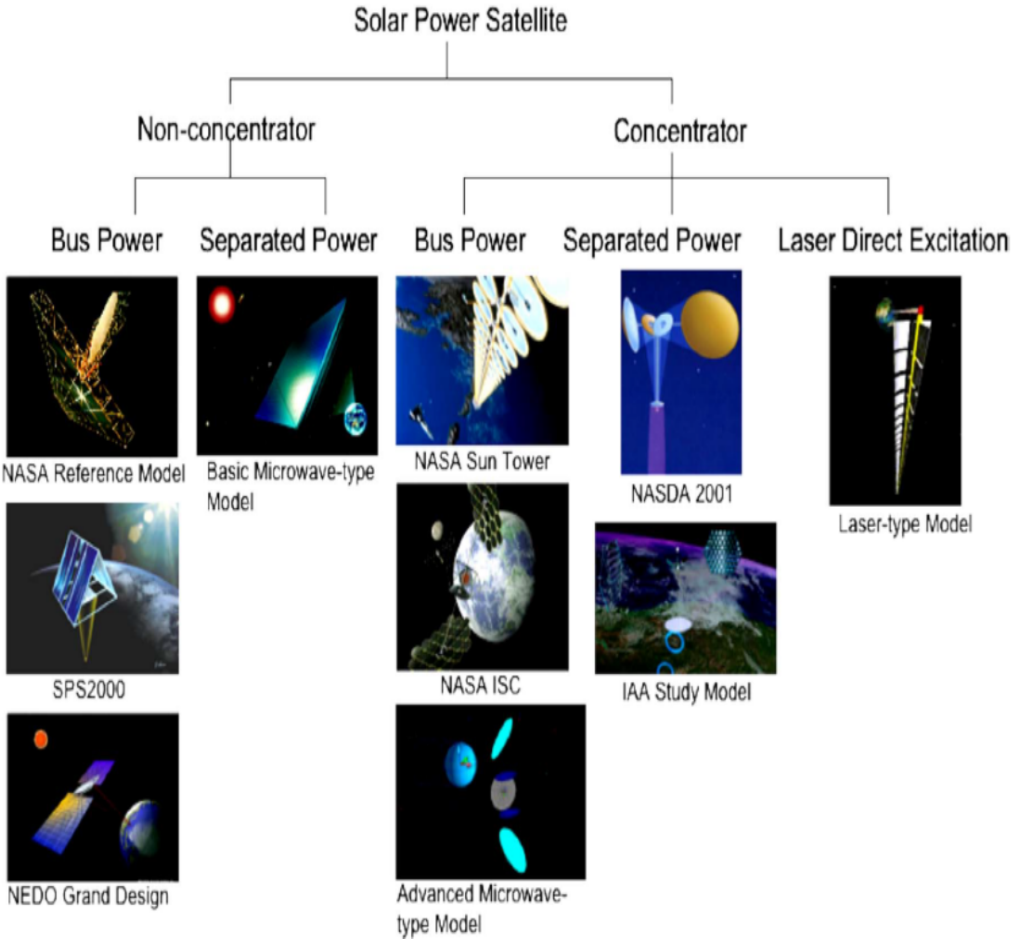

FIGURE 2.5: Different types of SPS Models.

2.2 Wireless Power Transmission towards SPS

2.2.1 19th Century

In 1864, prediction for existence of radiowaves was given by James C. Maxwell. In 1884, John H. Poynting identified role of poynting vector for calculating electromagnetic energy. Heinrich Hertz was firstly successful in 1881 to show evidence of radiowaves experimentally. Spark-gap radio transmitter was used by him [2].

1n 1899, Nikola Tesla carried out first WPT experiment by using Tesla Tower. Tesla tower, as shown in Figure 2.6, was a coil connected to 200 ft high mast with 3 ft diameter ball at its top. Tesla fed 300 kw to coil and resonant frequency was 150 KHz. Voltage at radio frequency at top sphere reached 100 MV. Experiment failed because transmitted power was diffused in all directions with wavelength of 21 km. After this WPT trial, area of radiowaves was dominated by wireless communication and remote sensing [2].

FIGURE 2.6: Tesla Tower.

2.2.2 20th Century

To work for transmitted power and to increase transmission efficiency, a higher frequency than that used by Tesla is needed. 1n 1930, by invention of magnetron and klystron, progress was made to get high power microwaves. With development of radar technology after world war II, high power microwave generating devices were advance.

1n 1960, W.C. Brown developed a rectifying antenna, called as "Rectenna" to convert microwave to dc. With the rectenna, Brown did MPT to a wired helicopter in 1964 and to a flying helicopter in 1968. In 1970, Brown did Mashall Space Flight Center tests to increase total DC-RF and RF-DC efficiency with 2.45 GHz radiowaves. DC-DC efficiency was 26.5% with output of 39 WDC. DC-DC efficiency was increased upto 54% in 1975 with output of 495 WDC by magnetron of Raytheon Laboratory [2]. P.E Glaser proposed idea of Solar Power Satellite (SPS) in 1968 [3].

At JPL Goldstone facility, MPT experiment was performed by Brown and Richard Dickinson in 1975, depicted in Figure 2.7. Transmitted power was 450 kw with 2.388 GHz and parabolic antenna of 26 was used as transmitter. Size of rectenna array was 3.4 m x 7.2 m. Distance between transmitter and rectenna was 1.6 km and 30 KWDC power was received [10].

FIGURE 2.7: Goldstone Experiment.

In 1983, MPT rocket experiment was performed by Hiroshi Matsumoto's group in Japan. Name of experiment was microwave Ionosphere Nonlinear interaction experiment (MINIX). Focus of this experiment was to evaluate interaction of microwave and ionosphere plasma. Another MPT rocket experiment, called International Space Year-Microwave Energy Transmission (ISY-METS) was conducted in 1993, shown in Figure 2.8. Transmitting antenna for MINIX was truncated waveguide and for ISY-METS, phased array antenna was used to control beam direction. 2.45 GHz frequency was used for transmitted signal [11].

FIGURE 2.8: ISY-METS.

Some MPT experiments were performed around 1990s for SPS and other applications of MPT. 1n 1987, stationary high altitude relay platform (SHARP) experiment was carried out by Canada to transfer microwave to a fuel free airplane, shown in Figure 2.9. 10 KW signal with 2.45 GHz was transmitted to airplane flying 150 m above ground level. Parabolic antenna was used to transmit beam [11].

FIGURE 2.9: SHARP experiment.

Figure 2.10 shows Microwave lifted Airplane experiment (MILAX), conducted by Japan in 1992. Phased array antenna with 4-b digital phase shifters was used to steer beam toward flying plane [10]. Transmitter was installed on roof of a car and car was driven under airplane. 1.25 kW power with 2.411 was sent and received dc power by rectenna was 88 W. In 1995, another experiment by japan was done to flying airship, named as Energy transmission toward High-altitude long endurance airship Experiment (ETHER). 2.45 GHz signal with 10 Kw power was sent by parabolic antenna to flying airship, 35-45m above ground. Ground to ground MPT experiment was also conducted by japan with 2.45 GHz in 1994-1995 [2].

FIGURE 2.10: MILAX Experiment.

2.2.3 21th Century

In 2000, Solar Power Radio Integrated Transmitter (SPRITZ) MPT system was made by Japan. Purpose of this system was to develop high efficient phased array for SPS applications. Solar cell panel, microwave generator, transmitting antenna and rectenna array were installed together in one package. Frequency of transmitting beam was 5.77 GHz and beam was steered by 3-b phase shifter [8].

Hawaii experiment was carried out by coordination of Japan and USA in 2008. Phased array transmitting antenna was used and 20 W power was sent. Target was 150km away from transmitter [10].

In 2010, Kyoto university and Mitsubishi Electric developed novel phased array for SPS. 5.8 GHz frequency was used for transmitting beam. 256 antenna elements were used in phased array and 5-b phase shifter was used. Output power from the array was 1.5 kW and Class-F amplifiers with GAN FETs was used to generate beam [10].

In 2012, a breadboard model (BBM) was developed by JAXA for MPT experiment from space to ground. 64 sub-arrays of microstrip patch antennas were used and output power was 160 w. 16 microwave modules were used, having 6-bit phase shifter, pre-amplifier and power amplifier, shown in Figures 2.11 and 2.12 [13].

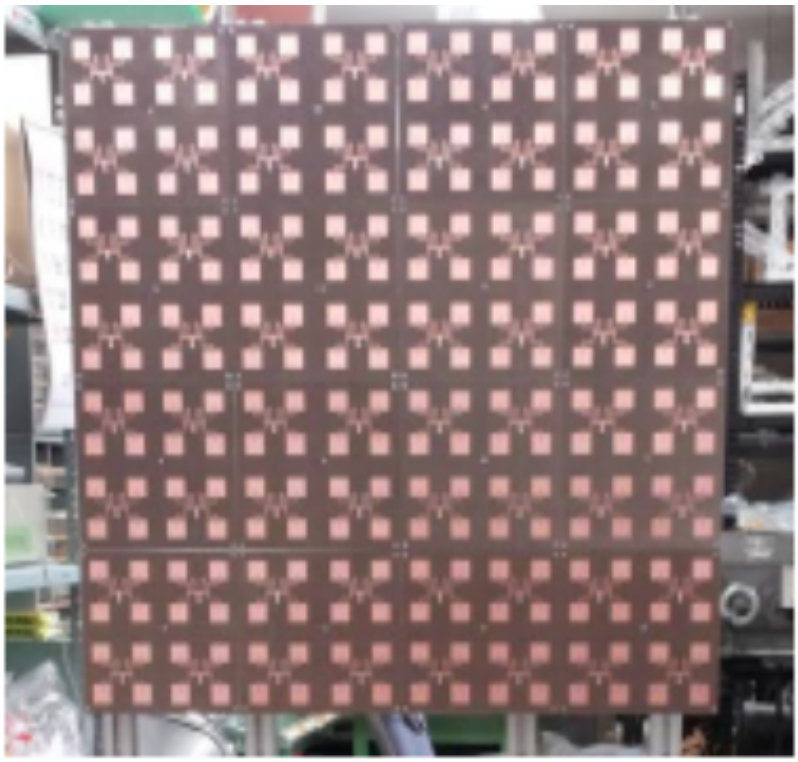

FIGURE 2.11: BBM Transmitting Antenna.

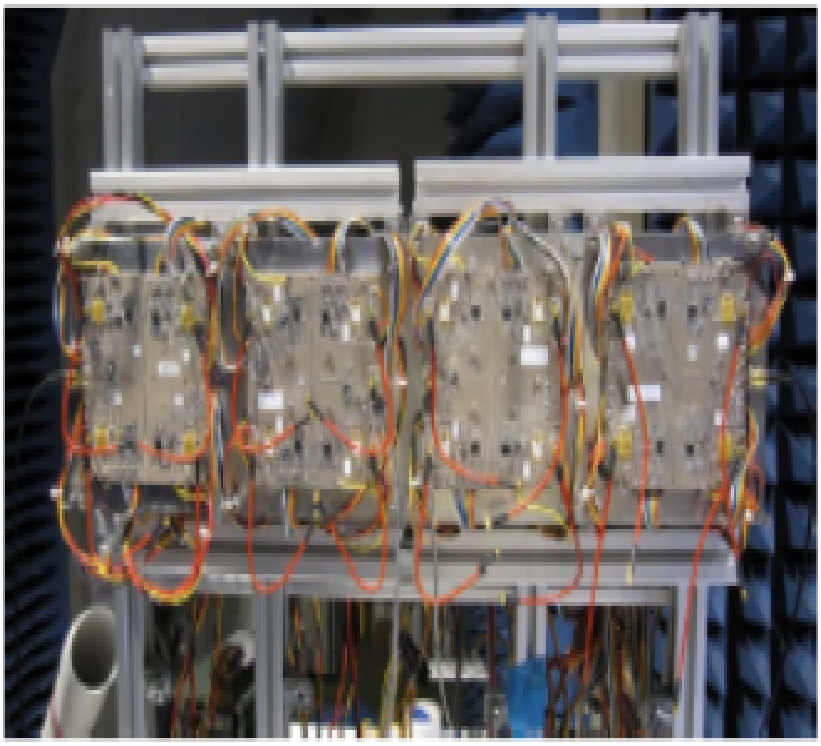

FIGURE 2.12: BBM Microwave Module.

2.3 Hardware Retrodirective System

In 1987, a retrodirective system, shown in Figure 2.13, was developed by Kyoto university and Mitsubishi Electric with using two asymmetric pilot signals for phase conjugate circuit. In conventional retrodirective system, same frequency was used for pilot signal and transmitting microwave. So, there was a problem of interference between pilot signal and transmitted signal. Therefore, it was proposed to use two asymmetric pilot signals. Frequency was 2.45 GHz and seven dipole antennas were used to transmit signal in direction of incoming pilot signals [10].

FIGURE 2.13: Hardware Retrodirective Experiment.

Kyoto university and Nissan Motor Company developed another retrodirective system in 1995, with using a pilot signal being one third of transmitting frequency. Frequency of transmitted signal was 2.45 GHz and that of pilot signal was 817 MHz. On both sides of transmitting antenna, pilot signal receiving antenna were placed [12].

In 2003, a PLL-heterodyne retrodirective system was developed by Mitsubishi electric and USEF SPS Study team [10]. Transfer frequency was 5.77 GHz and pilot signal frequency was 3.884 GHz. A successful retrodirective MPT experiment was performed from rocket to ground by Kobe University, ISAS, ESA in 2006 [2].

2.4 Direction Finding and Beam Forming Method

Kyoto university group suggested DF & Beam forming method (software retrodirective method) for outdoor MPT experiment and SPS. Conventional retrodirective system was hardware system with using analog phase conjugate circuits. Hardware system was complex and not flexible regarding frequency [14,15]. Flexible beam forming was also possible by software retrodirective system. An experiment was performed by the group and error of DOA estimation was less than 1.2 ° [16].

Novel phased array system by Kyoto university and Mitsubishi, depicted in Figure 2.14, used software retrodirective method for beam controlling. Amplitude monopulse method was used to detect direction of pilot signal. Frequency of pilot signal was 2.45 GHz. Accuracy of DF was 0.4 ° RMS [10].

FIGURE 2.14: Phased array model by Kyoto Uni.

An experiment was performed by JAXA for DF of pilot signal, shown in Figure 2.15. Phase comparison monopulse method and amplitude comparison method were used for DF. An array of two antenna elements was used with baseline of 1m and 5 m. Gain of the antenna elements was 6 dBi. Estimation of uplink power and noise level was done to achieve .0005° accuracy. It was suggested that 1 MW of uplink power with -110 dBm of noise level is required for 5m baseline to achieve required accuracy [17].

Another experiment was performed by JAXA with phased array antenna system for microwave power transmission. Gain of pilot signal receiving antennas was 5 dBi, baseline was 0.2 m and -140 dBm noise level was required with 1 MW uplink power for .0005° accuracy of direction finding [18].

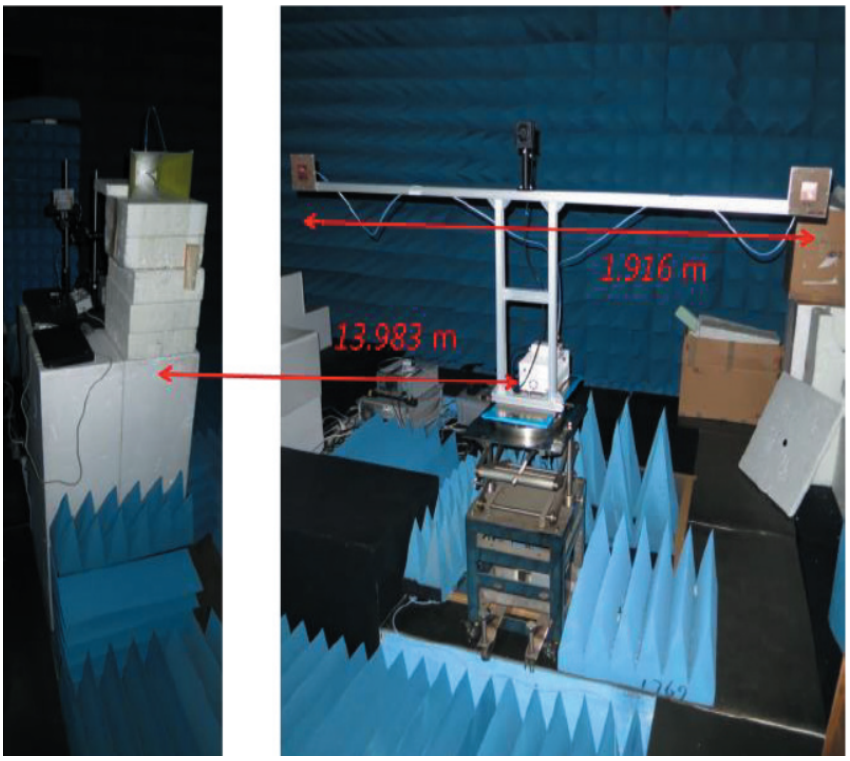

FIGURE 2.15: DOA experiment by JAXA.

Chapter 3

Precise Direction Finding

3.1 Introduction

For case of tethered SPS, required accuracy of beam forming with 10% of control error is .0005°[15,17,19]. Hardware Retrodirective system has been studied initially for purpose of microwave power transmission. It is difficult to implement amplitude tapering refinements, etc. and this method is also not flexible regarding frequency[14,15]. Direction Finding and Beam Forming method (Software retrodirective method) was proposed as alternative to Hardware Retrodirective method [14].

Direction Finding and Beam Forming method requires high uplink power of pilot signal for direction finding. With 6 dBi gain of pilot signal receiving antenna and using baseline of 5 m, 1 MW uplink power with -110 dBm noise level is required [17]. For purpose of DF with Direction Finding and Beam Forming method, phase comparison monopulse and amplitude comparison monopulse have been studied. Accuracy of Phase comparison monopulse is higher than that of Amplitude comparison monopulse [20-22].

There is a concern of antenna deformation due to space environmental conditions[23-25]. Some studies have been done to evaluate the effect for microwave power transmission. Cases of antenna deformation are evaluated regarding accuracy of power transmission[23,25-26]. There is a need to do study for evaluation of effect of antenna deformation on direction finding.

In Chapter 3, I did experiments with using phase comparison monopulse method. Array antennas with long baseline were used to increase accuracy with less uplink power. Effect of antenna deformation was also considered with using different cases of antenna deformation.

3.2 Phase comparison monopulse

Figure 3.1 represents concept of DF & Beam forming method. A pilot signal is sent from rectenna location and received by antennas, installed on transmitter. DOA of pilot signal is found by DF methods and then information of DF is sent to Phased array equipment of the transmitter. Phase shifters are used to change the transmitting beam direction. Beam is transmitted depending on the DF of the received pilot signal.

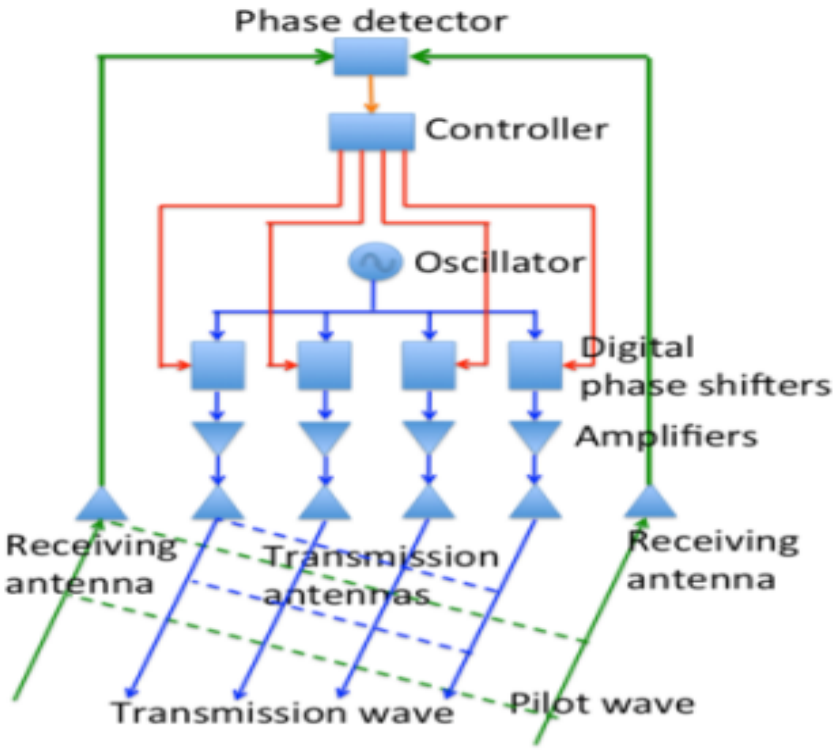

FIGURE 3.1: Software Retrodirective Method.

Figure 3.2 represents basic configuration of phase comparison monopulse method. A signal is sent from a target and received by separated antennas. Minimum requirement of receiving antennas is to have two antennas.

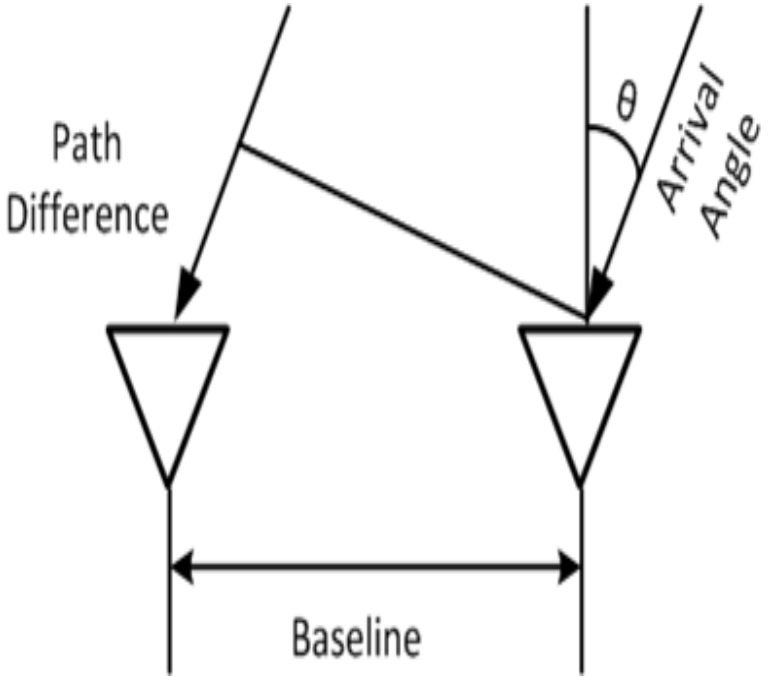

FIGURE 3.2: Phase Comparison Monopulse.

Path difference (Δx) in Figure 3.2 is calculated by Eq. (3.1) and then, phase difference ($\Delta\phi$) by Eq. (3.2). d is baseline and θ is angle of arrival (AOA).

$$\Delta x = d \sin\theta \tag{3.1}$$

$$\Delta\phi = \frac{2\pi d \sin\theta}{\lambda} \tag{3.2}$$

If we know the phase difference between two antennas, then AOA can be found by following Eq. (3.3).

$$\theta = \sin^{-1} \frac{\lambda\Delta\phi}{2\pi d} \tag{3.3}$$

Eq. (3.4) is about error of AOA and it depends on signal to noise ratio (SNR), baseline and angle of arrival.

$$\Delta\theta = \frac{\lambda}{\pi d \cos\theta \sqrt{SNR}} \tag{3.4}$$

For standard deviation of phase difference ($\sigma\phi$), error of AOA can be found, as in Eq. (3.5).

$$\Delta\theta = \sin^{-1} \frac{\lambda\sigma\phi}{2\pi d} \tag{3.5}$$

3.3 USRP

Universal Software Radio Peripheral (USRP) is a software defined radio hardware system. Received signals by antennas are fed to USRP. Motherboard of USRP provides following subsystem: Low noise amplifier (LNA), Phase-locked loop (PLL), Mixer and ADC. Figure 3.3 shows basic configuration of a USRP. Analog signal is converted to I and Q data and then digital signal processing is performed.

USRP is connected with personal computer and controlled by software like GNU Radio and Labview, etc. These software use signal processing blocks for implementation of signal processing functions.

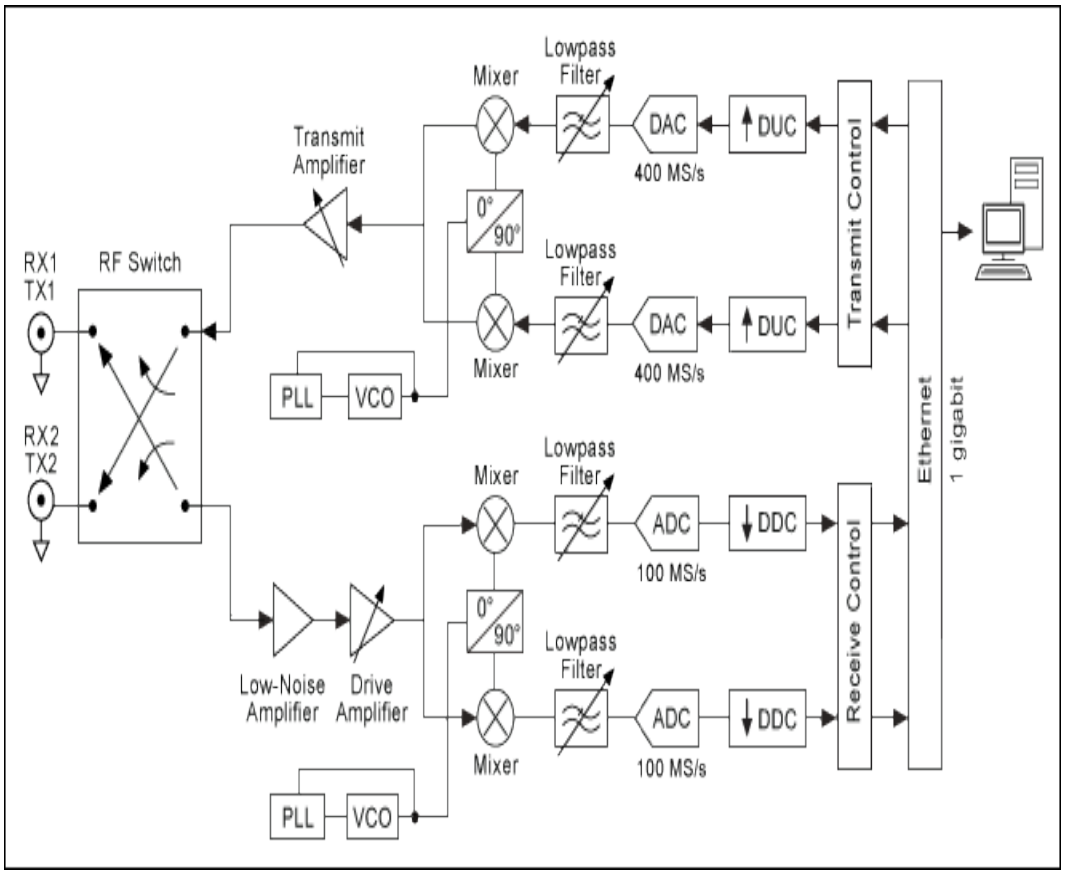

FIGURE 3.3: USRP.

3.4 Antenna

It is a metallic device to receive or radiate radio waves. It is a transitional structure between free space and guiding waves. Guiding device or transmission line can be in the form of coaxial cable or waveguide etc.

There are different types of antenna like wire antenna, Aperture antenna, Microstrip antenna and array antenna etc.

3.4.1 Half Wavelength Dipole antenna

It is type of wire antenna and its length is equal to half of wavelength, as in Figure 3.4. It has identical two conductive elements of metal wire or rod. Each side of feed line is connected with one conductor of dipole. Gain of half wavelength dipole antenna is 2.15 dBi.

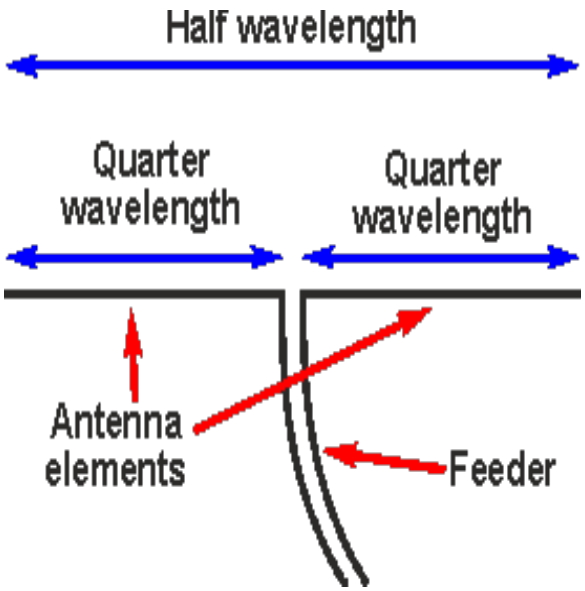

FIGURE 3.4: Half Wavelength Dipole antenna.

3.4.2 Microstrip Patch antenna

This antenna is printed directly on circuit board. It is low profile, conformable to planar and nonplanar surfaces. It is easy and cheap to manufacture patch antenna with prtinted circuit technology. Feed is given by microstrip transmission line. Patch antenna, transmission line and ground plane are made of high conductivity metal, as in Figure 3.5.

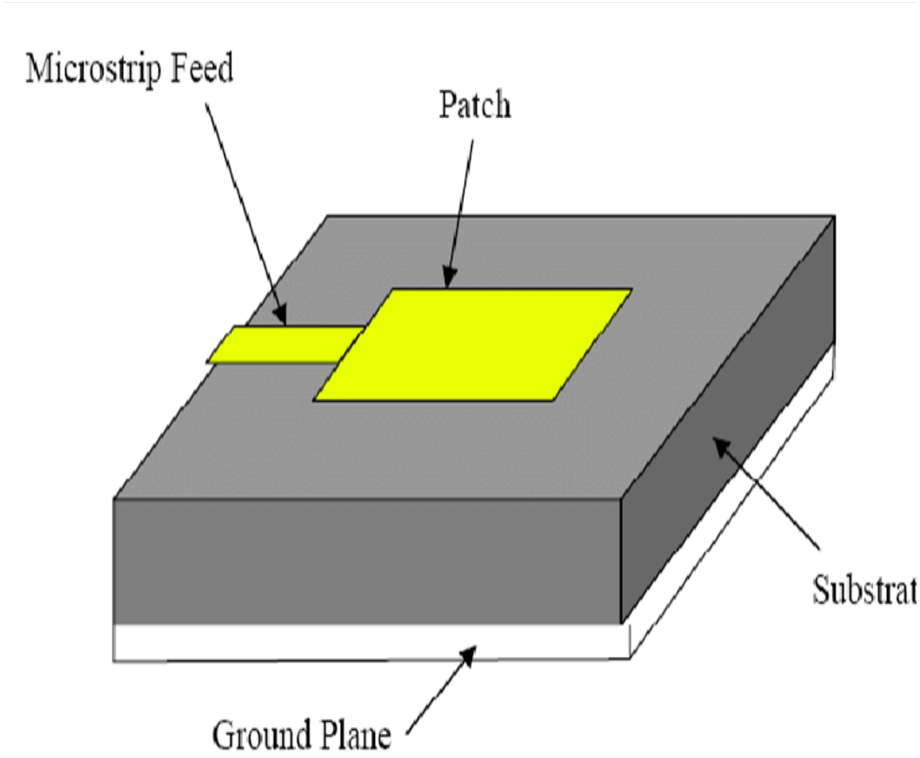

FIGURE 3.5: Patch Antenna.

3.4.3 Array antenna

It has multi elements, which are connected together. All antennas work together, being one antenna. Commonly, same antenna elements are used in an array. Antenna elements are connected to transmitter or receiver through feed line and there is a relationship of phase between elements. Radiowave transferred by each element interfere constructively in desired direction to radiate high power.

With using array antenna, gain is high and beam is narrow as compared to that of individual element. Larger the number of antenna, larger the gain band and beam will be narrower. Electric field is calculated by product of array factor and electric field of single element. Array factor is function of geometry of array and excitation phase. Figure 3.6 shows array of patch antenna. Planar array and phased array are some of types of array antenna.

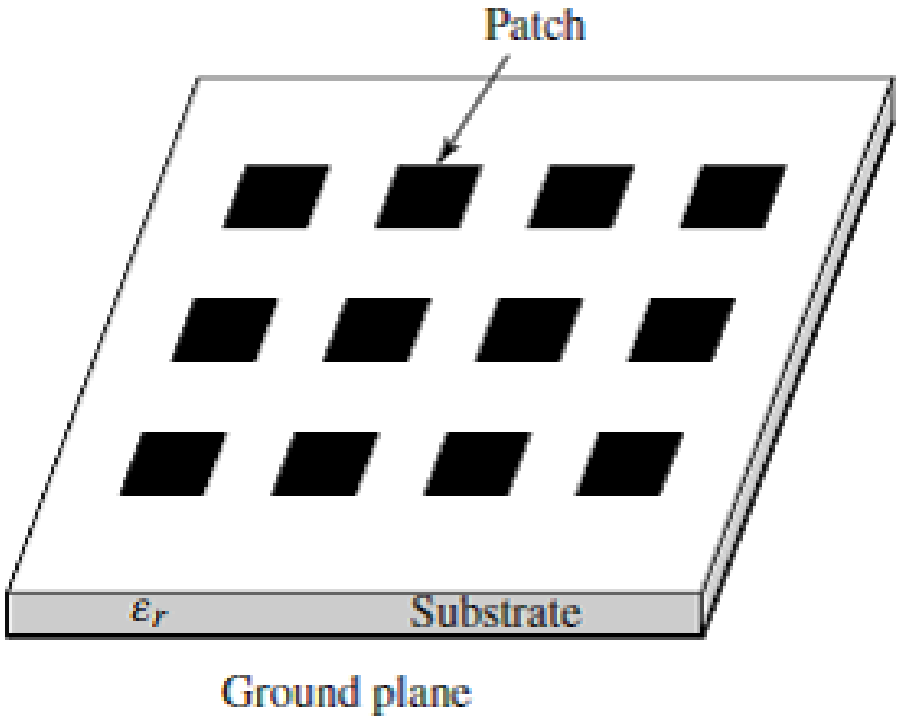

FIGURE 3.6: Array Antenna.

3.4.4 Phased Array

It is also known as scanning array to scan the radiated beam electronically in desired direction. This can transmit beam in any direction without moving the antenna. Progressive phase shift between elements is controlled by phase shifters and maximum radiation is transferred in any direction, shown in Figure 3.7.

Phase shift is controlled by using phase shifters. Different types of phase shifters are used like, ferrite or diode phase shifters. Active phased arrays use amplification with phase shift for scanning beam.

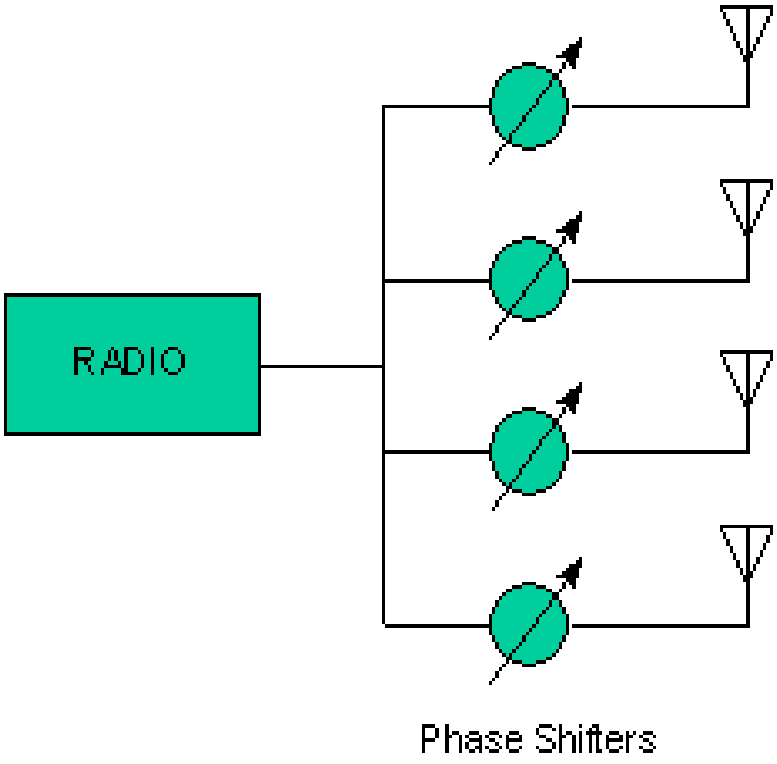

FIGURE 3.7: Phased Array Antenna.

3.4.5 Planar Array

In Planar array, antenna elements are positioned in form of rectangular grid. Planar array has more variables which can be used to control and shape the pattern. it can be used to scan the beam in any direction. Applications of planar arrays are tracking radar, search radar, remote sensing, communication, etc. Geometry of planar array is shown in Figure 3.8.

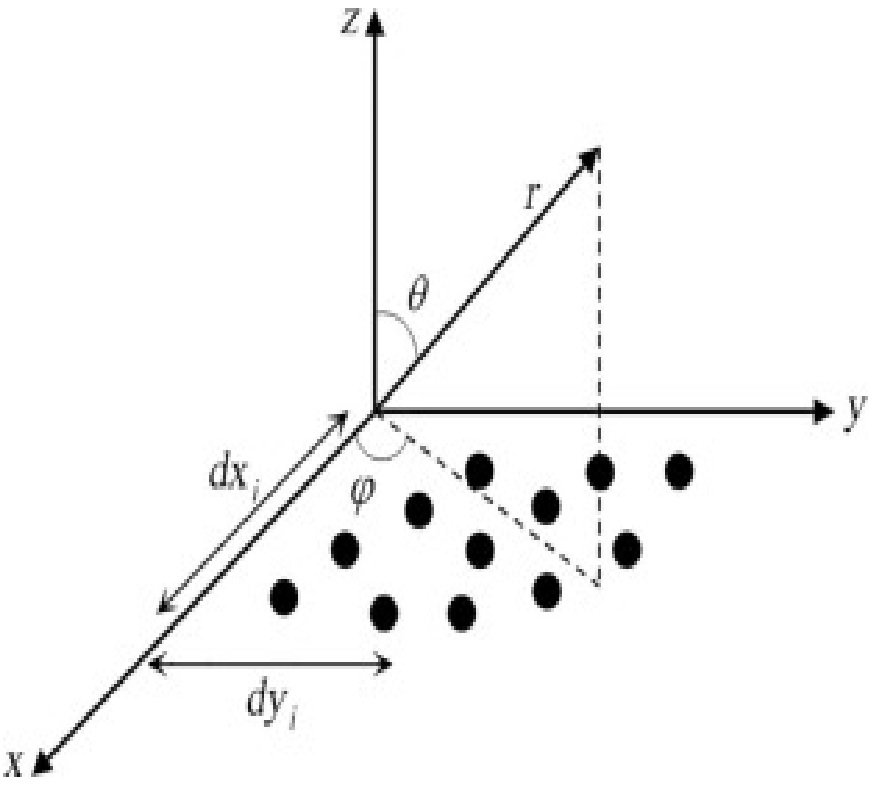

FIGURE 3.8: Planar Array Antenna.

3.5 DF with Array Antenna

With using phase comparison monopulse method, DF experiment was performed. Phase difference of pilot signal was found with using array antennas. Comparison was done for degradation of angle of arrival among 1 dipole, 2x2 and 3x3 array of dipole antennas. 4x4 and 2x2 array antennas were used to measure standard deviation of phase and error of AOA with changing SNR level. Effect of SNR and baseline was considered for antenna arrays. Proposed design for DF experimnetal setup is shown in Figure 3.9. Pilot signal is transmitted by Tx antenna and received by Rx1 and Rx2 array antennas. Phase measurement is performed for DF with signals received by Rx1 and Rx2.

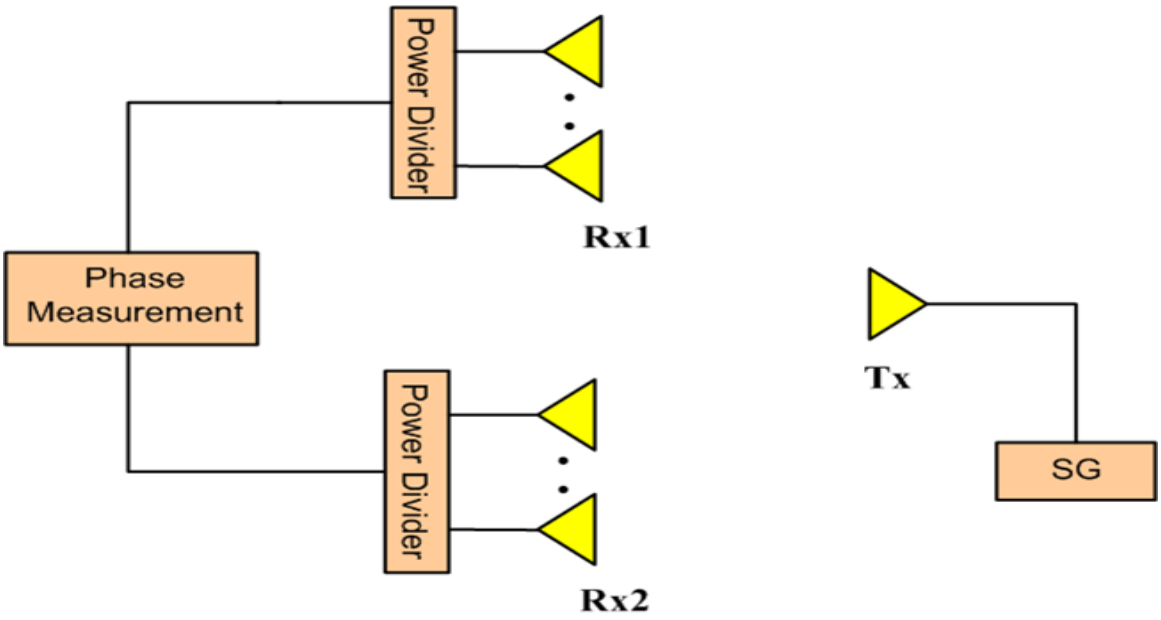

FIGURE 3.9: DF Setup.

3.5.1 Simulation Setup of Antennas

Half wavelength dipole antennas were designed with frequency of 2.45 GHz in CST. Antennas were placed on Aluminum sheet. Radiation pattern of antennas were found. Setup in CST for of 2x2 and 4x4 array antennas is shown in Figures 3.10 and 3.11. Patch subarray simulation model is shown in Figure 3.12

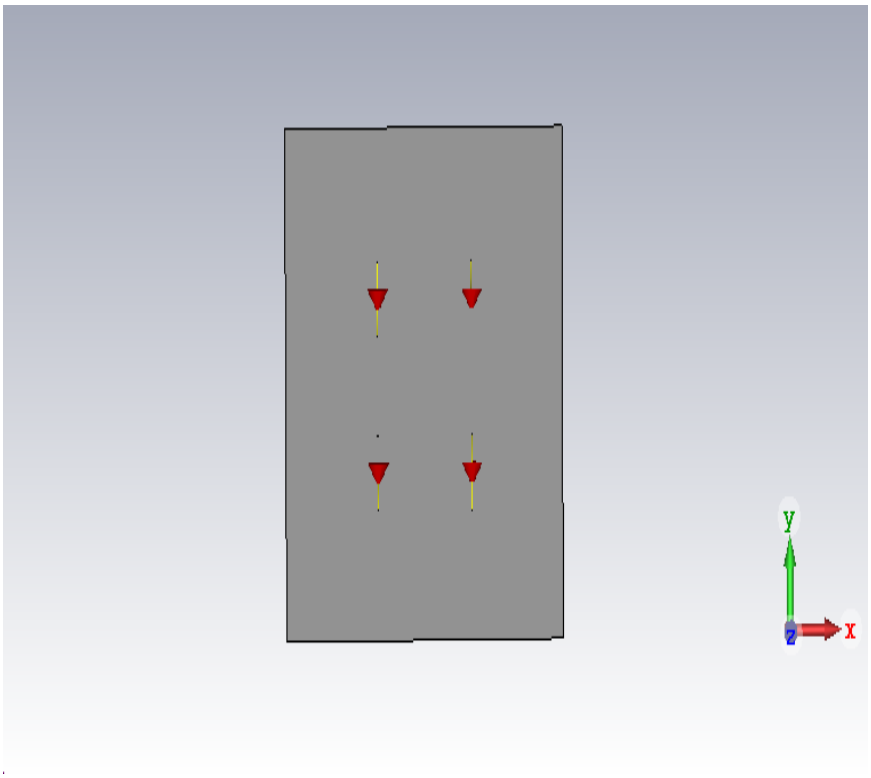

FIGURE 3.10: 2x2 dipole Antenna Array.

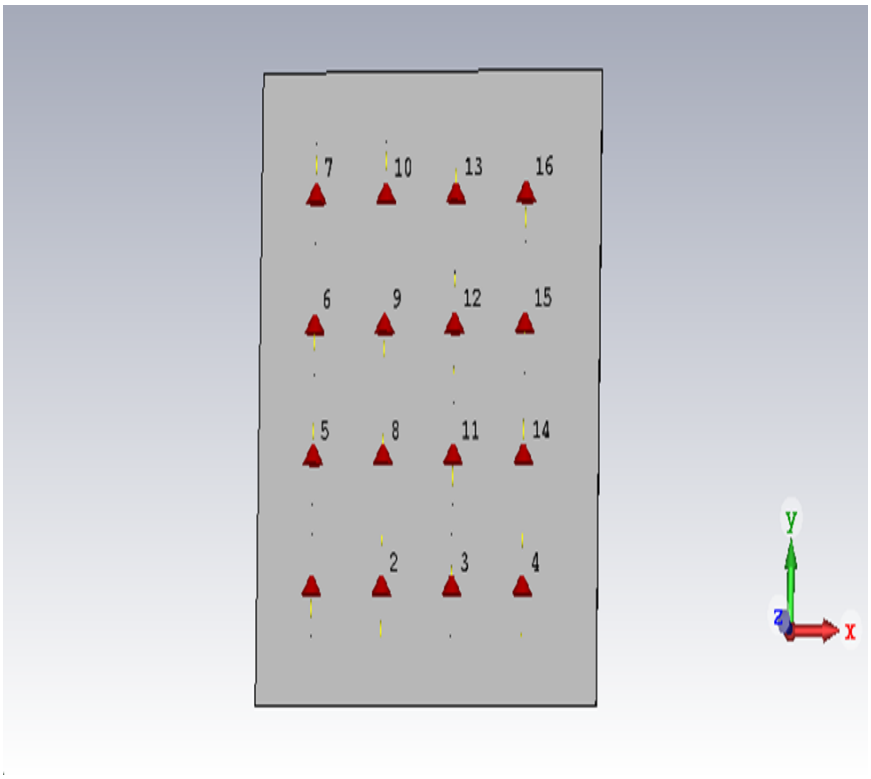

FIGURE 3.11: 4x4 dipole Antenna Array.

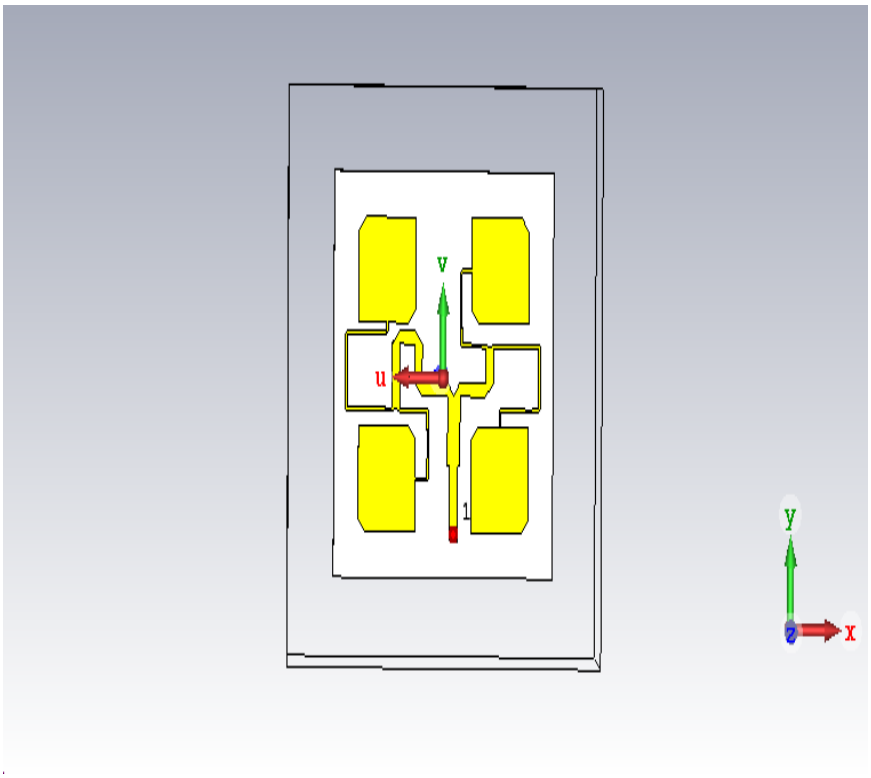

FIGURE 3.12: Patch Subarray.

3.5.2 Experimental setup for DF

Configuration of receiving antennas for DF is shown in Figure 3.13. Degradation of angle of arrival experiment was performed with 1-element, 2x2 array and 3x3 array. 2x2 and 4x4 array were used for DF Experiment with long baseline.

USRP 2945 was used to receive signals from pilot signal receiving antennas and perform phase measurement. Resolution of ADC for USRP 2945 was 14 bit [27]. Accuracy of turntable in anchenoic chamber was .05°. Phase difference between antennas for received pilot signal was calculated by Labview. Transmitted power was changed from 10 dBm to -30 dBm and received power was measured. Value of SNR for the setup was -80 dBm. Baseline of 5m, 2.5 m and 1 m were used. Figure 3.14 and 3.15 shows 4x4 array, installed on AL-panel and on Tx 8x8 subarray panel. Tx subarray panel was used as breadboard model (BBM) for MPT experiments.

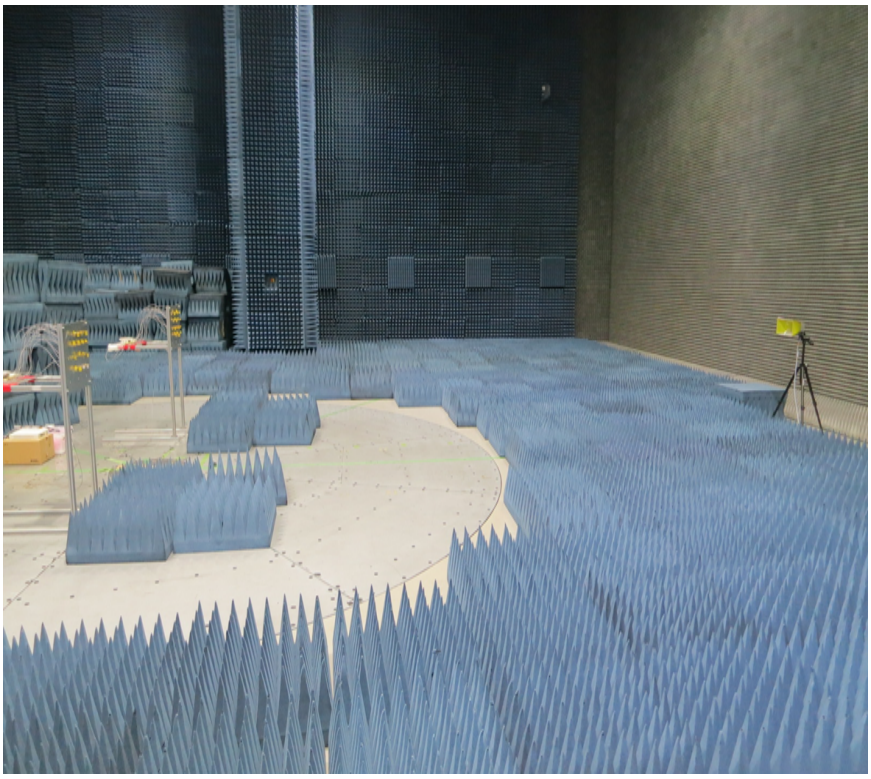

FIGURE 3.13: DF Experiment in Anechoic Chamber.

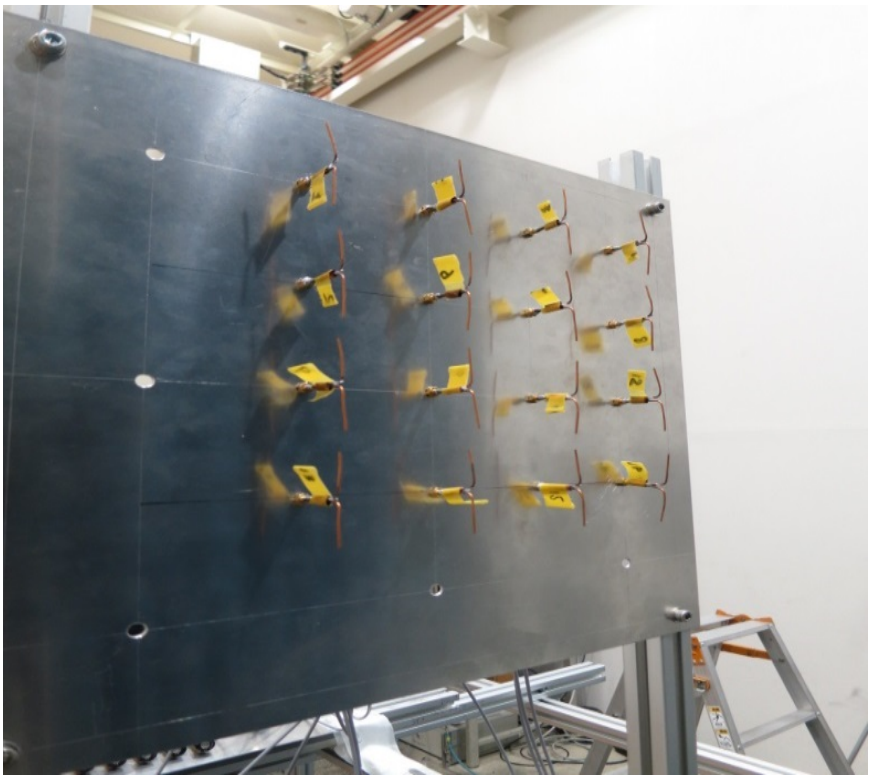

FIGURE 3.14: 4x4 dipole Array Setup.

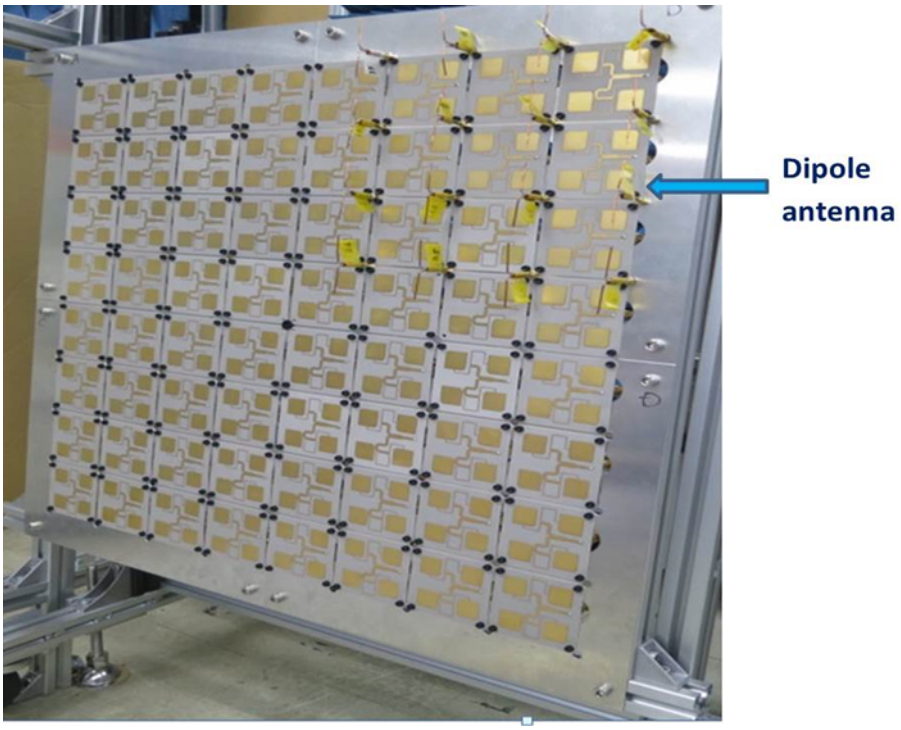

FIGURE 3.15: 4x4 dipole Antenna Array on Tx Panel.

3.5.3 Results and Discussion

Radiation Pattern of Antenna

Radiation patterns of 1 dipole and 4x4 array are shown in Figure 3.16 and 3.17. Pattern for 4x4 array compares when the array is installed on AL-frame and on BBM, and both radiation patterns are in good agreement. Radiation patterns of Tx panel is shown in Figure 3.18. It depicts the effect of installing dipole array antenna on transmitting array antenna. It can be observed that effect of dipole array is minimal on Tx panel.

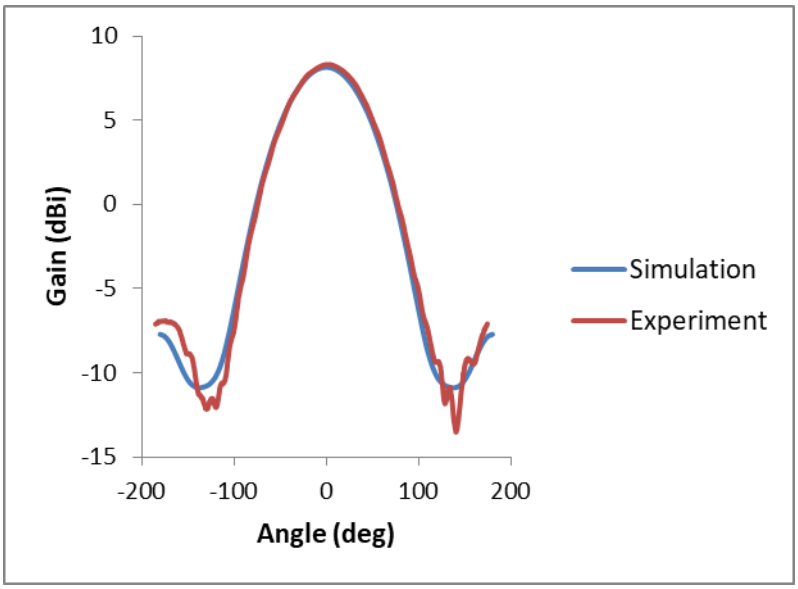

FIGURE 3.16: 1 dipole Antenna Pattern.

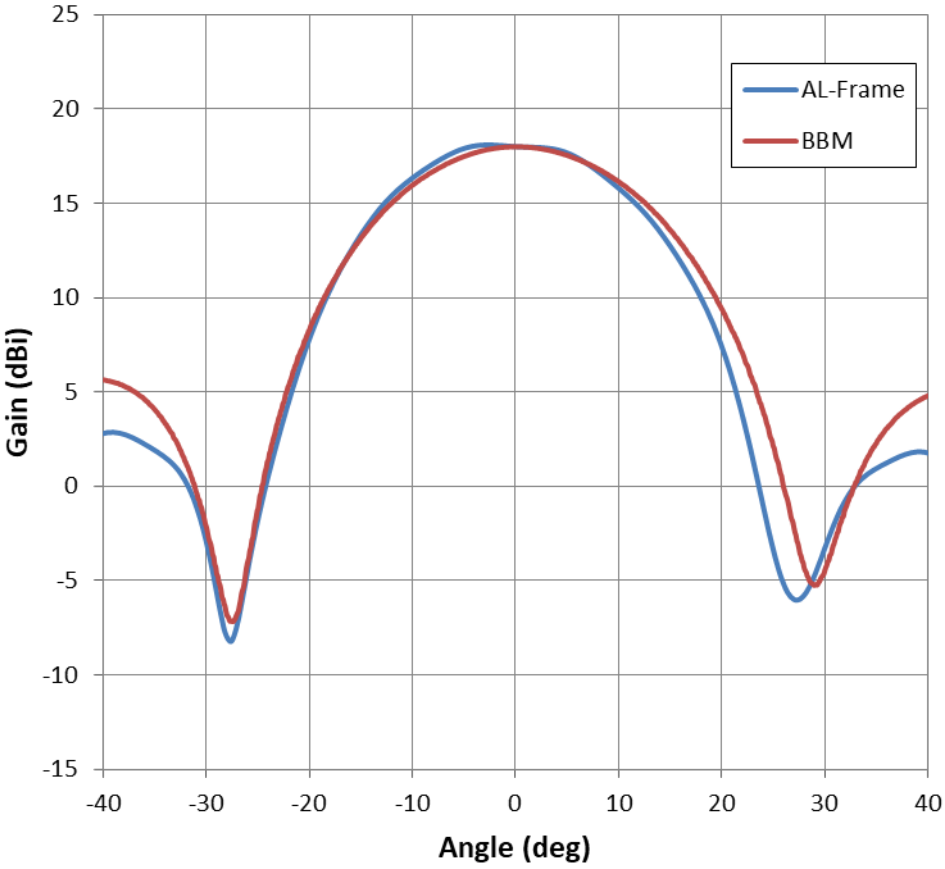

FIGURE 3.17: Comparison of radiation pattern of 4x4 dipole Array.

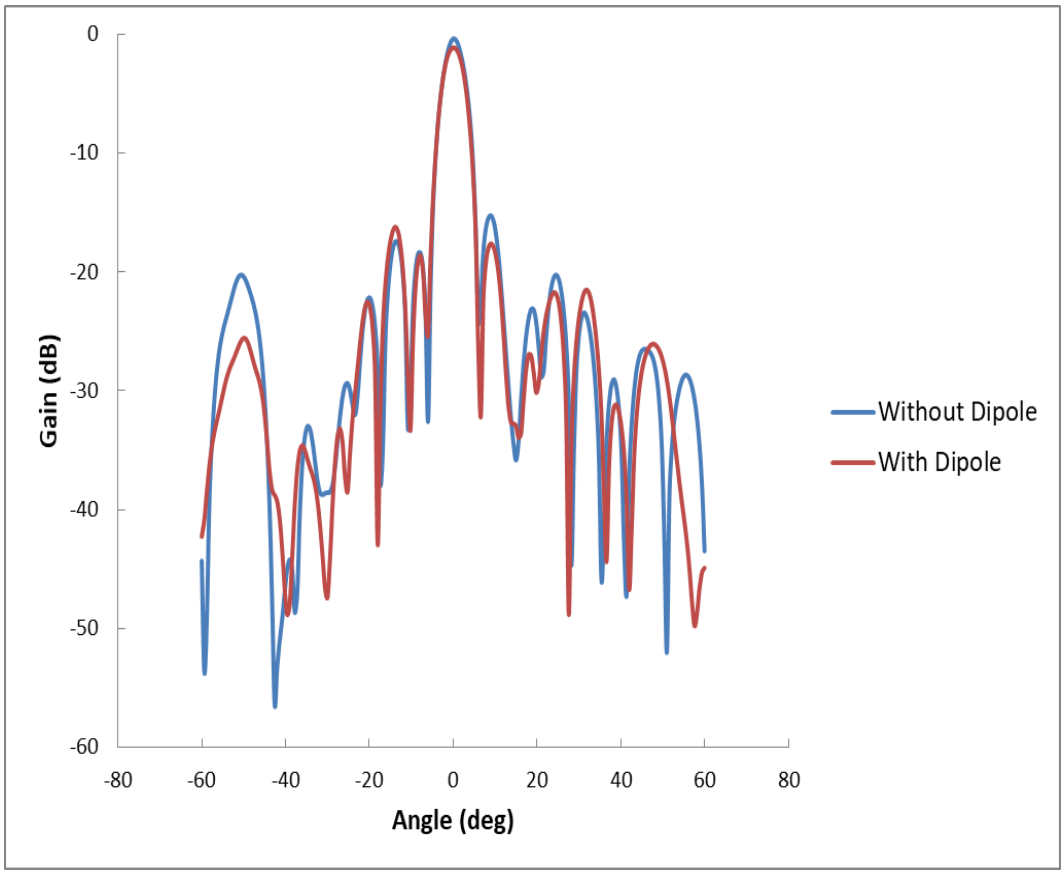

FIGURE 3.18: Effect of 4x4 dipole Antenna Array on Tx Panel.

Analysis for Degradation of AOA

Error of AOA was measured with 1 element, 2x2 array and 3x3 array of dipole antenna for same SNR values and it is shown in Figure 3.19 that same behavior was experienced among all antennas.

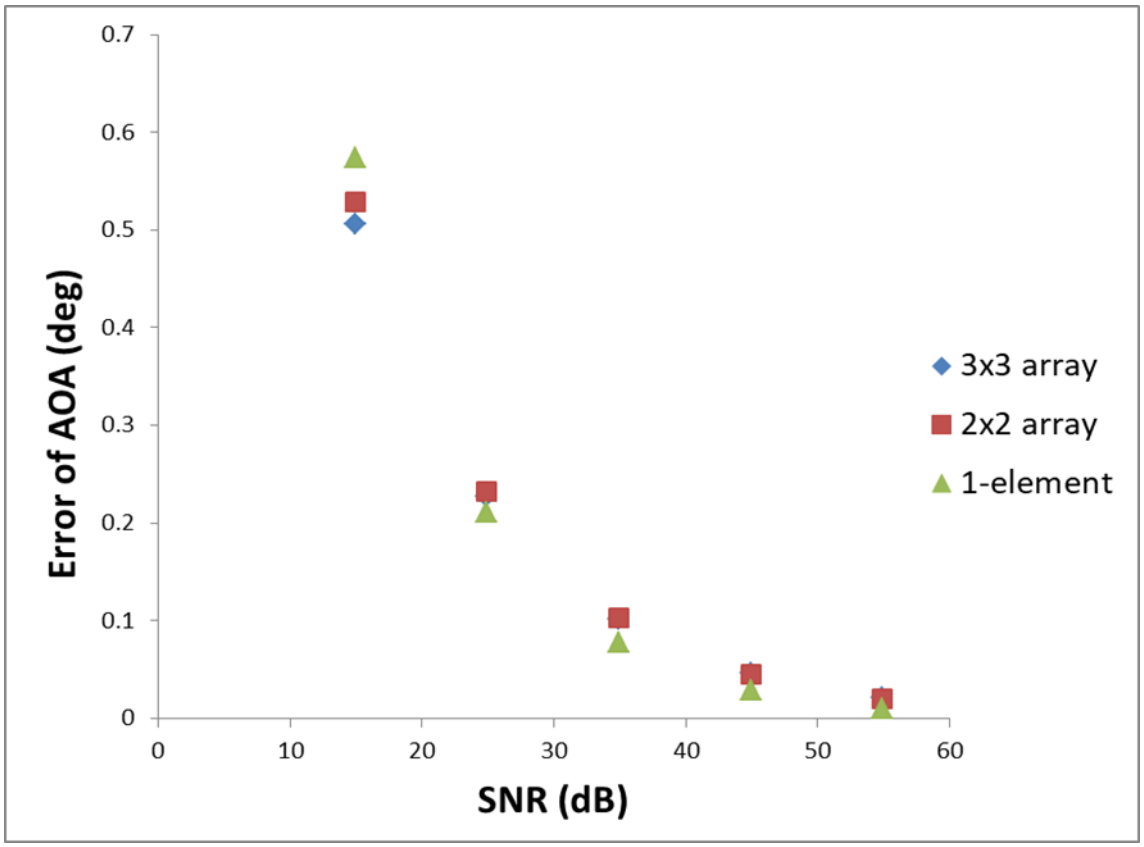

FIGURE 3.19: Checking for Degradation of AOA.

Comparison of Baseline

Error of AOA for 1m, 2.5m and 5m baseline is shown in Figure 3.20. For 5m baseline, .0005° error of AOA was achieved for 60 dB of SNR. Required accuracy was achieved with 2.5m and 1m baseline at around 70 dB and 75 dB respectively.

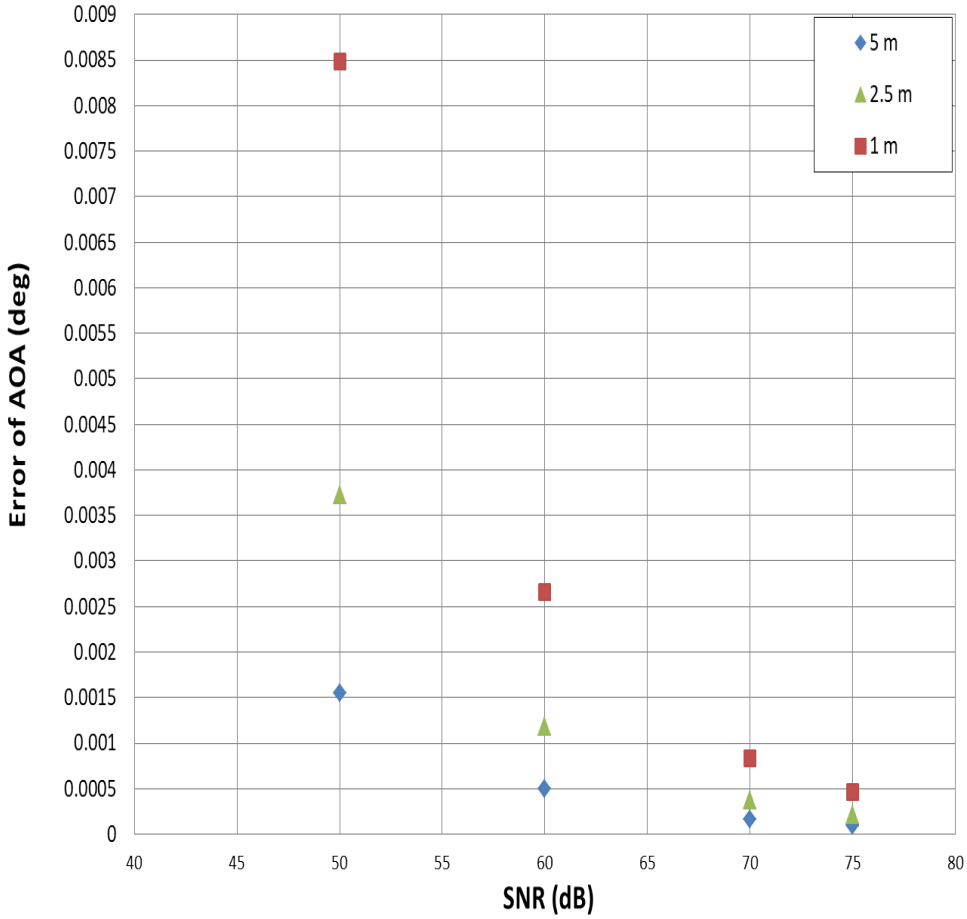

FIGURE 3.20: Effect of Baseline on error of AOA.

Comparison of Array Size

Table 3.1 shows phase difference samples for getting phase standard deviation. Accuracy of the experimental equipment is .05° and 10,000 samples are taken to get standard deviation. SNR is changed from 38 dB to 8 dB with using 4x4 array. Table 3.2 represents phase standard deviation and error of AOA for 4x4 dipole arrays. Values of standard deviation are measured values and error of AOA is calculated by Eq. (3.5). Table 3.3 represents phase standard deviation and error of AOA for 2x2 dipole array. Gain of 2x2 array is 6 dB less, so SNR for received pilot signal was from 32 db to 2 dB.

Comparison of theory and experiment regarding error of AOA is given in Table 3.4. SNR is changed from 0 dB to 70 dB and .0005° accuracy is obtained for 60 dB of SNR. Regarding approximation values, they were obtained with least square method. Details about approximation are given in next section. Absolute error was obtained by subtracting Theoretical data and approximation data. Absolute error is decreased with increasing SNR. Figure 3.21 gives comparison among experimental data, approximation and theoretical data. it can be observed that experimental data correlate with theory and approximation.

TABLE 3.1: Phase Standard Deviation.

SNR (dB)	38	28	18	8
Phase Samples (deg)	90.189	87.1	88.601	123.209
	91.121	89.438	110.138	29.947
	89.806	90.17	115.493	43.638
	88.976	94.236	99.332	87.031
	90.303	89.263	113.657	102.407
	89.145	88.294	111.908	119.806
	90.319	92.915	54.734	45.777
	91.563	87.249	111.478	83.496
	90.682	90.441	98.628	79.736
Standard Deviation of Phase (deg)	1.49565	5.09541	15.49318	46.37072

TABLE 3.2: Error of AOA for 4x4 array.

SNR (dB)	STD of Phase (deg) Measured	Error of AOA (deg) Calculated
38	1.49569	0.00582
28	5.09541	0.01985
18	15.49318	0.06035
8	46.37072	0.18065

TABLE 3.3: Error of AOA for 2x2 array.

SNR (dB)	STD of Phase (deg) Measured	Error of AOA (deg) Calculated
32	3.09340	0.01205
22	9.67236	0.03768
12	30.24325	0.11783
2	94.56364	0.36844

TABLE 3.4: Comparison of Theory and Approximation for error of AOA.

SNR (dB)	Theory (deg)	Approximation (deg)	Absolute Error (deg)
10	0.14112	0.14801	0.00688
20	0.04462	0.04733	0.00270
30	0.01411	0.01513	0.00102
40	0.00446	0.00484	0.00037
50	0.00141	0.00154	0.00013
60	0.00044	0.00049	4.89E-05
70	0.00014	0.00015	1.72E-05

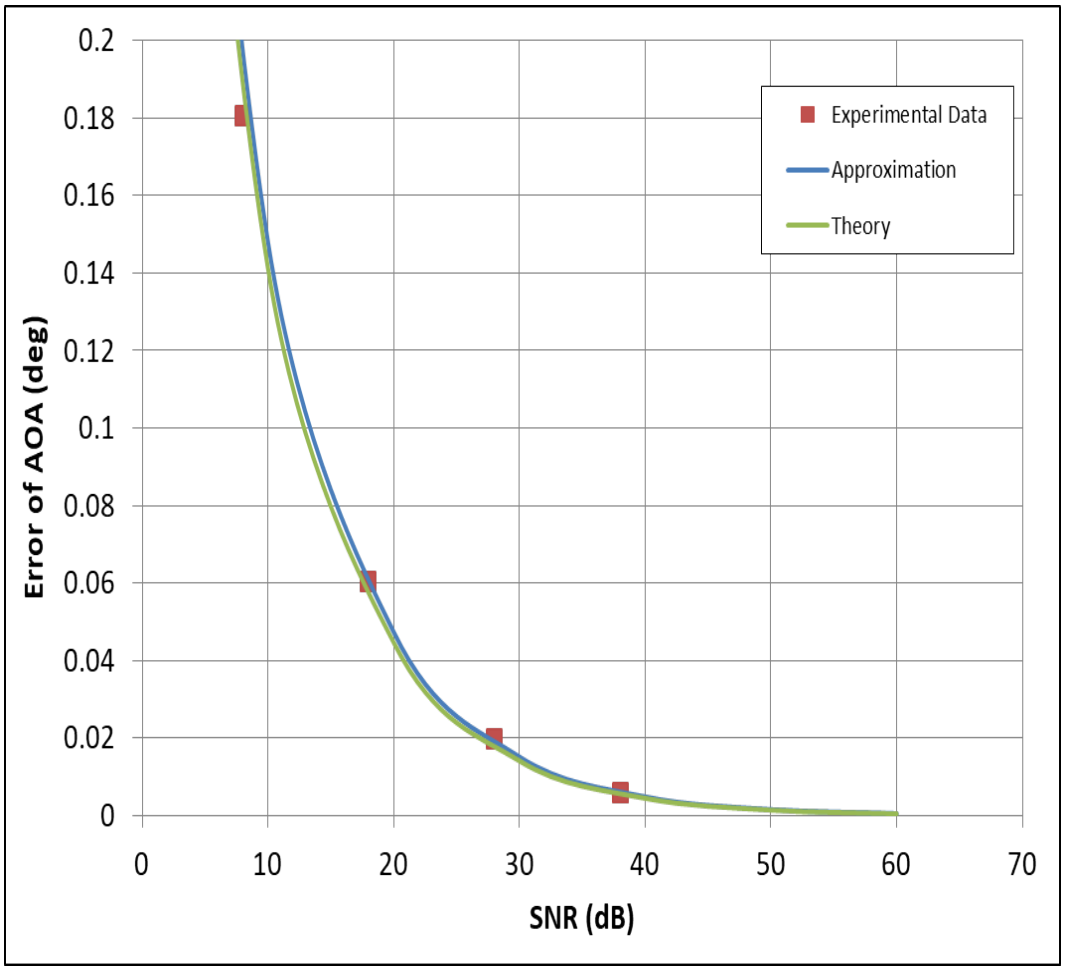

FIGURE 3.21: Comparison of Theory and Experimental data.

Analysis for Approximation

Experimental data was obtained with maximum SNR of 38 dB with using 4x4 array and error of AOA was .00582°. To get SNR data for required accuracy, approximation was done by least square method with using experimental data. Figure 3.22 shows comparison between experimental data and approximation for error of AOA. SNR was changed from 0 dB to 60 dB and .00049° was obtained, as shown in Table 3.5. Approximation was also done for getting values of phase standard deviation for 60 dB SNR. Table 3.6 shows that .1271° phase standard deviation accuracy is required for measurement data to obtain .00049° error of AOA. Figure 3.23 shows the comparison of experimental data and approximation for phase standard deviation.

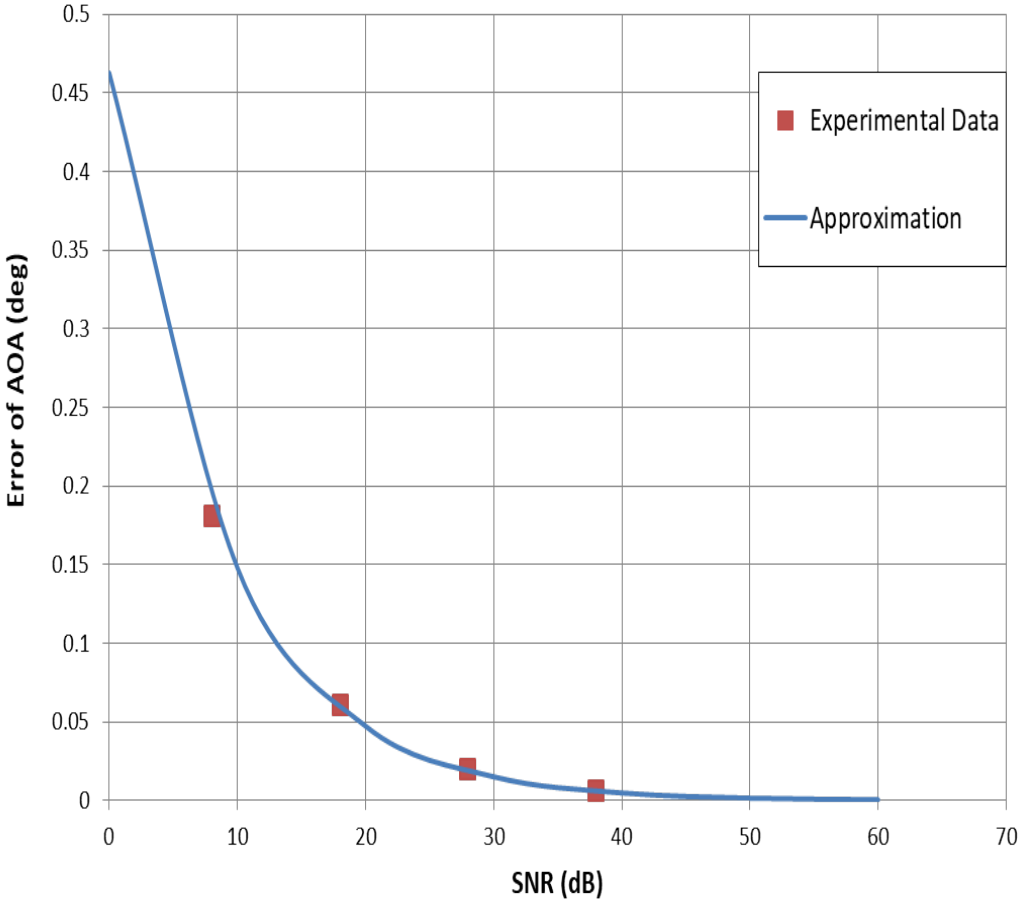

FIGURE 3.22: Comparison of Experiment and Approximation for Error of AOA.

TABLE 3.5: Approximation for error of AOA.

Approximation	
SNR (dB)	Error of AOA (deg)
0	0.4628
10	0.14801
20	0.04733
30	0.01513
40	0.00484
50	0.00154
60	0.00049

TABLE 3.6: Approximation for Phase Standard Deviation.

Approximation	
SNR (dB)	STD of Phase (deg)
0	118.78
10	37.9881
20	12.14931
30	3.88558
40	1.24268
50	0.39743
60	0.1271

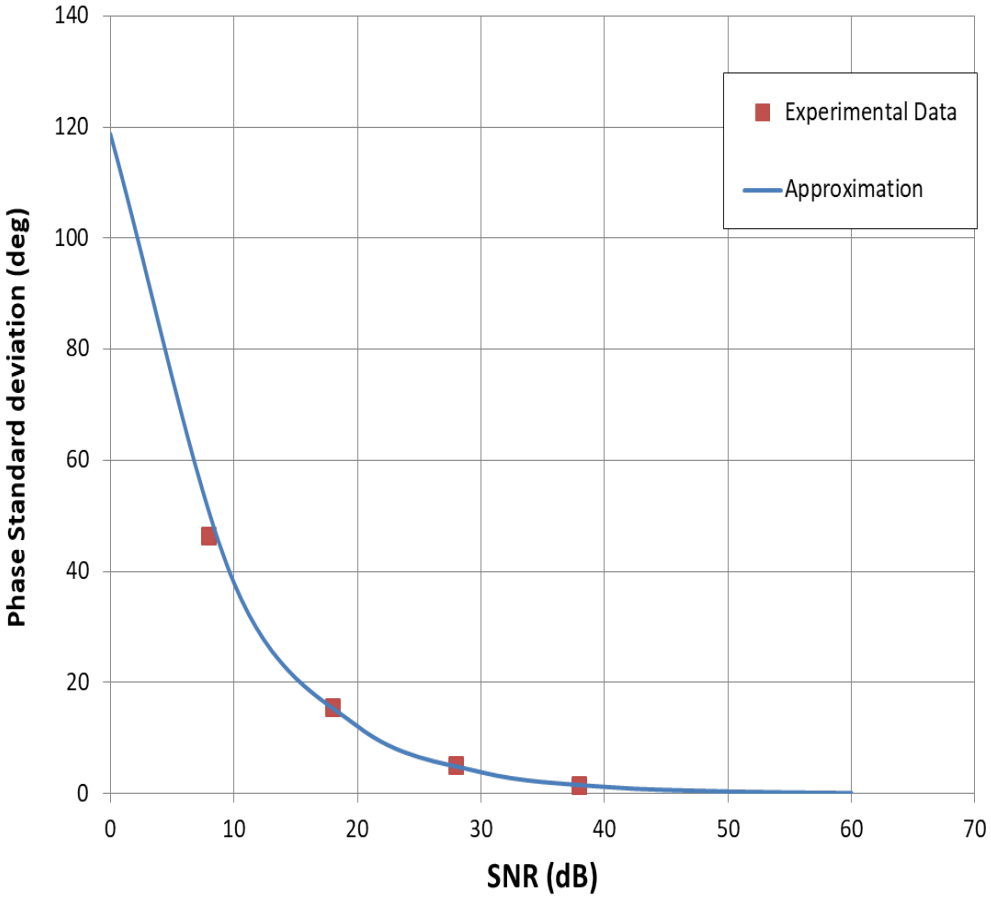

FIGURE 3.23: Comparison of Experiment and Approximation for Phase Standard Deviation.

Analysis of Ambiguity

Direction finding experiment was performed with 1m, 2.5m and 5m baseline. Large spacing between antennas has issue that ambiguities begin to occur when the antenna spacing is longer than haft of wavelength of signal. Purpose of the DF experiment was analysis of phase standard deviation and error of AOA regarding SNR value of pilot signal. SNR values were changed and analysis was performed. So, measurement for the experiment was done for 0° between pilot signal transmitting antenna and pilot signal receiving antenna arrays. Pilot signals from different angles were not required for purpose of the evaluation.

Regarding phase measurement between two complex pilot signals A and B by antennas RX1 and Rx2 respectively, Eq. (3.6) can be used.

$$\cos\theta = \frac{A.B}{Mag(A)xMag(B)} \tag{3.6}$$

But problem with measurement of θ with Eq. (3.6) is that there is an ambiguity for angle measurement, as shown in Figure 3.24. cos(160°) and cos(200°) has same value -0.939. So, to resolve this issue for phase measurement, Eq. (3.7) and (3.8) were used.

$$\cos\theta = \frac{Re(Conjugate(A)xB)}{Mag(A)xMag(B)} \tag{3.7}$$

$$Sign = \frac{Re(A)xImg(B) - Re(B)xImg(A)}{Mag(Re(A)xImg(B) - Re(B)xImg(A))} \tag{3.8}$$

Eq. (3.7) gives value for θ and ± is provided by Eq. (3.8). This measurement is done in real time with labview software to find the phase. Figure 3.25 shows the operation by using these equations. Angle for phase moves from 0° to 180° and then -180° to 0°. -180° is next value after 180° and operation is continuous without discontinuity. Phase measurement by these equation fulfils the need to measure phase change for deformation cases in section 3.6.

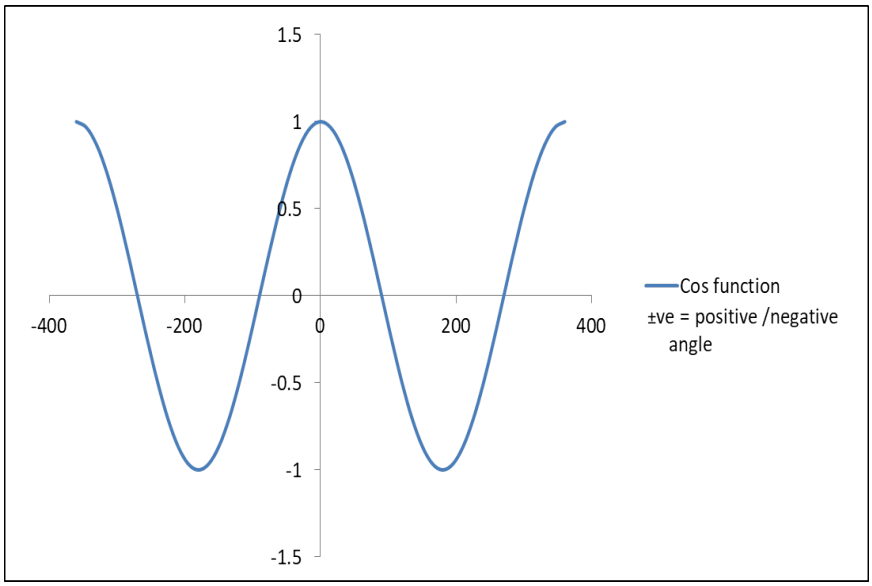

FIGURE 3.24: Cos Function.

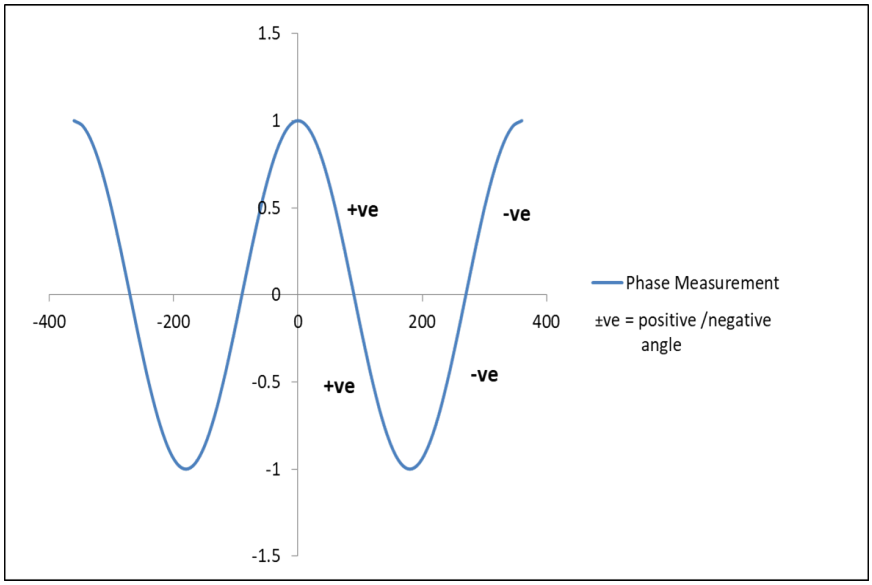

FIGURE 3.25: Phase Measurement.

To know the effect of phase difference by changing angles between pilot signal transmitting antenna and pilot signal receiving antenna arrays, measurement were taken for 1° and 5° turntable position. Table 3.7 compares the $\Delta\phi$ for 1° and 5° position between Eq. (3.9) and experimental data with 2.5m and 1m baseline.

$$\Delta\phi = \frac{2\pi d \sin\theta}{\lambda} \tag{3.9}$$

By Eq. (3.9), phase change ($\Delta\phi$) for 2.5m and 1m baseline is 128.33° and 51.33° respectively for 1° position. Phase change ($\Delta\phi$) for 2.5m and 1m baseline is 640.88° and 256.35° respectively for 5° position. Regarding measurement data in Table 3.7, error

between theory and experiment is increased with 2.5m baseline for 5° due to less received power at this position. Theoretical values of ($\Delta\phi$) with 5m baseline for 5° and 1° turntable position are 1281.77° and 256.66°. Regarding measurement, Phase will move from 0° to 180° and then -180° to 0°, which will generate ambiguity when using large position angles with long baseline. To resolve ambiguity with long baseline was not required for the DF experiment, so this issue should be addressed in future. A solution with unwrap phase function is given and it provides continuous angles from 0 degree to 360 degree, 720 degree and so on [35-37]. Another solution to resolve ambiguity is given to use antennas with different baseline for phase measurement [22].

TABLE 3.7: Phase data for Turntable position.

	Theory		Experiment	
	1 (deg)	5 (deg)	1 (deg)	5 (deg)
1m	51.33	256.35	50.4	254.35
2.5m	128.33	640.88	126.15	634.56

3.6 Effect of Deformation on DF

3.6.1 Experimental Setup

Regarding effect of antenna deformation on DF, experimental evaluation is performed. Partial antenna deformation and whole antenna deformation cases are considered. For partial antenna deformation, position of elements in an array was changed. For Whole antenna deformation, one whole antenna array was deformed. 2x2 dipole antenna arrays were used for the deformation evaluation and forward deformation case was considered. Figure 3.26 shows 2x2 array without deformation. Figures 3.27 and 3.28 show 2x2 array with 1-element and 2-element deformation respectively. Figure 3.29 represents whole antenna deformation.

Figure 3.30 represents setup for partial array deformation. Antenna elements are deformed in Rx2 dipole array antenna. Phase measurement is performed between Rx1 and Rx2 under deformation conditions. Figure 3.31 shows setup for whole array deformation. Rx2 dipole array is deformed in forward direction and phase measurement is performed. USRP 2945 was used for measuring the phase difference between Rx1 and Rx2. Configuration of USRP is given in Figure 3.3.

FIGURE 3.26: 2x2 dipole Antenna Array without Deformation.

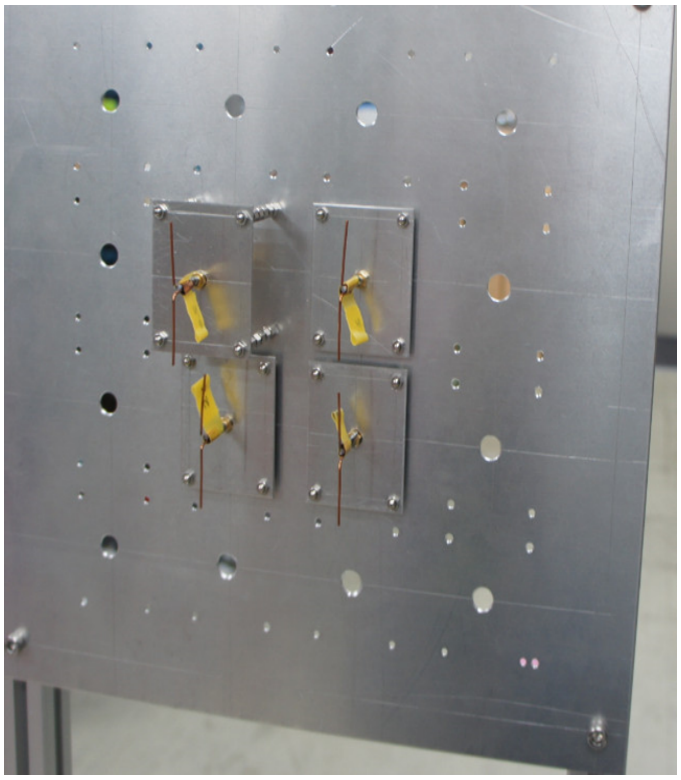

FIGURE 3.27: 2x2 dipole Antenna Array with 1 element Deformation.

FIGURE 3.28: 2x2 dipole Antenna Array with 2 element Deformation.

FIGURE 3.29: 2x2 dipole Antenna Array with whole antenna Deformation.

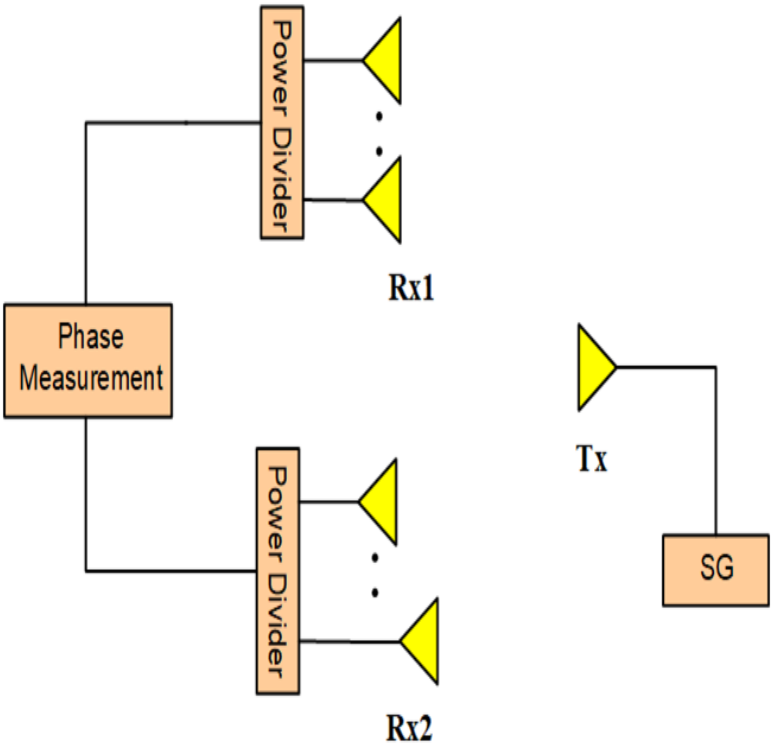

FIGURE 3.30: Partial Antenna Deformation.

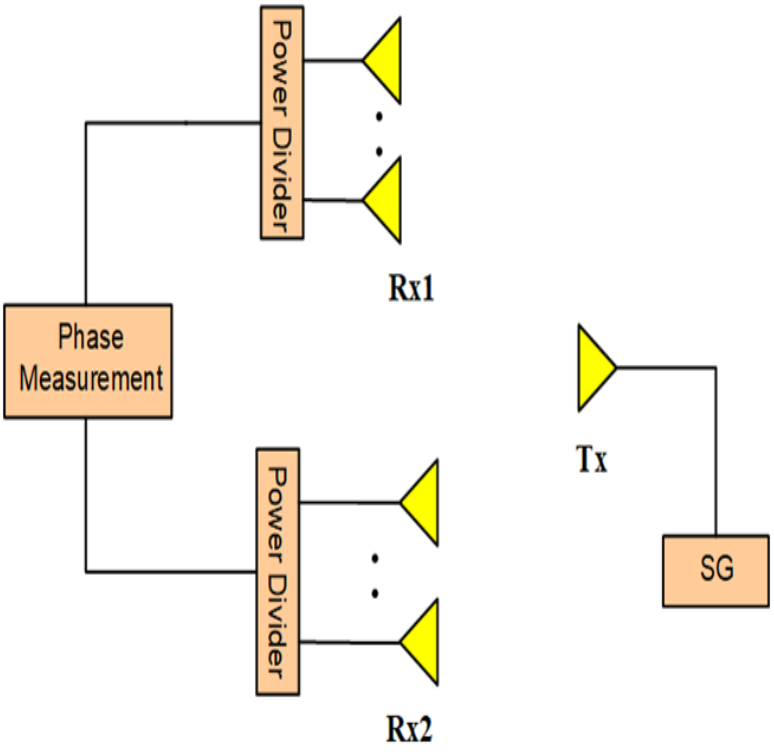

FIGURE 3.31: Whole Array Deformation.

3.6.2 Results and Discussion

Simulations are performed to get radiation patterns for deformation cases. Figure 3.32 shows pattern for 1 element deformation and Figure 3.33 indicates pattern for 2 element deformation. For 5mm deformation, radiation Pattern shifts to right side by 2° for 1 element deformation and shifts by 4° for 2 element deformation.

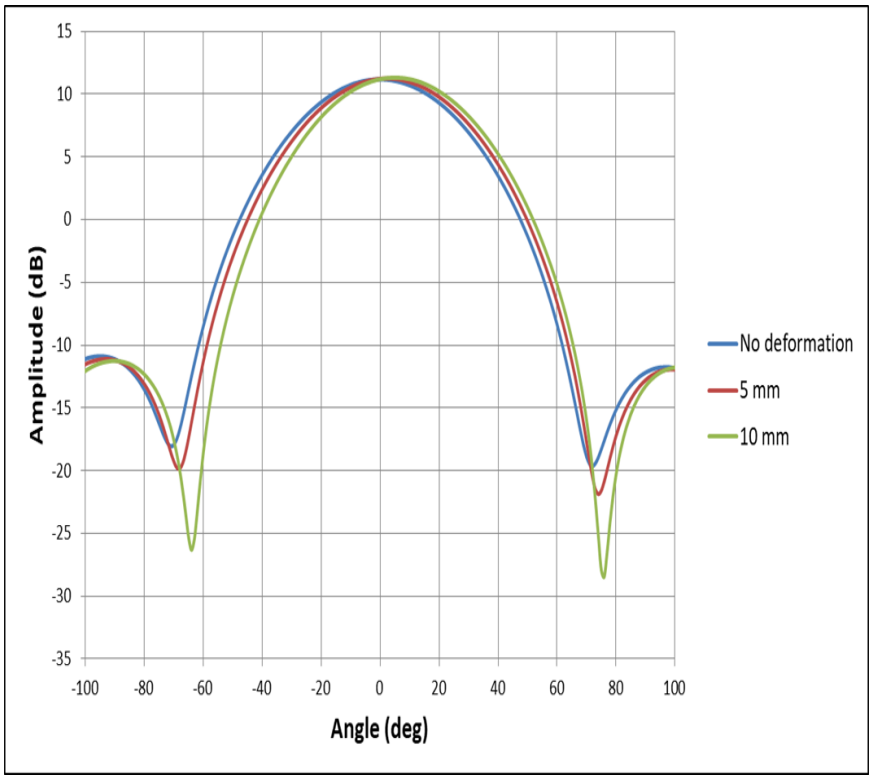

FIGURE 3.32: Simulation for 1 element Deformation.

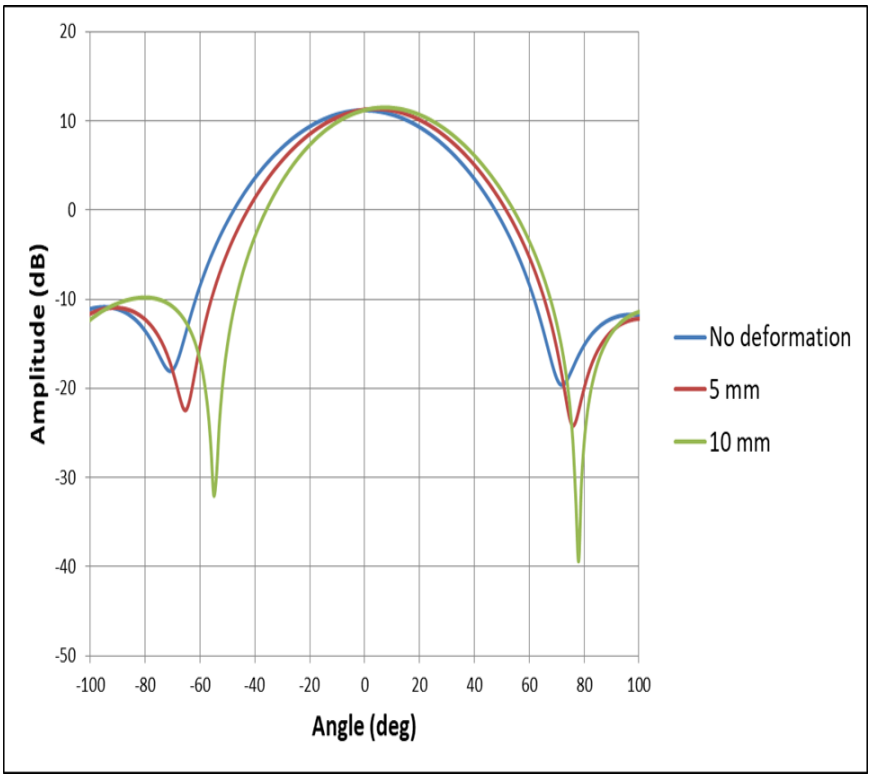

FIGURE 3.33: Simulation for 2 element Deformation.

Figure 3.34 shows phase change for 1 element deformation. Figure 3.35 represent phase difference for 2 element deformation. Figure 3.36 shows phase change for whole antenna deformation. 250cm baseline and 7mm (.05λ), 14mm (.11λ), 21mm (.17λ) and 28mm (.23λ) deformation cases are considered for the evaluation. Maximum phase change is obtained for whole array deformation and minimum is obtained for one element deformation case. For 7mm deformation, phase change is 5° for one element deformation and phase change is 20° for whole antenna array deformation case.

Theoretical data for the evaluation is obtained by Eq. (3.6),

$$\Delta\phi = \frac{2\pi\Delta x\Delta n}{\lambda M} \tag{3.10}$$

where $\Delta\ \phi$ is change in the phase difference due to deformation, Δx is antenna deformation in meters, Δn is number of deformed antennas and M is total number of antennas in the array.

Error of AOA is determined for all cases of deformation and is shown in Figure 3.37. Minimum value of error is 0.39° for 1 element deformation case.

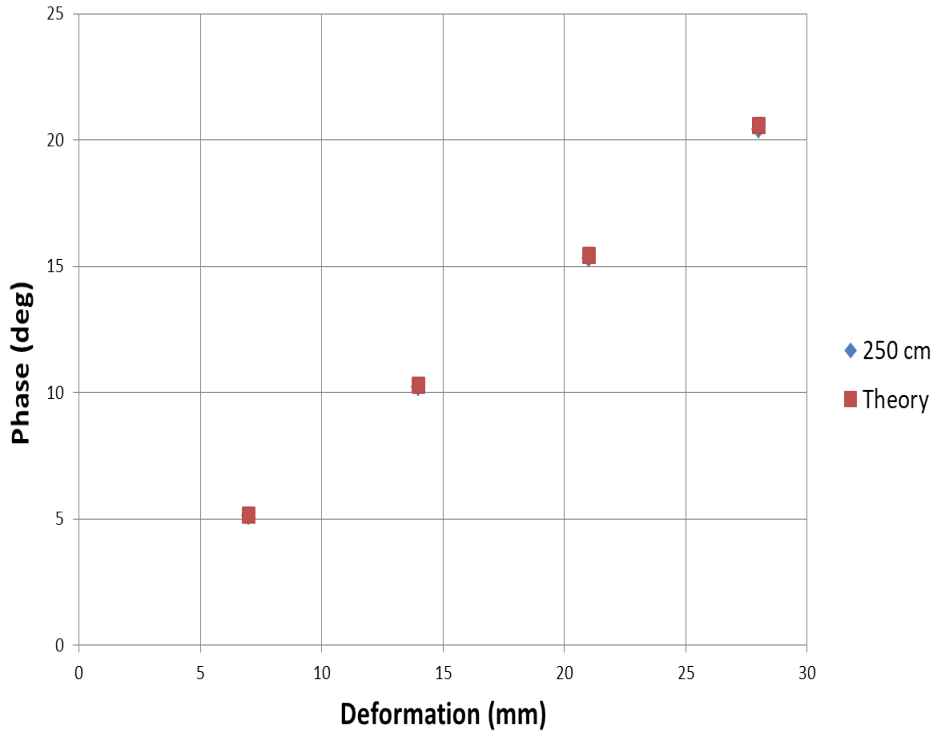

FIGURE 3.34: Phase Change for 1 element Deformation.

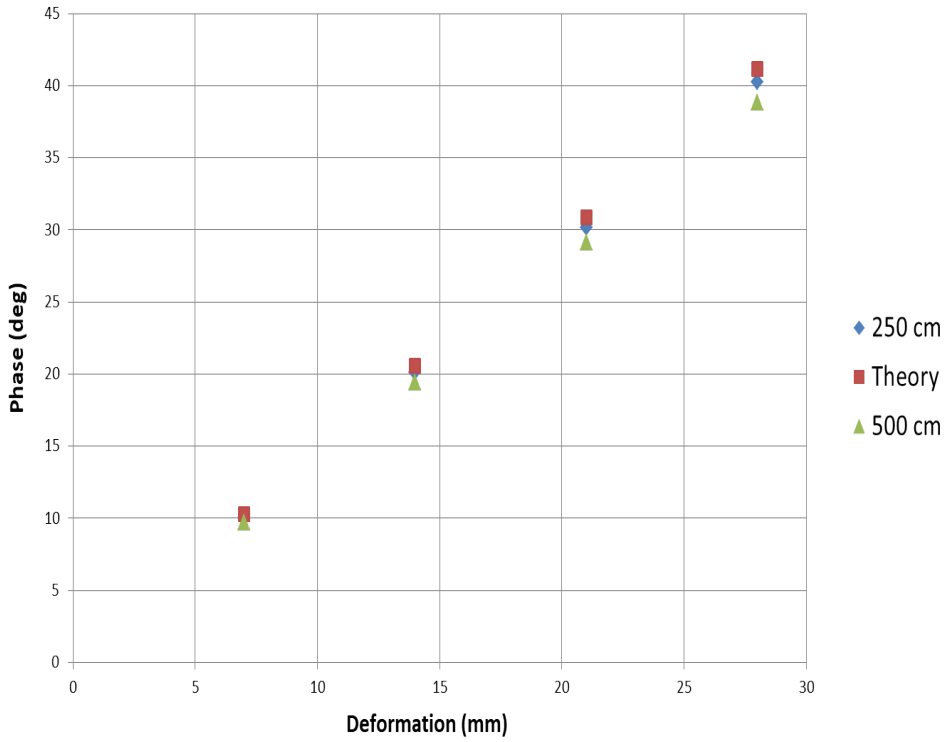

FIGURE 3.35: Phase Change for 2 element Deformation.

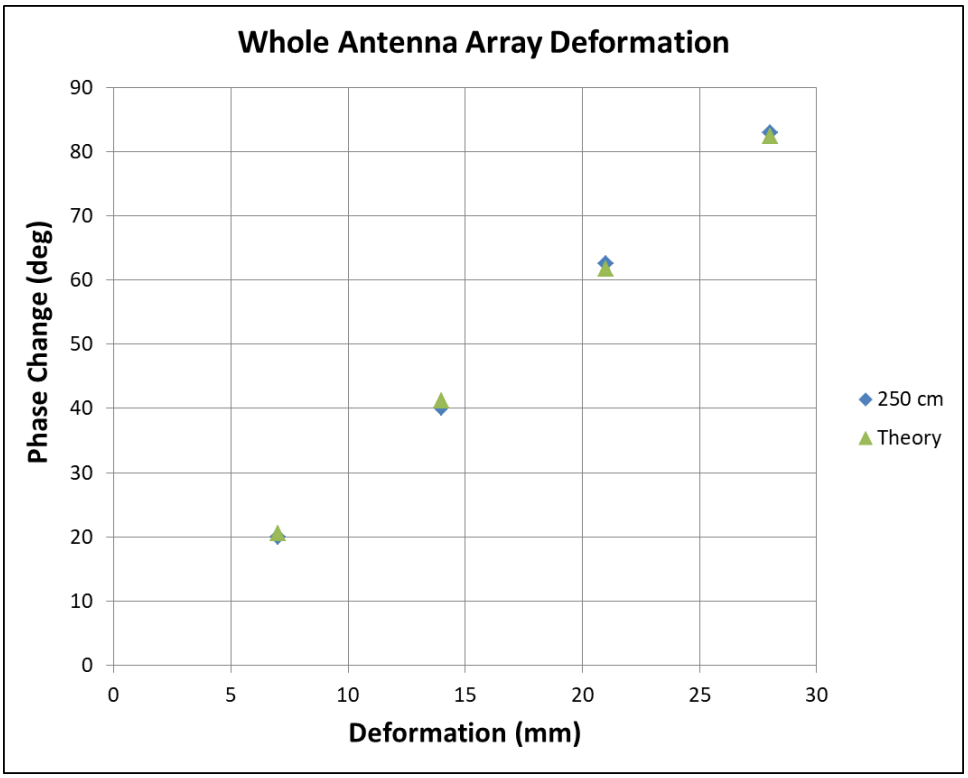

FIGURE 3.36: Phase Change for whole antenna deformation.

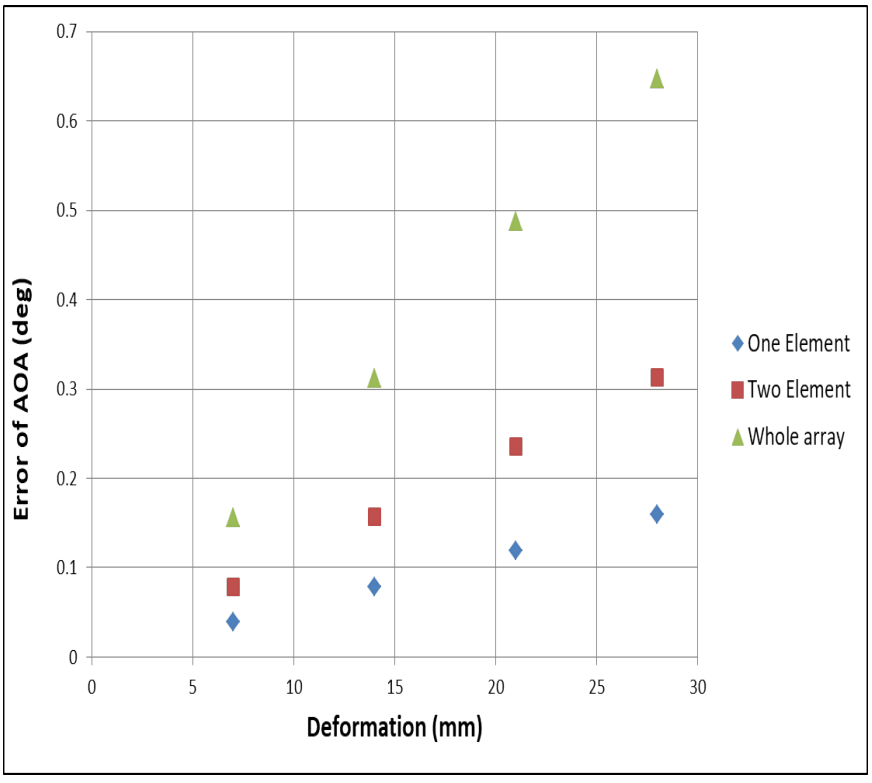

FIGURE 3.37: Error of AOA for Deformation.

3.7 Summary

DF experiments were performed by DF & Beam forming method. Phase comparison monopulse method was used with 2x2 and 4x4 array antennas and 5m, 2.5m, 1 m baselines. For 5m baseline, error of AOA was .00582° with 38 dB of SNR and -80 dBm of noise level. Accuracy of the measurement system was 0.05° and 10,000 samples were taken to measure standard deviation of phase. For 38 dB of SNR, phase standard deviation was 1.4956°. Approximation was performed with least square method for getting values of phase standard deviation and error of AOA by increasing SNR. For 60 dB SNR, error of AOA was .00049° and phase standard deviation was .1271° .

Deformation experiments were performed with 2x2 dipole array antennas. Partial deformation and whole deformation cases were considered to know the effect of deformation on direction finding. It was obtained by experiment that phase change by whole array deformation was higher than that of by partial antenna array deformation. For partial array deformation, with increasing number of deformed elements, phase change was also increasing.

Chapter 4

Digital Retrodirective Method

4.1 Introduction

Precise beam control accuracy of MPT is required for the SPS [15,19]. Beam pointing error of MPT should be less than 10% of the beam-width[19]. Flexible structures will be used for large array antenna system, and space environment conditions will deform antenna system [23-26].

Several types of methods have been studied to do MPT for SPS. The most studied methods are Hardware Retrodirective and Direction Finding and Beam forming method (Software Retrodirective method). Hardware Retrodirective method uses pilot signals from rectenna, and a power signal is generated by reflecting back or by phase conjugation of pilot signal. In Reference [23], hardware retrodirective method is demonstrated to correct antenna deformation, but accuracy of the method is not discussed. Hardware retrodirective method is complex and also not flexible regarding frequency selection. Software Retrodirective method uses direction finding methods for angle of arrival detection of pilot signal and beam forming is done with phased array antennas. In Reference [25,28], an experiment is performed to correct antenna deformation with software retrodirective method and 0.15 root-mean square (RMS) accuracy is achieved. Synchronization will be required among 23.75 million antenna modules of SPS with using software retrodirective method. This method uses rotating element electric field vector (REV) method for synchronization among antenna modules and for rectification of antenna deformation. REV method will take several hours to perform the said operations for the SPS.

Deep Neural Network (DNN)-based auto-encoders used for end-to-end learning of simultaneous wireless information and microwave power transfer (SWIPT) is a solution to do communication and power transfer simultaneously [29,30]. Currently, power transfer by SWIPT method is being studied to do wireless charging of batteries for wireless devices. To the best of author's knowledge, data is not reported about transmitting high power microwave by using this method.

Retro-reflective beamforming method is proposed to do microwave power transmission with phase conjugation. Digital signal processing (DSP) is used for phase detection and phase conjugation. This method requires phase shifters for power transmission. Study is also not provided regarding antenna deformation conditions and consequences [31,32].

Previously studied methods, as mentioned above have limitations regarding solving

the issues of MPT for SPS. Digital retrodirective method is proposed in Chapter 4 to resolve issues of flexibility for frequency, synchronization among antenna modules and deformation of antennas. DSP is used to achieve flexibility regarding frequency of MPT. Need of synchronization is removed by making antennas independent. The issue of antenna deformation is solved by measuring phase change of pilot signal for the deformation, and beam forming is done by phase conjugation of the pilot signal. The algorithm of the proposed method is also evaluated by comparing with REV method for antenna deformation.

4.2 Concept of Digital Retrodiretive method

Figure 4.1 represents concept of digital retrodirective method. Pilot signal is sent from rectenna towards retrodirective array. Retrodirective array consists of pilot signal receiving antennas (RX) and power signal transmitting antennas (TX). ϕ_{r1} is phase of pilot signal, received by RX1 and ϕ_{r2} is phase of pilot signal, received by RX2. RX1 antenna is used as reference pilot signal receiving antenna to measure average value of phase between RX1 and RX2. Phase detection of pilot signal is performed by DSP circuit. Then, DSP circuit performs beam forming for power signal by phase conjugation of pilot signal and considering frequency of power signal. Phase of the power signal (ϕ_t) is determined by Eq. (4.1),

$$\phi_t = -\frac{f_t}{f_r}\phi_r, \tag{4.1}$$

where f_t is frequency of the transmitted power signal, and f_r is frequency of received pilot signal. Power signals with phase ϕ_{t1} and ϕ_{t2} are radiated by power signal transmitting antennas TX1 and TX2, respectively. Figure 4.2 depicts configuration for deformation, RX2 and TX2 antennas are deformed from their original position. Each set of pilot signal and power signal transmitting antenna is working independently without synchronization among them.

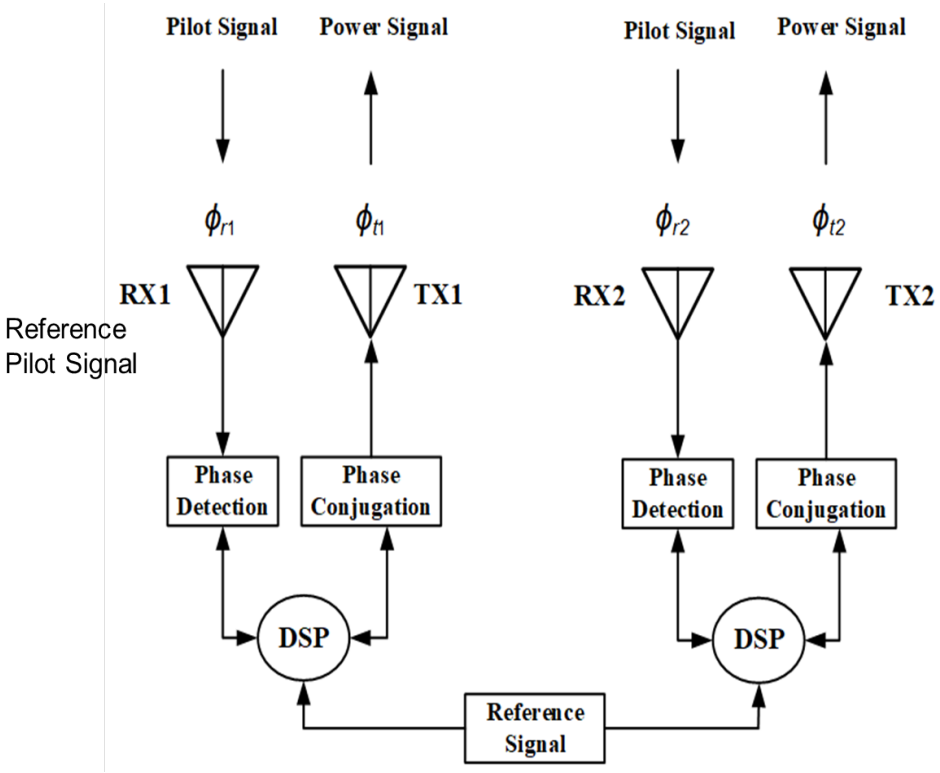

FIGURE 4.1: Digital Retrodirective method concept.

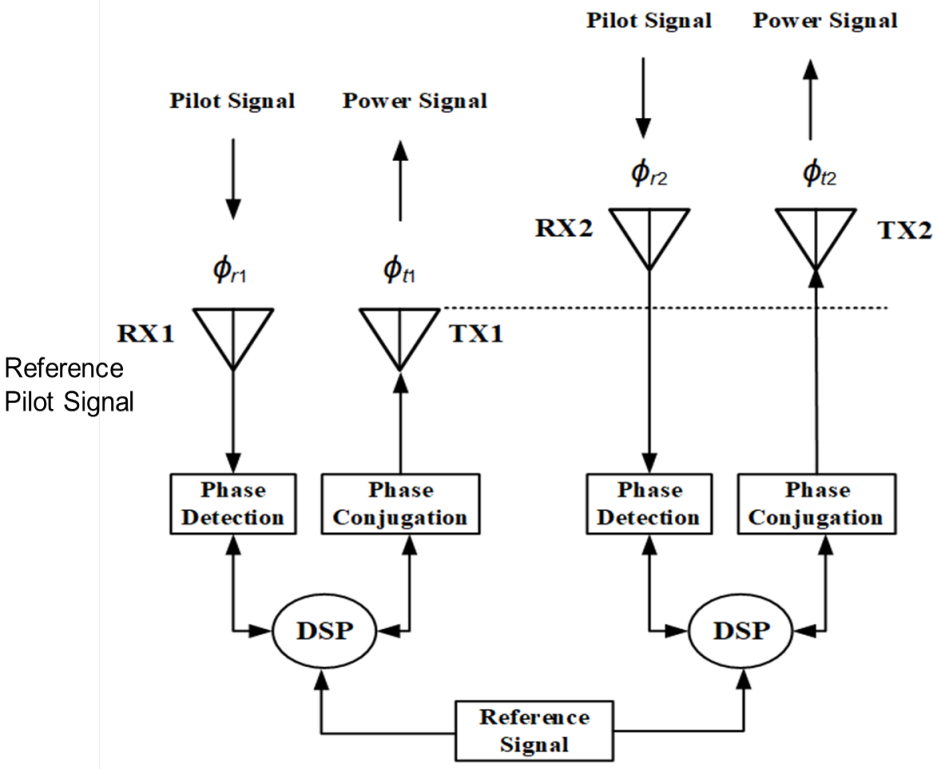

FIGURE 4.2: Digital Retrodirective method concept for Deformation.

4.2.1 Algorithm of Digital Retrodiretive method

Figure 4.3 shows algorithm for digital retrodirective method. Pilot signal is received and mixed with local oscillator signal. Then, conversion is performed to change complex signal to I and Q data. I and Q signal is digitized and phase detection is performed by DSP circuit. Analysis is also done at this position for antenna deformation conditions. Then, power signal for required frequency is generated. Phase of the power signal is determined by multiplying phase of pilot signal with ratio of frequency for power and pilot signal, as shown by Eq. (4.1). After that, Conjugation for the power signal phase is performed, and power beam is transmitted.

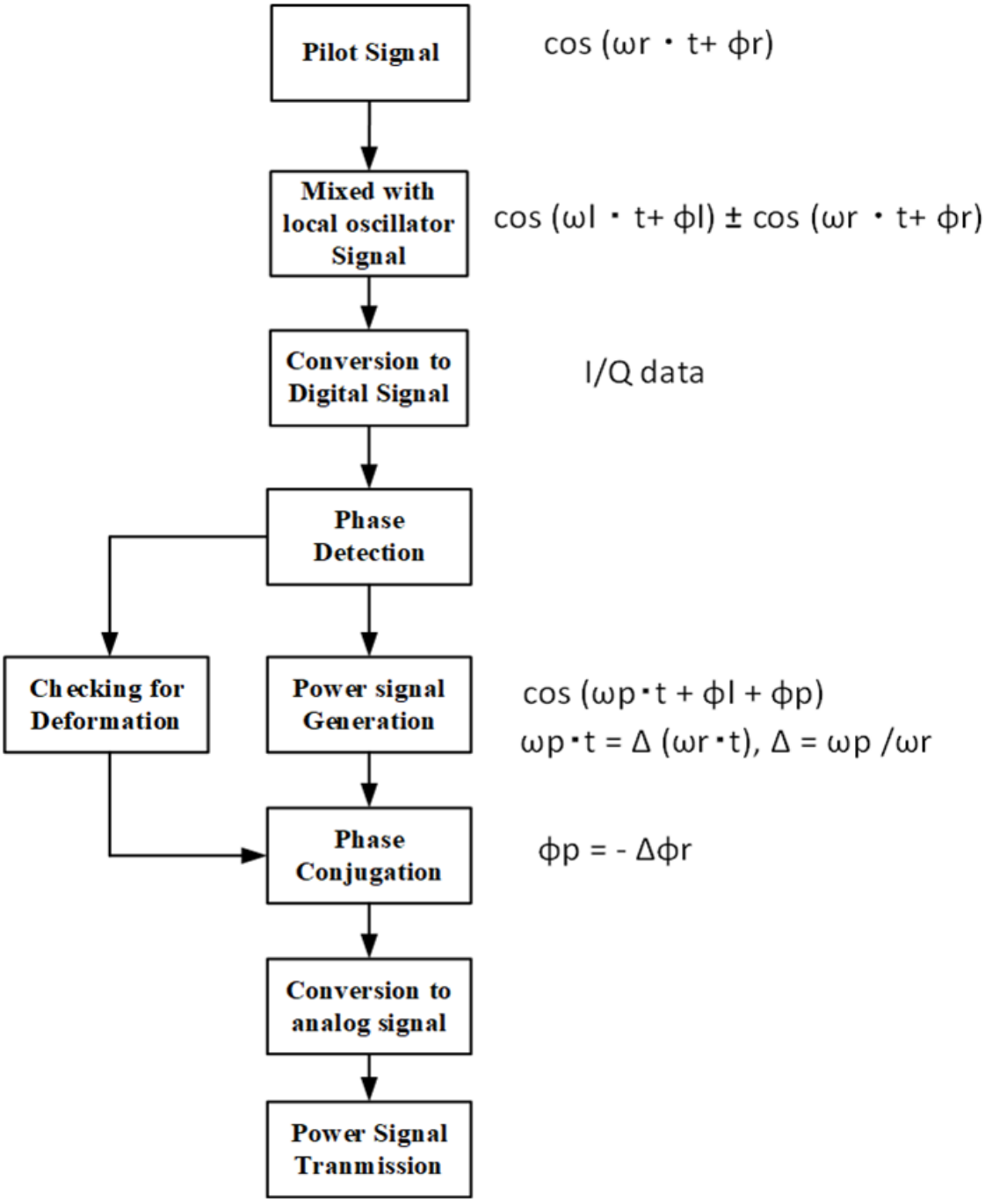

FIGURE 4.3: Digital Retrodirective method algorithm.

4.3 DSP Circuit

Details of DSP circuit are shown in Figure 4.4. DSP circuit has analog front-end, analog-to-digital conversion, and digital signal processing. Software defined radio (SDR) hardware is used for analog front-end and analog-to-digital conversion. Received pilot signal is amplified by low noise amplifier (LNA) and downconverted to baseband in-phase (I) and quadrature-phase (Q) components by mixer. Voltage controlled oscillator (VCO) provides reference frequency to mixer. Reference signal of 10 MHz is used for providing standard frequency to VCO. Phase-locked loop (PPL) is used to stabilize frequency and phase of VCO. Reference signal of 1 PPS is used as timing reference for retrodirective array. I/Q components are filtered by low pass filter (LPF) and then digitized by analog-to-digital converter (ADC). Digitized I/Q data is downconverted by digital downconverter (DDC) and passed to the host computer over a standard gigabit Ethernet connection.

For power signal transmission, I/Q baseband components with conjugate phases are generated by host PC and fed to digital up converter (DUC). After digital upconversion, digital-to-analog converter (DAC) converts the signal to analog. Then, LPF reduces high frequency components in the signal and mixer upconverts the signal to user-specified RF frequency.

The area within the dotted line indicates processing with field programmable gate array (FPGA), and it is controlled by LabVIEW software. LabVIEW performs phase detection of the pilot signal and generates power signal with phase conjugation. USRP 2943 software defined radio is used as DSP hardware system [34].

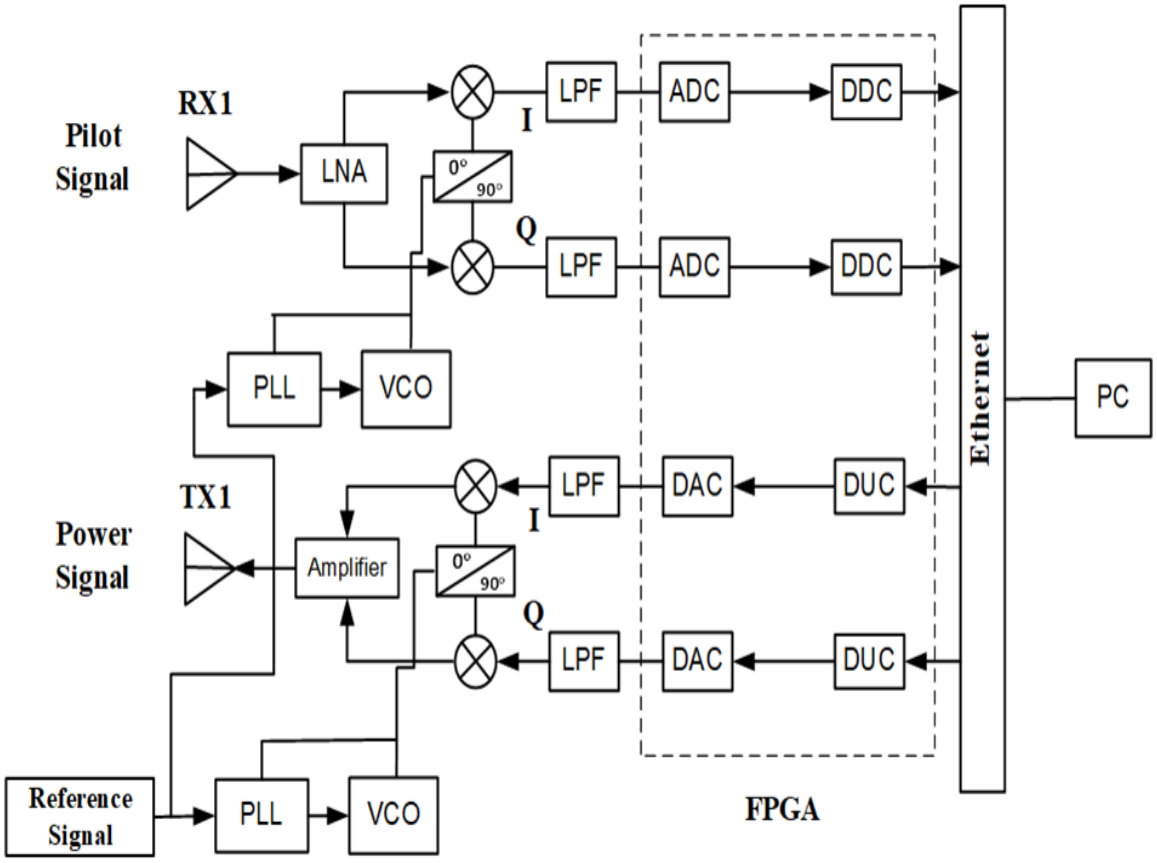

FIGURE 4.4: Digital Retrodirective algorithm.

There is a concern that aliasing can occur when using different frequencies for power signal and pilot signal. 5.8 GHz and 2.45 GHz frequencies are proposed for power signal and pilot signal, respectively. Aliasing can take place when reconstructing power signal from samples of the pilot signal. In the proposed method, power signal is generated by SDR hardware and phase information of pilot signal is used for getting phase of power signal, as given in Eq. (4.1) and represented by Figures 4.1– 4.4. So, aliasing will not occur for the proposed method with using different frequencies for power signal and pilot signal.

4.4 Experimental Setup

4.4.1 Experimental Setup for Bistatic Pattern Measurement

Bistatic radiation pattern measurement is performed for evaluation of digital retrodirective method, as shown in Figure 4.5. Retrodirective array is installed on turn table in anechoic chamber, and horn antenna is fixed. The horn antenna sends pilot signal, and it is received by pilot signal receiving antennas. Then, retrodirective array moves on turn table, and power signal transmitting antennas send power signal to horn antenna. Radiation pattern is measured for the power signal, received by horn antenna.

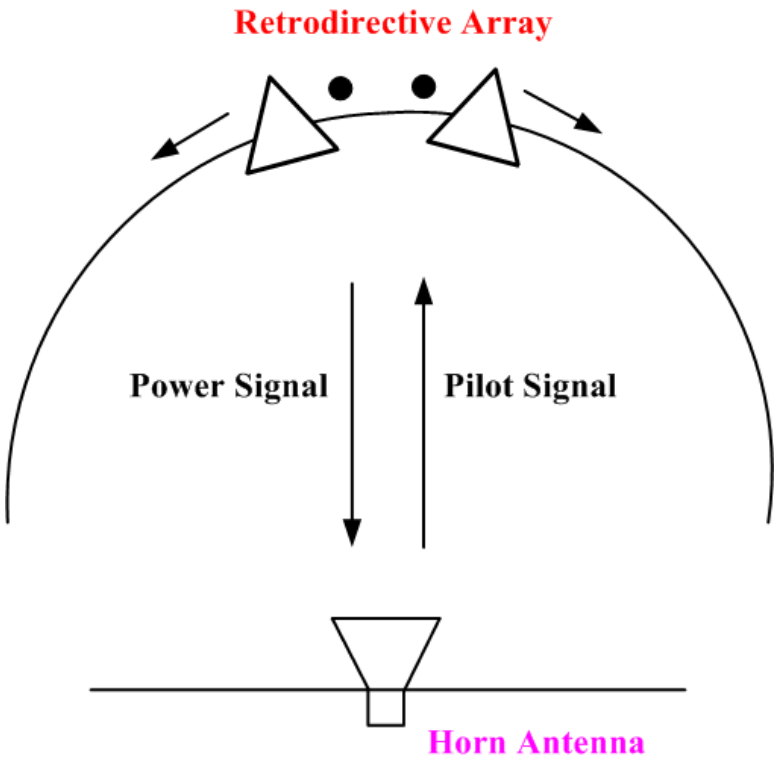

FIGURE 4.5: Bistatic radiation pattern measurement.

4.4.2 Detailed Experimental Setup Configuration

Detailed setup configuration for digital retrodirective experiment is depicted in Figure 4.6. Considering the case of the Tethered SPS, 2.45 GHz and 5.8 GHz frequencies are used for pilot signal and power signal, respectively. A two and forty-five hundredths gigahertz pilot signal is sent from signal generator (SG) to horn antenna. The horn antenna radiates pilot signal towards retrodirective array. Four sets of pilot signal receiving and power signal transmitting antennas are used for retrodirective array. Antennas are working independently, so this small scale demonstration can determine the usefulness of proposed method for SPS. Half wavelength dipole antennas are used to receive pilot signal. Right-hand circular polarized patch subarray antennas are used to transmit power signal. For SDR hardware, two USRP 2943 are used. Power signal is received by horn antenna, and radiation pattern analysis is performed by network analyzer and spectrum analyzer. Figure 4.7 represents configuration for providing reference signals of 10 MHZ and 1 PPS to each DSP circuit. Same cable lengths are used between source and each DSP circuit of receiving and transmitting antennas.

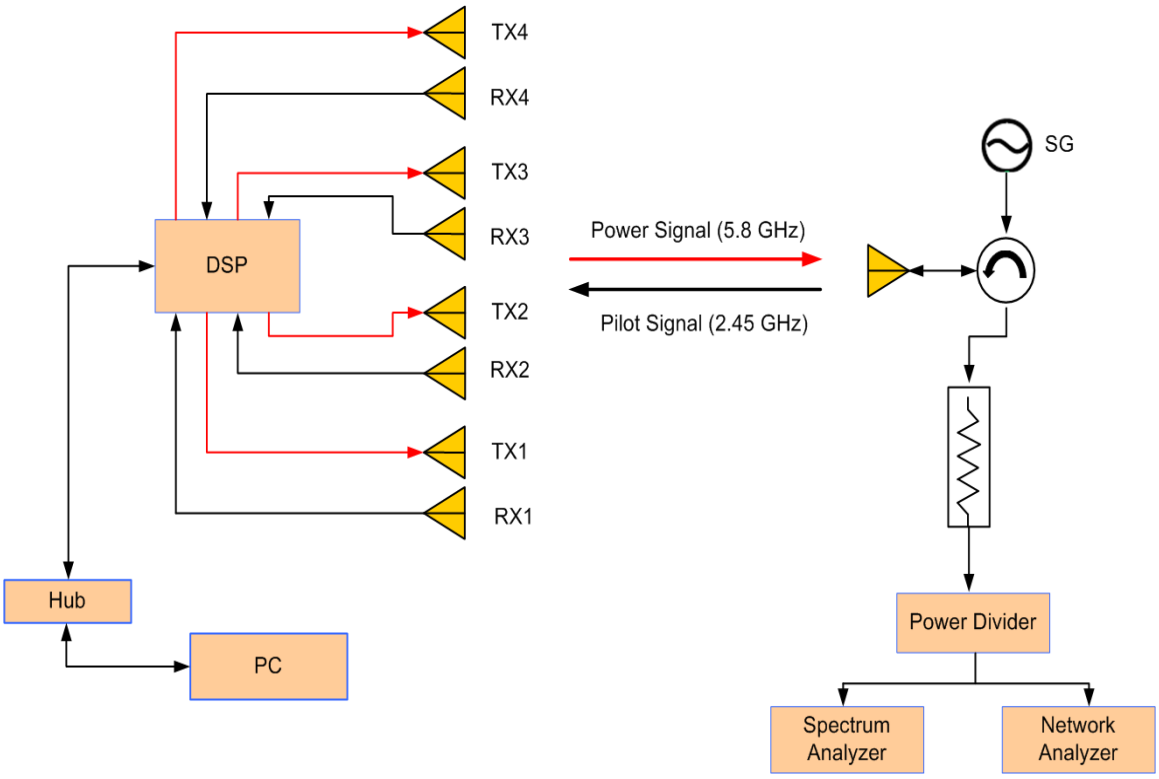

FIGURE 4.6: Digital Retrodirective method experimental setup.

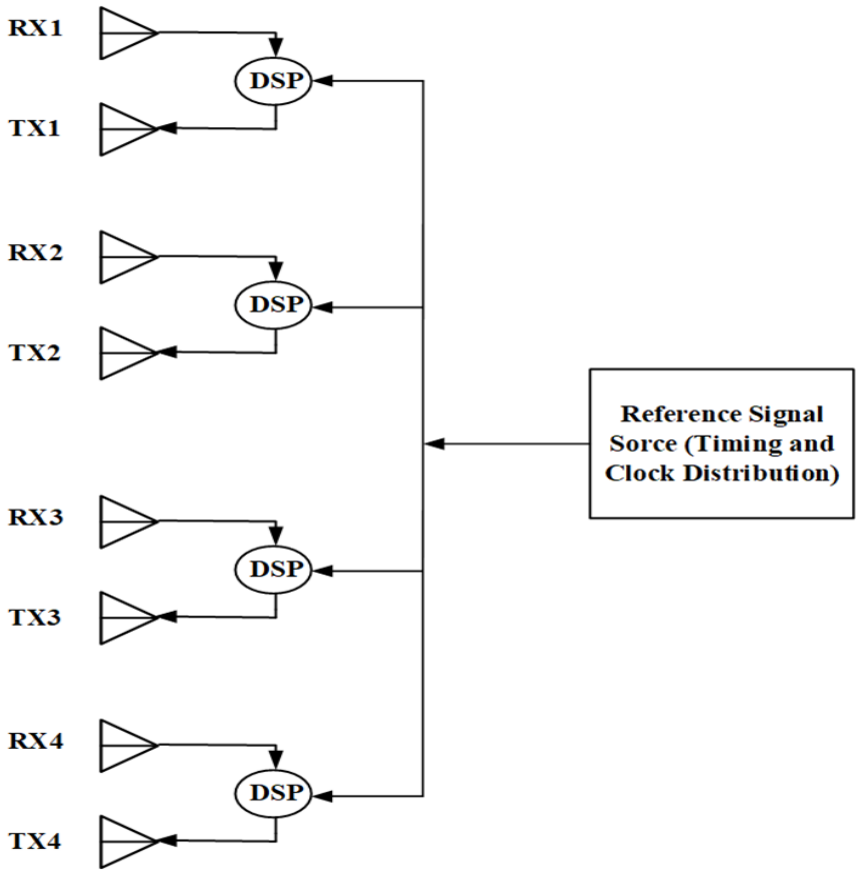

FIGURE 4.7: Configuration for Refernce signal.

Figure 4.8 shows retrodirective array setup with patch subarray antennas and dipole antennas. Each patch subarray is working independently with respective dipole antenna. Spacing between each patch subarray is 1.3λ, and spacing between elements of a subarray is 0.65λ. For no deformation case, antennas are in original position. Forward and backward deformation cases are represented in Figures 4.9 and 4.10 respectively. One patch with respective dipole antenna is deformed in forward and backward direction.

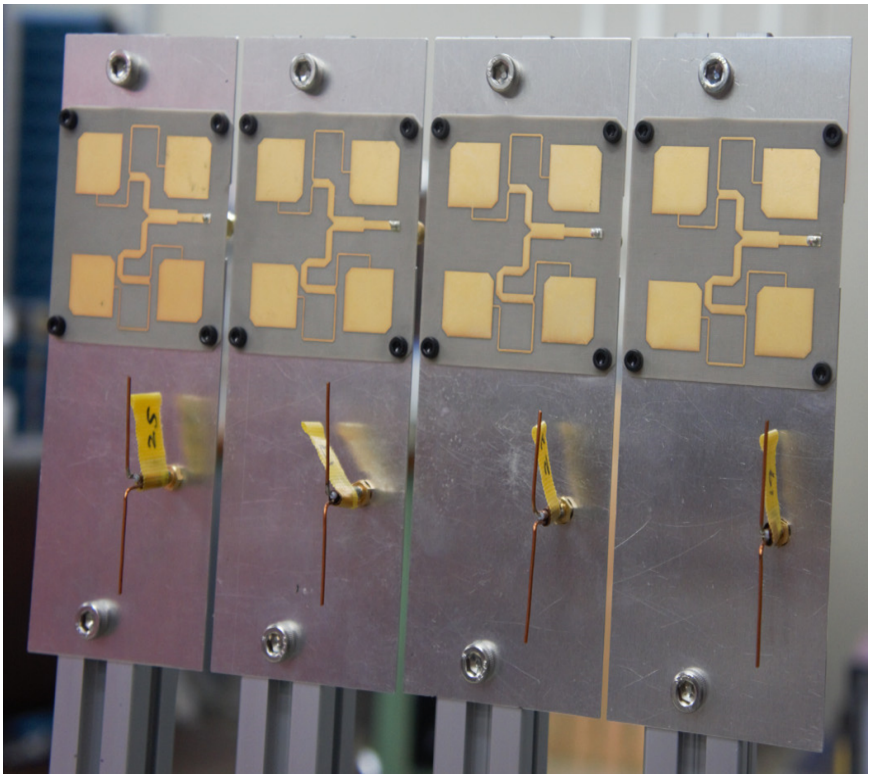

FIGURE 4.8: Patch subarrays with dipole antennas.

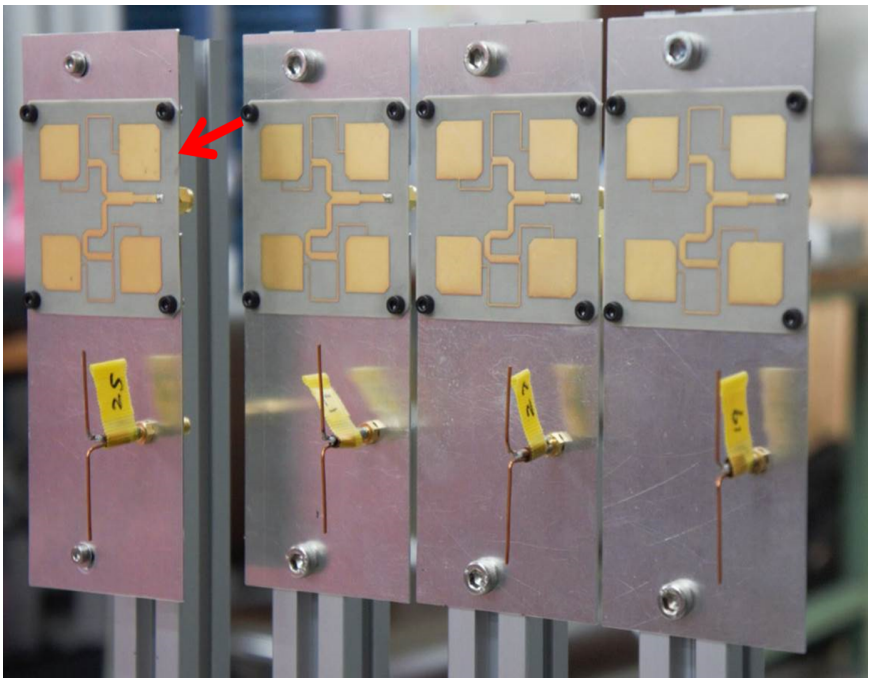

FIGURE 4.9: Forward antenna deformation configuration.

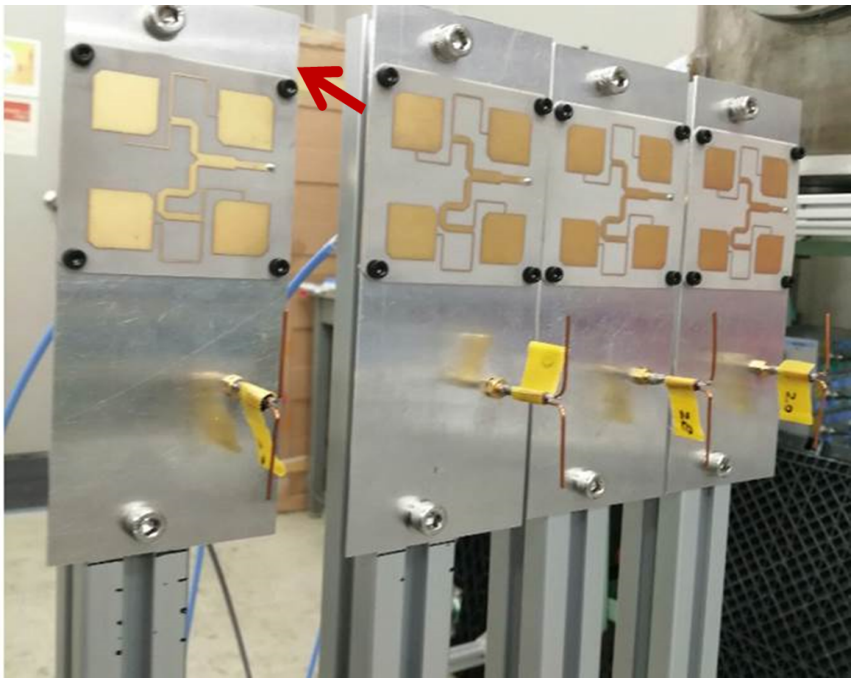

FIGURE 4.10: Backward antenna deformation configuration.

4.5 Results and Discussion

4.5.1 No Deformation Case

Digital retrodirective method is confirmed for beam forming towards 0° and 5°. Pilot signal is sent towards 0° and 5° positions of retrodirective array. Figure 4.11 represents radiation pattern of power signal for 0° beam forming. Radiation pattern

is measured from -30° to 30°. Three decibels beam-width is 9.8° and side lobe level is -13 dB. The measured pattern, especially the main lobe matches those simulated closely. Simulations are performed by using CST software. Figure 4.12 shows radiation pattern of power signal for 5° beam forming. Half power beam-width is 9.5°, and side lobe level is -12 dB. Simulated and measured results are in good agreement and represent that digital retrodirective method is performing well.

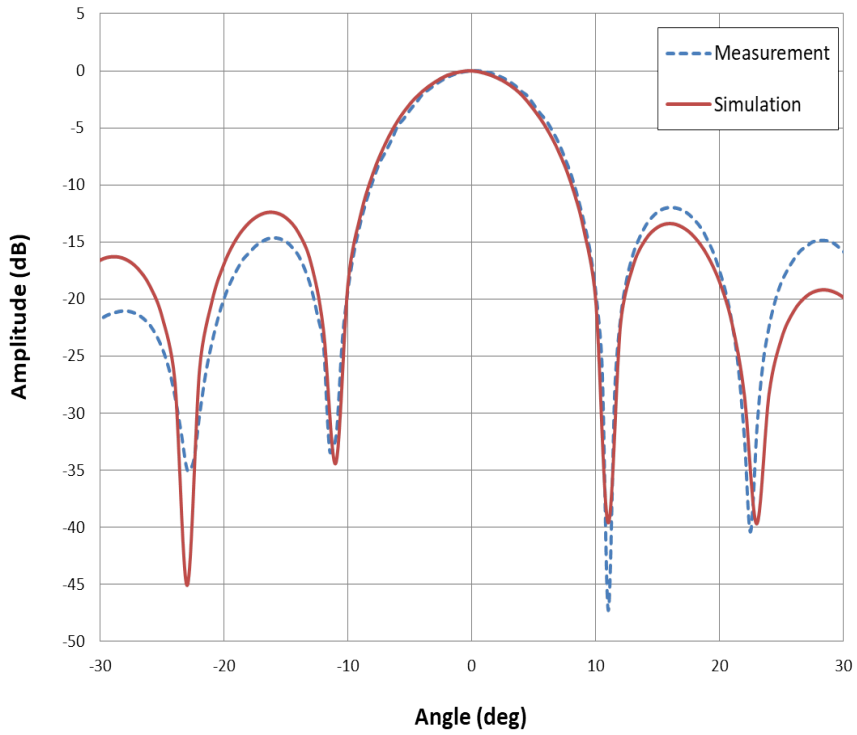

FIGURE 4.11: No deformation with Digital Retrodirective method for pilot signal from 0°.

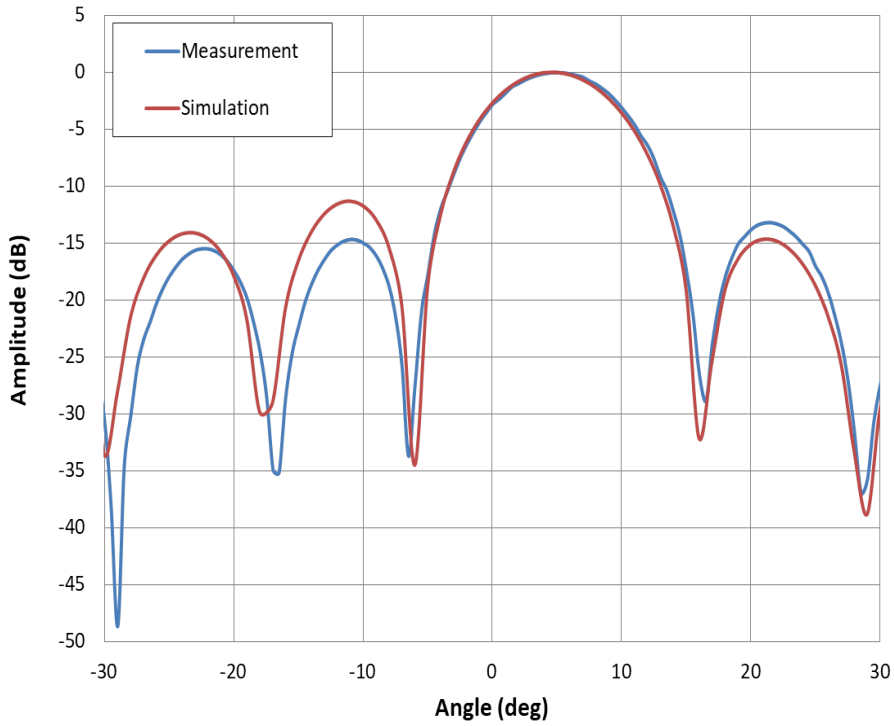

FIGURE 4.12: No deformation with Digital Retrodirective method for pilot signal from 5°.

4.5.2 Deformation case

For deformation cases, analysis is performed for phase change of pilot signal with deformation. Figure 4.13 depicts comparison between theoretical data and measured data. Theoretical data is obtained by Eq. (4.2):

$$\Delta\phi = \frac{2\pi\Delta x}{\lambda}, \tag{4.2}$$

where $\Delta\phi$ shows phase change of pilot signal by deformation, and Δx represents dimension for deformation. Then, 0.2λ, 0.4λ, 0.5λ, 0.6λ, and 0.8λ deformation cases are compared. Theoretical and measurement data is correlated in Figure 4.13.

TABLE 4.1: Root-mean square (RMS) phase error measurement..

Deformation	Phase Error
0.2	1.8
0.4	4.31
0.5	5
0.6	3
0.8	2.3
	3.495 (RMS)

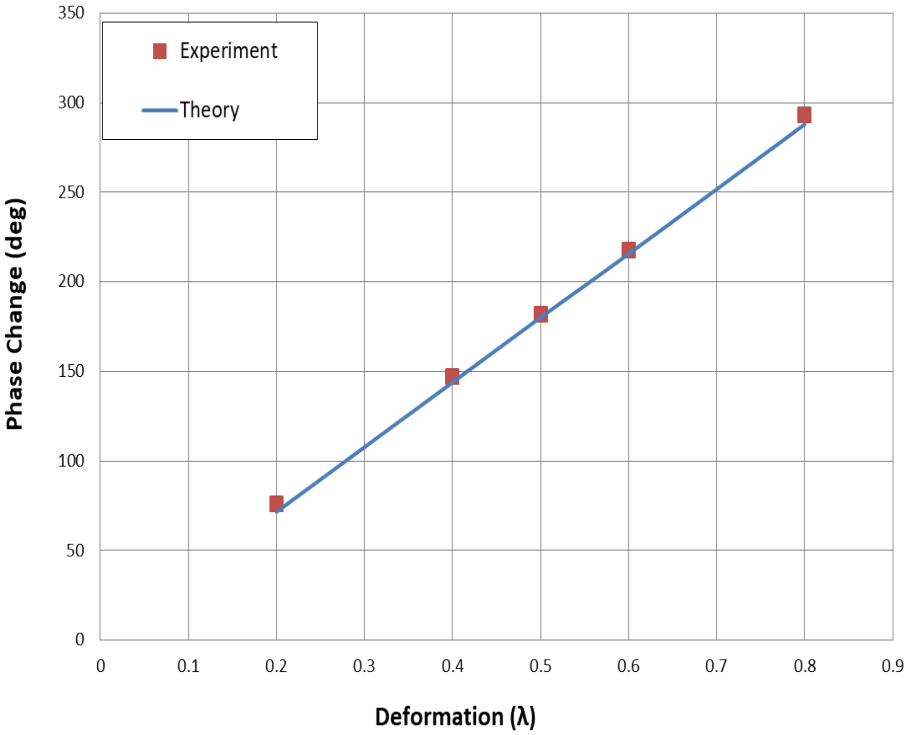

FIGURE 4.13: Deformation analysis for phase.

DSP circuit, as shown in Figure 4.4, has ADC component, and it generates main quantization error. Analysis is performed to measures phase change error and power signal beam pointing error. Phase measurement error for antenna deformation cases is represented in Table 4.1, and RMS error for phase change is 3.495°. Power signal beam pointing RMS error is calculated by Eq. (4.3) [33]:

$$\Delta\theta = \frac{2\lambda}{\pi d \cos\theta, M^{1.5}}\delta\phi, \tag{4.3}$$

where $\Delta\theta$ is beam pointing RMS error, d is spacing between antenna subarray, M is number of elements in the array, and $\delta\phi$ is phase RMS error. For M=4, θ=0°, d=1.3λ, $\delta\phi$=3.495°, $\Delta\theta$ was determined as 0.21° RMS. Beam width of power signal beam is 9.8° and 10% of beam-width is 0.98°. So, beam pointing error by digital retrodirective method satisfies accuracy requirement for SPS. Each subarray is working independently and will be working in the same manner for SPS. Probability density distribution for phase change error is also represented in Figure 4.14.

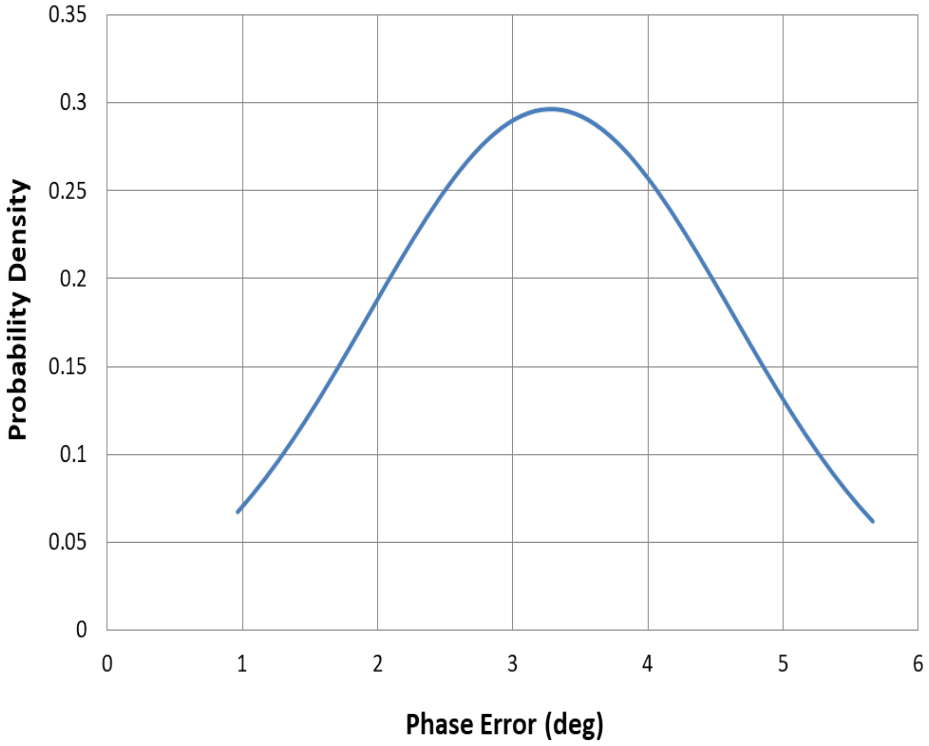

FIGURE 4.14: Probability density function of phase error.

Further, 0.5λ deformation case produces maximum phase change of pilot signal. So, radiation patterns with 0.5λ case are analyzed. Figure 4.15 represents radiation pattern for 0.5λ forward deformation case. With retrodirective plot is measured data for digital retrodirective method with deformation. Simulation plot is simulated data for the deformation with digital retrodirective method. Without retrodirective pattern is when digital retrodirective method is not used for deformation. Simulated and measured data with retrodirective method are in good agreement. Without retrodirective plot shows that main lobe is directed to $-8°$, and side lobe level is -3 dB. So, the effect of deformation is resolved by using the digital retrodirective method.

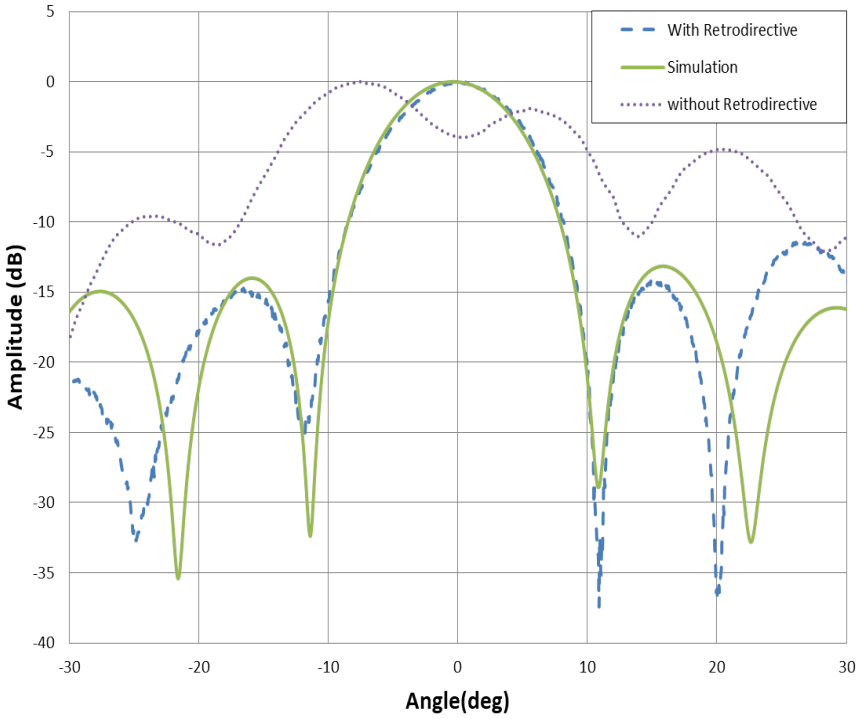

FIGURE 4.15: Forward deformation with digital Retrodirective method.

Figures 4.16 represents comparison of digital retrodirective method and REV method for antenna deformation. We compare the 0.5λ deformation case, and the radiation pattern shows that both methods are in good agreement with the simulation. REV method takes long time for the process, so digital retrodirective method has advantage over REV method to correct radiation pattern for antenna deformation.

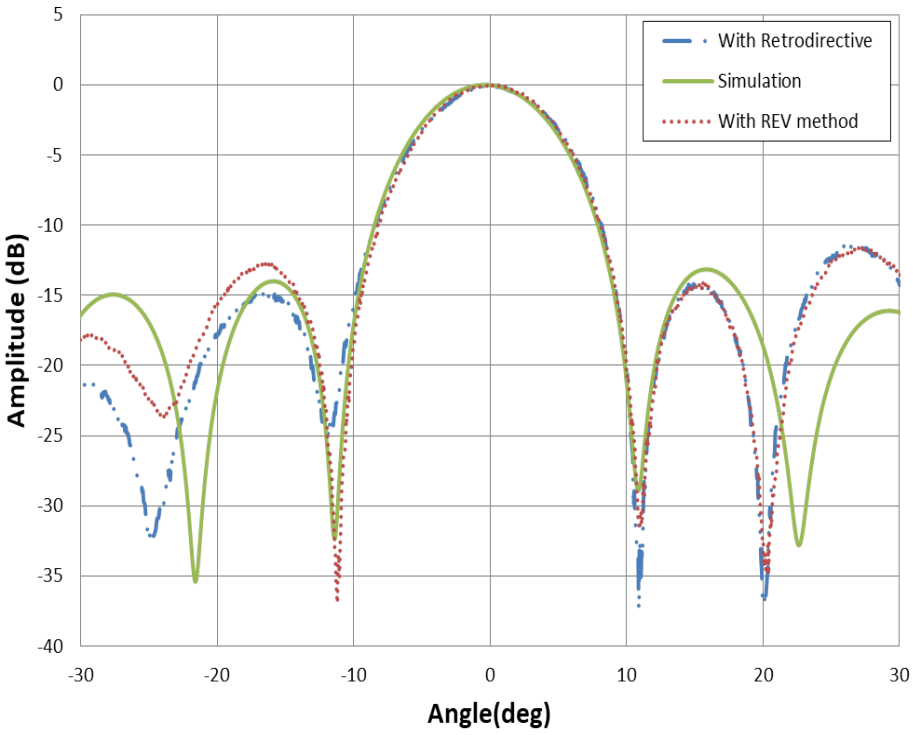

FIGURE 4.16: Comparison of Digital Retrodirective method with REV method.

Figure 4.17 represents radiation pattern for 0.5λ backward deformation case. With retrodirective plot correlates with the simulation, having beam-width of 9.7° and side lobe level of -12 dB. Without retrodirective pattern has -5.1° main lobe direction of and -3.4 dB side lobe level. Figure 4.18 depicts comparison of digital retrodirective method for no deformation and deformation case. Pilot signal is sent from 5°, and measured patterns are compared. Both plots are in good agreement, and this shows that effect of antenna deformation is resolved successfully by digital retrodirective method.

Experimental results of digital retrodirective method show that appropriate radiation patterns are obtained for no deformation and deformation cases.

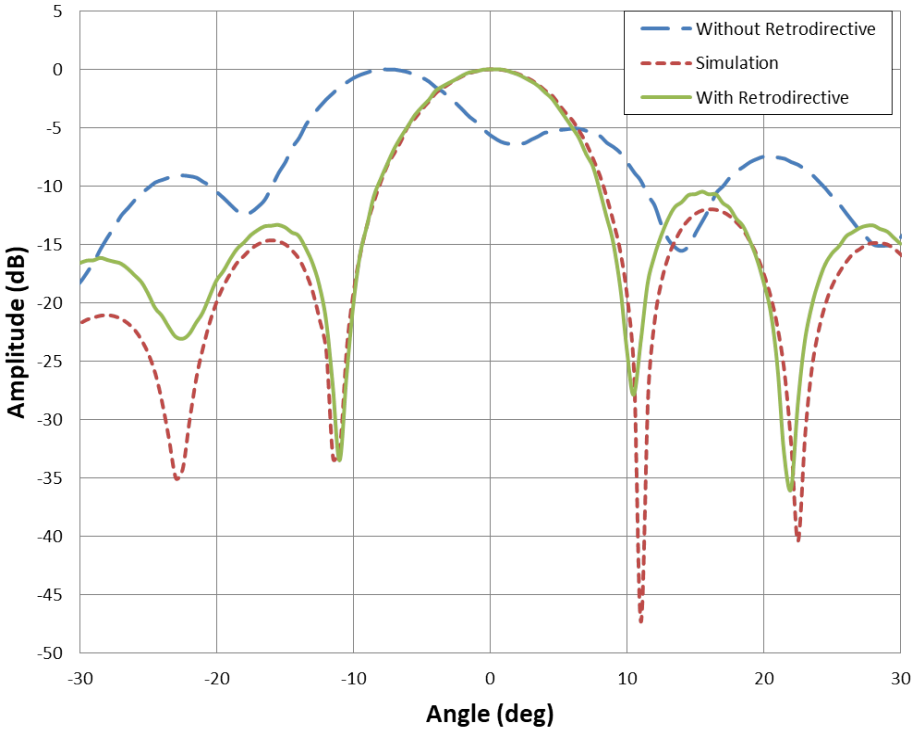

FIGURE 4.17: Backward deformation with Digital Retrodirective method.

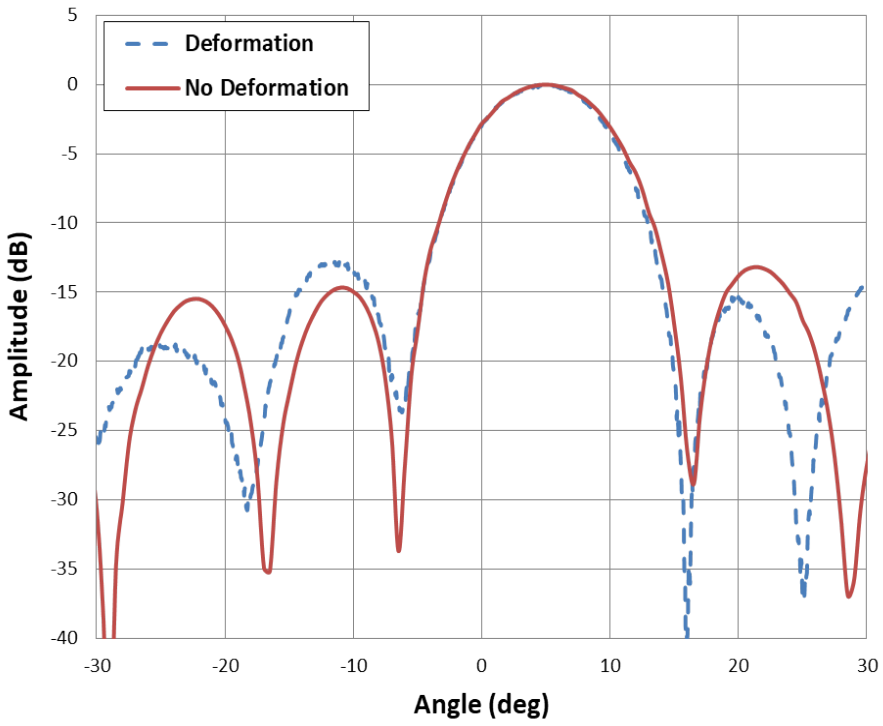

FIGURE 4.18: Comparison of no deformation and deformation case.

4.6 Summary

Chapter 4 presented digital retrodirective method to perform MPT for SPS. Four dipole antennas received pilot signal from the rectenna, and four patch subarrays transmitted power signal towards rectenna. DSP circuit was used for pilot signal phase detection and power signal beam forming with phase conjugation. Digital retrodirective method's algorithm performed well for correction of antenna deformation effect. Each subarray worked independently with respective dipole antenna, and synchronization was not required for beam forming. Phase change measurement error was 3.495° RMS, and beam pointing error was 0.21° RMS. Comparison was also done for antenna deformation and no deformation cases. REV method was also in correlation with digital retrodirective method. This study suggests that the proposed method is a suitable candidate to resolve issues of previous methods to do beam forming for SPS.

Chapter 5

System Study of WPT Technologies for SPS

5.1 Introduction

Direction finding experiments with using pilot signal receiving array antennas are discussed in Chapter 3. Digital Retrodirective method is evaluated in Chapter 4 with using retrodirective antenna arrays. chapter 5 mentions application of DF experiment and digital retrodirective method for system study of SPS. Use of array antenna with long baseline is studied to estimate uplink power and noise level to perform pilot signal direction finding for SPS. Digital retrodirective method is investigated for large array size and concept about providing reference signal for large antennas arrays is proposed.

5.2 Estimation of Uplink Power

It is required to estimate uplink power for pilot signal. As by Chapter 3, 4x4 dipole array with 18 dBi gain was used for DF and .00582° error of AOA were achieved with 5m baseline. For required accuracy of .0005°, if we consider that transmitted power (P_t) of 100 W - 10 MW is sent from a parabolic antenna of 54.49 dBi gain (G_t). Then, received power (P_r) by 4x4 dipole arrays of 18 dBi gain (G_r) will be -68 dBm to -18 dBm, as shown in Table 5.1. Required noise level will be -127 dBm to -77 dBm. Values of (P_r) and noise level are obtained by Eq. (5.1) and (5.2) respectively. By Table 5.1, If a standard receiver with -110 dBm noise level is used, then .0005° accuracy can be achieved with 6 kW uplink power. As mentioned in Chapter 2 that, 1 MW of uplink was required with using 6 dBi gin of pilot signal receiving antenna. So, by increasing gain of pilot signal receiving antenna to 18 dBi, required uplink power was decreased to 6 KW with -110 dBm noise level. Figure 5.1 shows the transfer of uplink power to SPS with parabolic antenna.

$$P_r = P_t G_t G_r (\frac{\lambda}{4\pi r})^2 \tag{5.1}$$

$$\Delta\theta = \frac{\lambda}{\pi d \cos\theta \sqrt{SNR}} \tag{5.2}$$

TABLE 5.1: Uplink Power Estimation.

Pt (w)	Pr (dBm)	Noise (dBm)
100	-68.85	-127.8
1,000	-58.85	-117.8
10,000	-48.85	-107.8
100,000	-38.85	-97.8
1,000,000	-28.85	-87.8
10,000,000	-18.85	-77.87

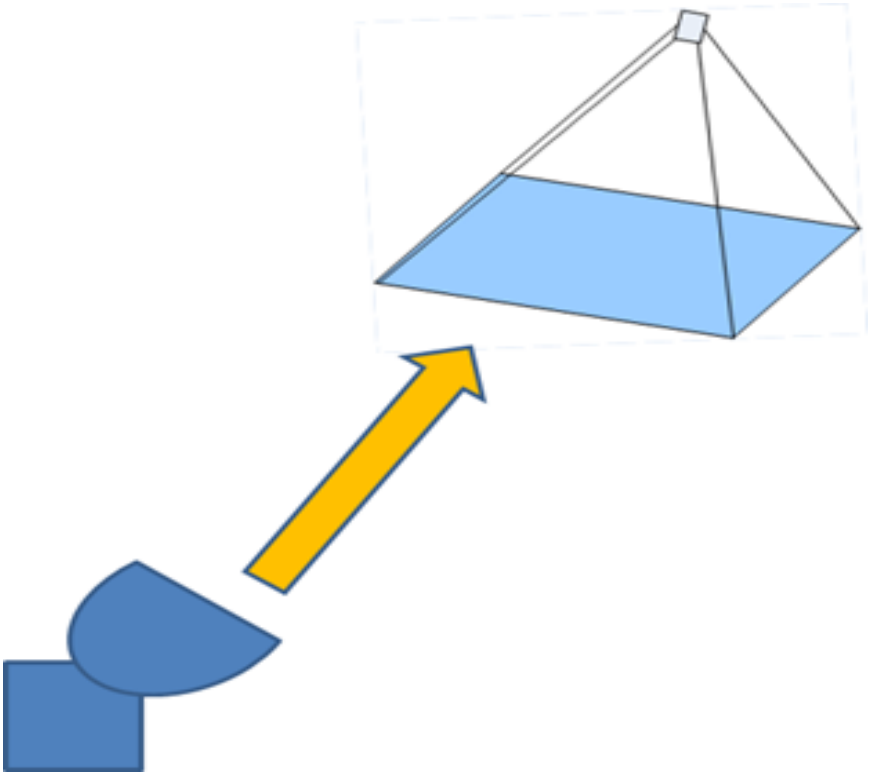

FIGURE 5.1: Uplink pilot SIgnal.

5.3 Array Size Estimation

If array size of pilot signal receiving antenna is increased, then uplink power will be decreased more. Simulations are performed to measure gain with increasing array size, as shown in Table 5.2. 14x7 array has 26 dB gain and baseline size is decreased to 4.2 m. 7x7 array has 23 dB gain and baseline size is 4.6 m.

For 0.0005° accuracy, noise level and uplink transmitted power is calculated, as given in Table 5.3.

TABLE 5.2: Array Size and Gain.

Array	Gain	Beam width	Baseline
7x7	23 dB	13.3 deg	4.6 m
14x7	26 dB	13.3 deg	4.2 m

TABLE 5.3: Uplink power with noise level.

Power	Noise level of 7x7	Noise level of 14x7
100 W	-122 dBm	-120 dBm
1000 W	-112 dBm	-110 dBm
10,000 W	-102 dBm	-100 dBm
100,000 W	-92 dBm	-90 dBm

5.4 Configuration of Pilot Signal Receiving Antennas for SPS

Figure 5.2 shows Tethered SPS with using 4x4 pilot signal receiving antenna array for one dimensional direction finding. Pilot signal receiving antennas are installed on power transmitting antenna. Two pilot signal receiving antenna arrays are required for 5 m baseline, so it also decreases number of pilot signal receiving antennas for direction finding.

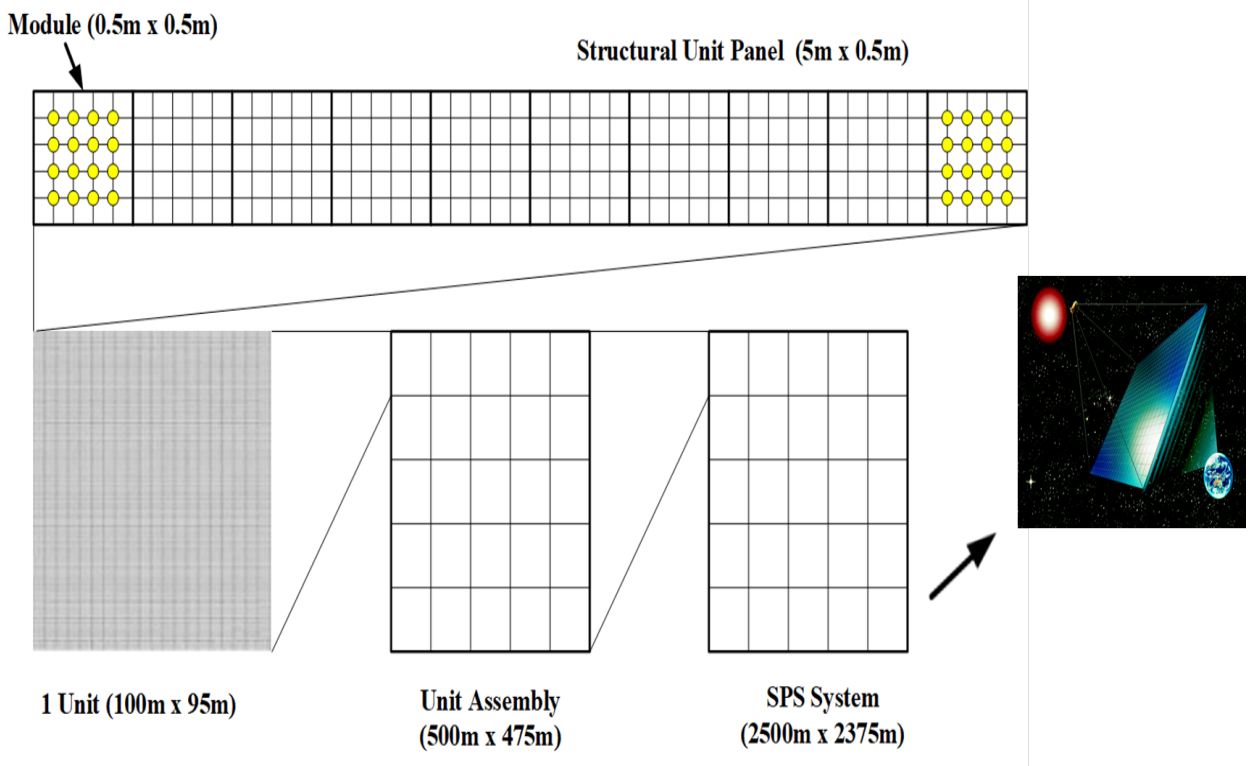

FIGURE 5.2: Configuration of 4x4 array for SPS.

5.5 Application of Digital Retrodirective Method for SPS

Digital Retrodirective method is demonstrated by simulation for 8x8 deformed antenna subarray. Antennas are deformed in forward and backward direction. Figure 5.3 shows configuration for 8x8 subarray with deformation. Figure 5.4 represents simulation result for correction of antenna deformation with digital retrodirective method. Results of 8x8 array without deformation and 8x8 deformation compensation by digital retrodirective method are in good correlation.

Regarding antenna modules with SPS, there is a concern of angular deformation [24,25,38,39]. By [25], antenna deformation experiments were performed in z-direction and with rotation in elevation. Rigid antenna modules were used and whole antenna module arrays were deformed, while individual antennas were not deformed. But with elevation deformation, there is a concern that relative position for pilot signal and power signal antenna will be different for retrodirective array in Figures 4.8 and 5.3. Deformation angle for SPS structure regarding power transmission has limitation of ± 5° [38,39]. So, it is need to know that regarding ± 5° deformation angle for SPS, how much deformation angle is required for 1 module or individual retrodirective array. There is also need to confirm the deformation angle for individual retrdodirective array with using rigid and thin antenna module.

Evaluation of digital retrodirective method was confirmed with deformation in z-direction in chapter 4 and 5. Regarding angular deformation, future study is required to know deformation angles for individual retrodirective array depending on the limitations of SPS. By Figure 3.15, spacing between pilot signal and power signal antennas is less and this configuration can decrease effect by angular deformation case. So, the issue of angular deformation for retrodirective array with digital retrodirective method is an open question and should be investigated in the future.

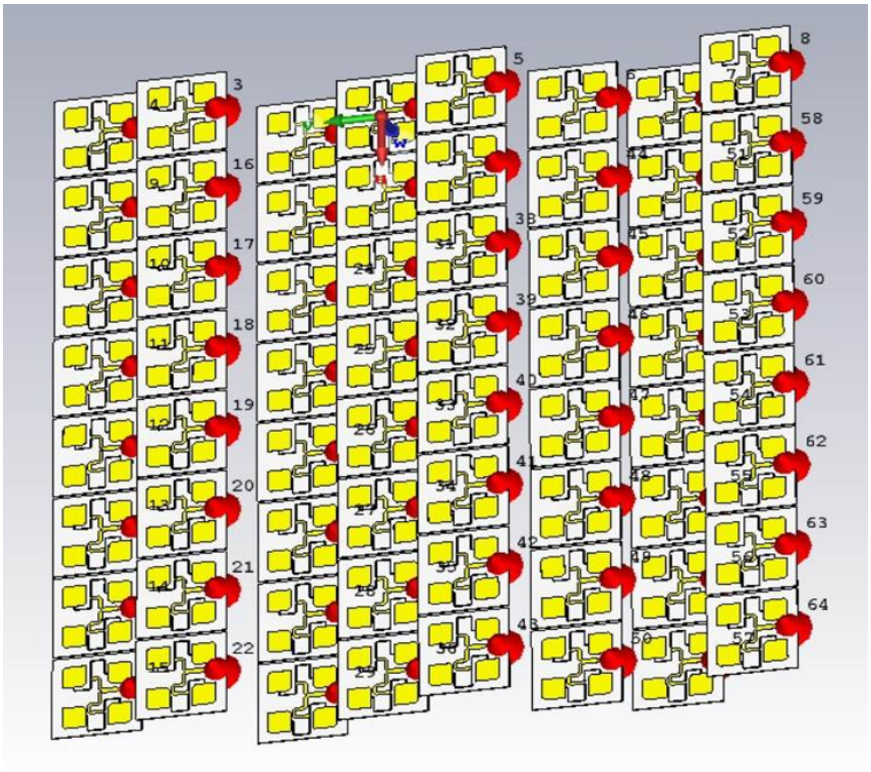

FIGURE 5.3: Configuration of 8x8 subarray.

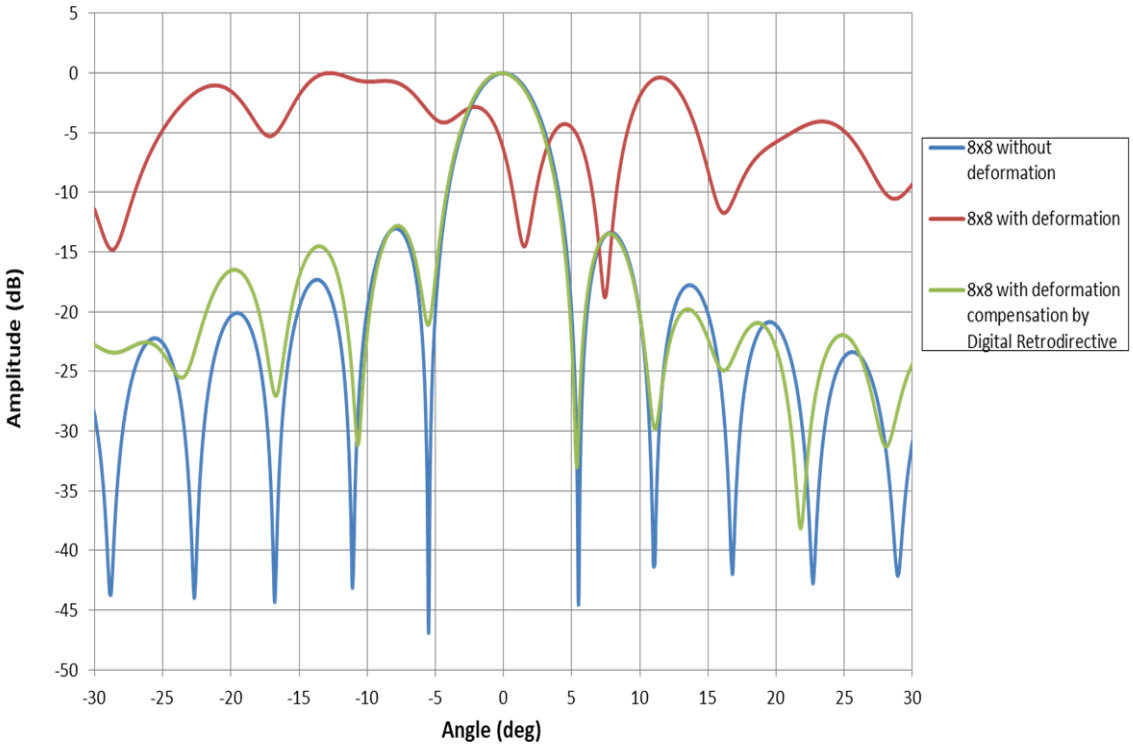

FIGURE 5.4: Simulation for of 8x8 deformed subarray.

Configuration for providing reference signal is represented for large scale in Figure 5.5. Each GPS antenna will provide reference signal for a group of retrodirective

array antenna (Rx and TX). Reference signals are not needed to be synchronized among group of retrodirective array antenna. Each RX/TX set will work independently for phase detection and phase conjugation.

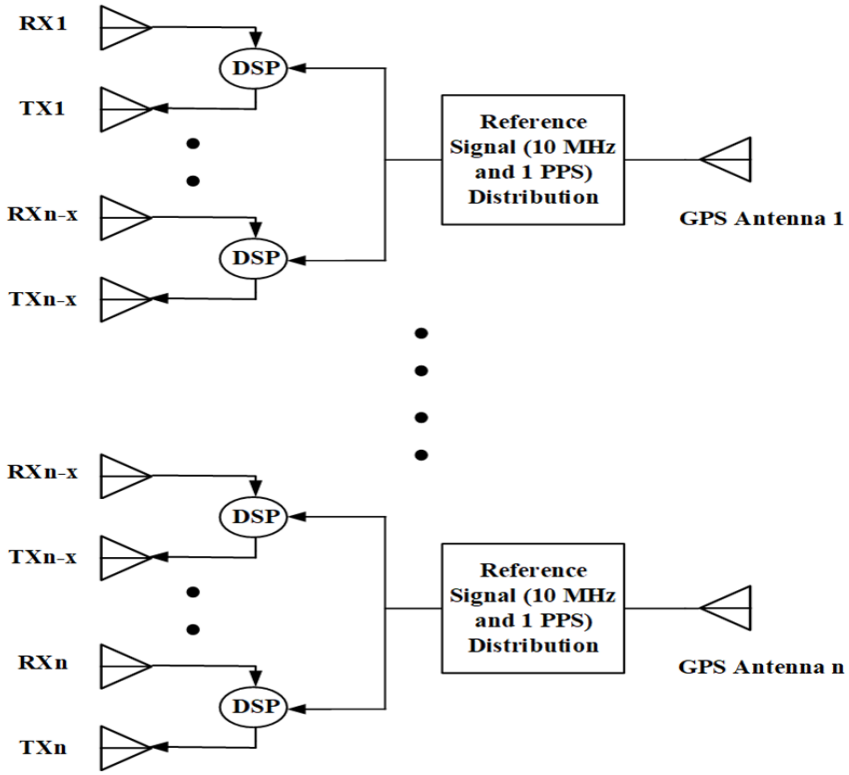

FIGURE 5.5: Configuration of reference signal for large scale.

5.6 Summary

Improvement of DF & Beam Forming method with respect to required accuracy of direction of arrival for pilot signal was required regarding uplink power. In previous studies, required uplink power was 1 MW. I proposed idea of using array antenna to decrease uplink power with long baseline. I was able to achieve the required accuracy of DF for SPS with 6 KW uplink power.

Chapter 4 discussed about development of Digital Retrodirective method. This method was proposed as alternative to Hardware retrodirective and Direction Finding and Beam Forming method. Application of Digital Retrodirective method was discussed for large array size in Chapter 5. Analysis was done for deformation with 8x8 subarray and effect of deformation was successfully resolved. Configuration was proposed for the providing reference signals of 10 MHz and 1 PPS for large antenna system.

Chapter 6

Conclusion

My study goal was to achieve the .0005° accuracy for power transmission and to compensate effect of antenna deformation effectively. My study objectives to achieve the goal were improvement of DF & Beam Forming method regarding uplink power, estimation of antenna deformation effect on direction finding and development of Digital Retrodirective method as alternative to Hardware retrodirective and DF & Beam Forming method.

Chapter 2 provides details about overall background regarding solar power satellite, proposed models of SPS and history of wireless power transmission. Previously proposed methods to transmit microwave power for SPS were also discussed and limitations were described.

Chapter 3 is about direction finding experiments. Comparison of array sizes and baseline was provided. Accuracy of direction finding was discussed regarding standard deviation of phase and error of AOA. 0.00049° accuracy was obtained for 60 dB of SNR with 4x4 array and 5m baseline. For case of deformation effect, experiments were performed with partial and whole antenna array deformation cases. Change of phase was measured to evaluate the effect of antenna deformation.

Chapter 4 discusses concept and evaluation for digital retrodirective method . Linear retrodirecrive array antenna was used for the experiment. Digital circuit was used for pilot signal phase detection and power signal beam forming with phase conjugation. Digital retrodirective method's algorithm performed well for correction of antenna deformation effect. Each subarray worked independently with respective dipole antenna and synchronization was not required for beam forming. Phase change measurement error was 3.495° RMS, and beam pointing error was 0.21° RMS. Comparison was also done for antenna deformation and no deformation cases. REV method was also in correlation with digital retrodirective method. So, digital retrodirective method solved issues of hardware retrodirective and DF and Beam forming method. Limitation of digital retrodirective method is that it needs pilot signal receiving antennas for each power transmitting antenna. So, there is trade-off between efficiency and cost.

Chapter 5 discusses about application of proposed ideas for SPS. Estimation of uolink power was done for SPS with 4x4 dipole array antenna. It was found that with standard receiver noise level of -110 dBm, 6 kw uplink power is required to get .0005° error of DF with 5 m baseline. Digital Retrodirective method was also evaluated for large 2 dimensional array system. scheme was given to provide the stable frequency and phase by reference signal for SPS.

Contribution of my research is that i was able to provide the update for system study of SPS regarding uplink power of pilot signal. Evaluation for antenna deformation effect on direction finding was reported first time. I proposed digital retrodirective method to do microwave power transmission for SPS under deformable antenna conditions. This method was able to solve issues of conventional microwave power transmission methods.

Bibliography

[1] Sasaki S, Tanaka K. Demonstration Experiment for Tethered-Solar Power Satellite. TRANSACTIONS OF THE JAPAN SOCIETY FOR AERONAUTICAL AND SPACE SCIENCES, SPACE TECHNOLOGY JAPAN. 2009;7(ists26):Tr_1_1-4.

[2] Shinohara, Naoki. Wireless power transfer via radiowaves. John Wiley & Sons, 2014.

[3] Glaser, P.E., “The Future of Power from the Sun,” Intersociety Energy Conversion Engineering Conference, published by IEEE Transactions on Aerospace and Electronic Systems, 1968, 68C-2 l-Energy, pp. 98-103.

[4] Glaser, P.E., “Solar Power via Satellite,” IEEE ’73 lNTERCON Conference Record.

[5] Glaser, P. E., “The Use of the Space Shuttle to Support Large Space Power Generation Systems,” presented at Meeting of the American Astronautical Society held in conjunction with the American Association for the Advancement of Science Annual Meeting, Washington, D. C., December 26-30, 1972.

[6] Brown, W. C., “Satellite Power Stations: A New Source of Energy?”, IEEE SPECTRUM, March 1973, pp. 38-47.

[7] Sasaki S, Tanaka K, Maki KI. Microwave power transmission technologies for solar power satellites. Proceedings of the IEEE. 2013 Jun;101(6):1438-47.

[8] Sasaki S, Tanaka K. Wireless power transmission technologies for solar power satellite. In Microwave Workshop Series on Innovative Wireless Power Transmission: Technologies, Systems, and Applications (IMWS), 2011 IEEE MTT-S International 2011 May 12 (pp. 3-6).

IEEE.

[9] Sasaki S, Tanaka K, Higuchi K, Okuizumi N, Kawasaki S, Shinohara N, Senda K, Ishimura K. A new concept of solar power satellite: Tethered-SPS. Acta Astronautica. 2007 Feb 1;60(3):153-65.

[10] Shinohara N. Beam control technologies with a high-efficiency phased array for microwave power transmission in Japan. Proceedings of the IEEE. 2013 Jun;101(6):1448-63.

[11] Strassner B, Chang K. Microwave power transmission: Historical milestones and system components. Proceedings of the IEEE. 2013 Jun;101(6):1379-96.

[12] Matsumoto H. Research on solar power satellites and microwave power transmission in Japan. IEEE microwave magazine. 2002 Dec;3(4):36-45.

[13] Maki KI, Takahashi M, Miyashiro K, Tanaka K, Sasaki S, Kawahara K, Kamata Y, Komurasaki K. Microwave characteristics of a wireless power transmission panel toward the orbital experiment of a solar power satellite. InMicrowave Workshop Series on Innovative Wireless Power Transmission: Technologies, Systems, and Applications (IMWS), 2012 IEEE MTT-S International 2012 May 10 (pp. 131-134). IEEE

[14] K. Hashimoto and H. Matsumoto, "Microwave beam control system for solar power satellite," 2004 Asia-Pacific Radio Science Conference, 2004. Proceedings., 2004, pp. 616-617, doi: 10.1109/APRASC.2004.1422583.

[15] Hashimoto, K.; Matsumoto, H. Retrodirective system for solar power satellites. In Proceedings of the 57th International Astronautical Congress, Valenica, Spain, 2–6 October

2006,
[16] Hashimoto K, Shinohara N, Matsumoto H. Beam control of microwave power beam for a solar power station/satellite. In2nd Sustainable Energy and Environment Conference 2006 (pp. 21-23).

[17] Shotaro Katano, Taishi Kobayashi, Makoto Tanaka, Koji Tanaka. Experiment of Direction Finding by pilot signal for Solar power satellite. ISTS 2015

[18] Koji Tanaka , Shotaro Katano, Maki KI, Sasaki S, 65th International Astronautical Congress, Toronto, Canada

[19] T. Miyakawa, M. Yajima, Y. Fukumuro, S. Sasaki, T. Sasaki, Y. Homma, and k. Namura, “Development status of the beam steering control subsystem for the microwave power transmission ground experiment,” IEEE MTT-S International Microwave Workshop Series on Innovative Wireless Power Transmission: Technologies, Systems, and Applications, Japan., pp. 231-234, 2011.

[20] Lim JS, Jung CG, Chae GS. A design of precision RF direction finding device using circular interferometer. InIntelligent Signal Processing and Communication Systems, 2004. ISPACS 2004. Proceedings of 2004 International Symposium on 2004 Nov 18 (pp. 713-716). IEEE.

[21] Park CS, Kim DY. The fast correlative interferometer direction finder using I/Q demodulator. InCommunications, 2006. APCC'06. Asia-Pacific Conference on 2006 Aug (pp. 1-5). IEEE.

[22] Van Doan S, Vesely J, Janu P, Hubacek P, Tran XL. Algorithm for obtaining high accurate phase interferometer. InRadioelektronika (RADIOELEKTRONIKA), 2016 26th

International Conference 2016 Apr 19 (pp. 433-437). IEEE.

[23] Iwashita, M.; Kaya, N. The demonstration of microwave-beam control in international symposium on solar energy from space. In Proceedings of the International Symposium on Space Technology and Science,Ginowan, Okinawa, Japan, 5–12 June 2011.

[24] Yamagami, T.; Nakamura, T.; Sekiya, N.; Arai, K.; Tanaka, K. Modeling and Simulation of Carbon Nanotube based Electro-active Polymers for Shape-keeping of the Large-scale Space structure. In Proceedings of the International Symposium on Space Technology and Science, Fukui, Japan, 15–21 June 2019.

[25] Takahashi, T.; Sasaki, T.; Homma, Y.; Mihara, S.; Sasaki, K.; Nakamura, S.; Makino, K.; Joudoi, D.; Ohashi, K. Phased array system for high efficiency and high accuracy microwave power transmission. In Proceedings of the 2016 IEEE International Symposium on Phased Array Systems and Technology, Waltham, MA, USA, 18–21 October 2016.

[26] S. Dong, Y. Dong, S. Liu, Y. Wang and X. Li, "Analysis on Local Deformation of Microwave Power Transmitting Antenna Array," 2018 International Applied Computational Electromagnetics Society Symposium - China (ACES), 2018, pp. 1-2, doi 10.23919/ACESS.2018.8669166.

[27] https://www.ni.com/documentation/en/usrp-software-defined-radio-reconfigurable-device/latest/specs-usrp-2945/specs/

[28] Mihara, S.; Sato, M.; Nakamura, S.; Sasaki, K.; Homma, Y.; Sasaki, T.; Ozawa, Y.; Tanaka, N.; Fujiwara. T. The result of ground experiment of microwave wireless power transmission. In Proceedings of the 66th Int. Astronautical Congress, Jerusalem, Israel, 12–16 October 2015.

[29] Varasteh, M.; Piovano, E.; Clerckx, B. A Learning Approach to Wireless Information and

Power Transfer Signal and System Design. In Proceedings of the ICASSP 2019—2019 IEEE International Conference on Acoustics, Speech and Signal Processing (ICASSP), Brighton, UK, 12–17 May 2019; pp. 4534–4538, doi: 10.1109/ICASSP.2019.8682485.

[30] Perera1, T.D.P.; Jayakody, D.N.K.; De. S.; Ivanov, M.A. A Survey on Simultaneous Wireless Information and Power Transfer. Journal of Physics: Conference Series, Volume 803. In Proceedings of the International Conference on Information Technologies in Business and Industry, Tomsk, Russian, 21–26 September 2016

[31] X. Wang, J. He, L. Guo, S. Sha and M. Lu, "Wireless charging for low-power mobile devices based on retro-reflective beamforming," 2014 IEEE Antennas and Propagation Society International Symposium (APSURSI), 2014, pp. 1411-1412, doi: 10.1109/APS.2014.6905031.

[32] S. Sha and M. Lu, "A hardware demonstration of wireless power transmission based on retro-reflective beamforming," Proceedings of the 2012 IEEE International Symposium on Antennas and Propagation, 2012, pp. 1-2, doi: 10.1109/APS.2012.6349063.

[33] Tanaka, K.; Maki, K.; Sasaki, S. Development of Phased-Array Antenna System for Wireless Power Transmission Experiment. In Proceedings of the 64th Int. Astronautical Congress, Beijing, China, 23–27 September 2013.

[34] https://www.ni.com/pdf/manuals/374193d.pdf

[35] https://forums.ni.com/t5/LabVIEW/unwrap-phase-7-1/td-p/525871?profile.language=ja

[36] https://forums.ni.com/t5/LabVIEW/wrap-phase/td-p/686071?profile.language=en

[37] https://zone.ni.com/reference/en-XX/help/371361R-01/lvanls/unwrap_phase/

[38] D. Sato, N. Yamada and K. Tanaka, "Thermal Design of Photovoltaic/Microwave Conversion Hybrid Panel for Space Solar Power System," in *IEEE Journal of Photovoltaics*, vol. 7, no. 1, pp. 374-382, Jan. 2017, doi: 10.1109/JPHOTOV.2016.2629843

[39] Nakamura, T.; Sekiya, N.; Yamagami, T.; Tanaka, K. Modeling and Simulation of Carbon Nanotube based Electro-active Polymers for Shape-keeping of the Large-scale Space structure. In Proceedings of the International Symposium on Space Technology and Science, Fukui, Japan, 15–21 June 2019.